# USE OF ACTIVATED CARBONS PRODUCED FROM INDIGENOUS RAW MATERIALS IN GOLD METALLURGY AS AN ALTERNATIVE TO COCONUT SHELL CARBONS

A THESIS SUBMITTED TO
THE GRADUATE SCHOOL OF NATURAL AND APPLIED SCIENCES
OF
THE MIDDLE EAST TECHNICAL UNIVERSITY

BY

MUSTAFA YALÇIN

IN PARTIAL FULFILLMENT OF THE REQUIREMENTS FOR THE DEGREE
OF

DOCTOR OF PHILOSOPHY

IN

THE DEPARTMENT OF MINING ENGINEERING

JANUARY 1996

Approval of the Graduate School of Natural and Applied Sciences of the Middle East Technical University

for Prof. Dr. İsmail TOSUN
Director

I certify that this thesis satisfies all the requirements as a thesis for the degree of Doctor of Philosophy.

Prof. Dr. A. Günhan PAŞAMEHMETOĞLU
Head of Department

This is to certify that we have read this thesis and that in our opinion it is fully adequate, in scope and quality, as a thesis for the degree of Doctor of Philosophy.

Assoc. Prof. Dr. A. İhsan AROL
Supervisor

Examining Committee Members

Prof. Dr. Gülhan ÖZBAYOĞLU

Prof. Dr. Çetin HOŞTEN

Prof. Dr. Ümit ATALAY

Assoc. Prof. Dr. A. İhsan AROL

Assoc. Prof. Dr. Suna BALCI

## ABSTRACT

### USE OF ACTIVATED CARBONS PRODUCED FROM INDIGENOUS RAW MATERIALS IN GOLD METALLURGY AS AN ALTERNATIVE TO COCONUT SHELL CARBONS

Yalçın, Mustafa

Ph.D., Department of Mining Engineering

Supervisor: Assoc. Prof. Dr. A.İhsan Arol

January 1996, 120 pages

Coconut shells are the most widely used raw material for the production of activated carbon sought after in the gold production by cyanide leaching. There have been efforts to find alternatives to coconut shells. Shells and stones of certain fruits; olive , peach, almond etc., have been tested. Although promising results to some extent were obtained, coconut shells remain the main source of activated carbon used in gold metallurgy.

Türkiye has become a country of interest in terms of gold deposits of epithermal origin. Four deposits have already been discovered and mining and milling operations are expected to start in the near future. Türkiye is also rich in fruits which can be a valuable source of raw material for activated carbon production. In this study, hazelnut shells, peach and apricot stones, abundantly available locally, have been tested to determine whether they are suitable for gold metallurgy. Parameters of carbonization and activation have been optimized. Gold loading capacity and adsorption kinetics have been studied. The gold loading capacities in the range of 19.5-30.7 mg.Au/g, 25.8-27.5 mg.Au/g and 24-27 mg.Au/g were obtained for hazelnut shell carbons, apricot and peach stone

carbons, respectively. These values although lower than that of the coconut shell carbons fell in the range of K-values of activated carbon used in the industry.

The kinetic results indicated that apricot stones with an R value of 0.060 and $t_{50}$ of 120 minutes had the same adsorption rate as coconut shells with 0.059 and 120 minutes, R and $t_{50}$ values, respectively; hazelnut shells and peach stones seemed to give slower adsorption rate.

It was found that apricot stones among the other two yielded the best activated carbon from the standpoint of mechanical strength and adsorption characteristics.

Keywords: Activated Carbon, Gold Adsorption

# ÖZ

## ALTIN METALURJİSİNDE HİNDİSTAN CEVİZİ KÖKENLİ KARBONLARA ALTERNATİF OLARAK YERLİ HAMMADDELERDEN ÜRETİLMİŞ AKTİF KARBONLARIN KULLANIMI

Yalçın, Mustafa
Doktora, Maden Mühendisliği Bölümü
Tez Yöneticisi: Doç.Dr. A.İhsan Arol

Ocak 1996, 120 sayfa

Altının siyanür liçi yöntemi ile üretiminde kullanılan aktif karbon en yaygın olarak Hindistan cevizi kabuğundan üretilmektedir. Diğer bazı meyve kabuklarından da üretim çalışmaları yapılmış olmasına rağmen Hindistan cevizi kabukları aktif karbon üretiminde önemini korumaktadır.

Türkiye son zamanlarda epitermal altın yatakları bakımından ilgi çekici ülke durumuna gelmiştir. Dört depozit tesbit edilmiş olup, madencilik ve zenginleştirme işlemlerinin yakın zamanda başlayacağı beklenmektedir. Türkiye aynı zamanda aktif karbon üretiminde değerli bir kaynak olabilecek meyve üretim kapasitesi bakımından da zengin bir ülke durumundadır. Bu çalışmada, Türkiyede yaygın olarak bulunan fındık kabukları, şeftali ve kayısı çekirdeklerinden aktif karbon üretim çalışması yapılmıştır. Karbonlaştırma ve aktifleştirme parametreleri belirlenmiş ve üretilen aktif karbonların altın yükleme kapasitesi ile birlikte altın adsorplama karakteristikleri tesbit edilmiştir. Deneyler sonucunda, fındık kabuğu kökenli aktif karbonlarda 19.5-30.7 mg.Au/g, kayısı ve şeftali çekirdeği kökenli aktif karbonlarda ise sırasıyla 25.8-27.5 mg.Au/g ve 24-27 mg.Au/g arasında değişen altın yükleme kapasite değerleri elde edilmiştir. Bu değerler hindistan cevizi

kabuğundan üretilmiş aktif karbonların altın yükleme kapasite değerlerinden düşük olmasına rağmen, endüstriyel kullanım limitlerinin üzerinde olduğu tesbit edilmiştir.

Kinetik deneyleri sonucunda, 0.060 R ve 120 dk $t_{50}$ değerleri ile kayısı kabuğundan üretilen aktif karbonların, 0.059 ve 120 dk, R ve $t_{50}$ değerleri ile hindistan cevizi kabuğundan üretilen aktif karbonlarla aynı adsorplama kinetiğine sahip olduğu belirlenmiştir. Fındık kabukları ve şeftali çekirdeklerinden üretilen aktif karbonlar ise daha yavaş altın adsorplama kinetiğine sahip olmuşlardır.

Elde edilen sonuçlardan, diğer iki hammaddeden farklı olarak kayısı kabuklarının mekanik dayanımı ve adsorpsiyon özellikleri bakımından aktif karbon üretiminde en iyi hammadde olduğu ortaya çıkmıştır.

Anahtar Kelimeler: Aktif Karbon, Altın Adsorpsiyonu

## ACKNOWLEDGMENTS

I express sincere appreciation to Assoc. Prof. Dr. A.İhsan Arol for his guidance and insight throughout the research. Thanks go to the other faculty members, Prof. Dr. Gülhan Özbayoğlu, Prof. Dr. Çetin Hoşten and Prof. Dr. Ümit Atalay for their suggestions and comments. The technical assistance of Süleyman Kırıcı and Tuncer Gençtan is gratefully acknowledged. To my wife, Nuray, I offer sincere thanks for her unshakable faith in me and her willingness to endure with me the vicissitudes of my endeavors.

TABLE OF CONTENTS

## LIST OF TABLES

TABLE

## LIST OF FIGURES

FIGURES

# CHAPTER I

# INTRODUCTION

Carbon has been known throughout history as an adsorbent, its usage dating back centuries before Christ. In about 1500 BC, the Egyptians, who were aware of the adsorbent properties of wood charcoal , used it for medicinal purposes and as a purifying agent , as did the ancient Hindus, who filtered their drinking water through charcoal (Hassler, 1963 and 1974 and Mattson and Mark, 1971).

The decolorization and gas-adsorption properties of various carbon products were first investigated in the late nineteenth century, their development having gained impetus from the need for gas adsorbents to protect people against the poisonous gases used in World War I and also from new applications that arose in the sugar industry and that are related to decolorization ( Bailey, 1986 ).

Activated carbon is a generic term for a family of highly porous carbonaceous materials, none of which can be characterized by a structural formula or by chemical analysis (Hassler, 1963 and 1974; Smisek and Cerny, 1970; Mattson and Mark, 1971). It is prepared by carbonizing and activating the carbonaceous material under conditions that give a very large adsorptive power due to that of highly developed porous sturucture and internal surface area.The volume of the pores of activated carbons is generally defined to be greater than 0.2 ml/g and the internal surface area is generally larger than 400 $m^2/g$ as measured by Nitrogen BET method ( Mc Dougall, Lecture Notes and Mc Dougall and Fleming, 1987).

Active carbon was initially classified as amorphous carbon together with the carbon blacks and unactivated products of carbonization such as chars, wood-charcoal (Kipling, 1956). Recently, after X-Ray diffraction studies this classification has turned out to be unsuitable since active carbon, carbon blacks and other carbonaceous materials are observed to be not amorphous but have a microcrystalline structure which depending upon the conditions of preparation, resembles more or less closely the structure of graphite(Smisek and Cerny, 1970; Mc Dougall and Hancock, 1980 and Mc Dougall, 1980 ). The same studies have shown that the size of these microcrystalline regions increases with temperature of activation, which might relate to the adsorptive properties of the carbon since these depend strongly on the temperature of activation.

Important applications relate to the use of activated carbons to render water potable by the removal of taste, color, odor and undesirable organic impurities, in the treatment of domestic and industrial waste water, in the removal of color from various types of sugar syrups, in a variety of gas-phase applications, in the purification of many chemical and pharmaceutical products, in wine and beer industries, in paper and pulp treatments and in food, petroleum and petro-chemical industries. Likewise, activated carbons adsorb gases and vapors and are extensively used for oil pollution control and vapor recovery operations in such applications as gas-masks, cigarette filters, solvent recovery, cooker hoods and catalytic supports. Recently, activated carbon also found increased application in the field of hydrometallurgy, particularly in the recovery of gold, silver and; to a lesser extent , molybdenum (Cheremisinoff and Ellesbusch, 1978).

The ability of activated carbon to adsorb gold from chloride solutions was first reported in 1847 (Streat and Naden, 1987). This information attracted considerable interest and, in 1880, Davis patented a process in which wood charcoal was used to recover gold from chloride leach liquors ( Adamson, 1972).This process has subsequently been popular, particularly in Australia.

Shortly after the discovery by Mac Arthur and the Forrest brothers in 1890 that cyanide was a good solvent for gold, in 1894 Johnson patented the use of wood charcoal for the recovery of gold from cyanide solutions (Mc Dougall, 1991). Since then, major developments have occurred in the technology relating to the manufacture of activated carbons, which are currently employed commercially in a wide range of industries. But, fundamental explanations and theories to fit the facts are still being evolved.

In recent years, many hydrometallurgical processes have been proposed for the recovery of gold (that is dissolved from the gold bearing ores under the attack of cyanide solutions) from solutions and pulps in which granular or powdered activated carbon is used as an adsorbent for the gold (Davidson et al., 1979; Laxen et al., 1979; Nicol, 1979; Mc Dougall et al., 1980 and Laxen, 1984). Undoubtedly, that which enjoys the greatest prominence at present is the carbon-in-pulp (CIP) process.In this, carbon granules are added directly to the cyanide pulp and moved counter-current to it. The gold loaded carbon is latter recovered by screening and then sent to the elution columns using a caustic cyanide at elevated temperatures to strip the gold off the carbon. Gold is recovered from the eluate by either electrowinning or zinc precipitation (Simmons et al., 1985).

Activated carbon can be manufactured from any carbonaceous raw material under the carefully controlled processes of carbonization and activation (Mc Dougall, 1991). However, active carbons with adequate adsorptive power, strengh, chemical purity etc. can be produced, in commercial practice concerning the low production cost, from peat, coal, lignite, wood and agricultural byproducts such as coconut shells, almond shells, hazelnut shells, peach and apricot stones etc. In hydrometallurgical studies to recover gold and silver, mostly, activated carbons of vegetable origin are preferred since they largely meet the metallurgical requirements.

Charcoal, the product of simple carbonization of the starting material with exclusion of air without the addition of any chemical reagents is usually an inactive material with a specific surface area 2-4 m2/g (essentially the

external surface area) and has low adsorptive capacity. Carbon having finely crystalline form with extended internal surface area and permeated by greatest number of randomly distributed pores of various shapes and size, hence high adsorptive power, can be prepared by activating the carbonized products with reactive gases such as $CO_2$, $O_2$, and steam etc. The majority of activated carbon used throughout the world is produced by steam activation. In this process, the carbonized product is reacted with steam over 700 °C. Another procedure used in the production of activated carbon involves the use of chemical activating agents such as $ZnCl_2$ , $H_3PO_4$ and salts of sodium and potassium etc. These chemicals act as dehydration agents and they may restrict the formation of tar during carbonization (Smisek and Cerny,1970).

Although the activation procedure and the after-treatment employed mainly determine the chemical nature of the surface oxides and the surface area of the resultant product, the structure of the pores and the pore-size distribution are largely predetermined by the nature of the starting materials. This is apparent from photomicrographs of the pore structure of activated carbon which indicate that the structure of original source material (cellular structure in the case of coconut, peach stones etc.) is still present in the carbon skeleton of the final product (Mc Dougall and Handcock,1980 and 1981). Therefore, the inherent cellular structure (extremely microporous) of raw materials of vegetable origin imposes a constraint on the degree to which the properties of the product can be be modified for special applications. It is this property that makes carbon from vegetable origin, eg., coconut shells suitable for gas-phase , solvent recovery processes and for the recovery of small gold-dicyanoaurite complex in carbon-in-pulp (CIP) and carbon-in-leach (CIL) processes. However, active carbons of vegetable origin generally fare poorly in applications involving the treatment of industrial effluents because the molecules that have to be adsorbed are often too large to penetrate into the microporous carbon matrix , and are therefore adsorbed less efficiently.

Although the source material of activated carbon mainly predetermines the structural properties and hence, fields of applications, process routes chosen to produce active carbon also characterize the final product. For instance, activated carbon produced by incorporating chemical agents before carbonization are generally characterized by macroporous pore size distribution and are mainly used in applications that require the removal of large molecular from solution e.g., in the decolorization of sugar syrups. These carbons do not show semi-conductor properties due to the lack of the graphitic zones under low temperature used in the production. However, activated carbons produced by steam show semi-conductor/redox properties since high temperature. production entails the creation of graphitic zones in the structure. The reduction potential of these carbons has been measured by a graphite-rod technique and found to be about -0.14 volts versus the saturated calomel electrode, at a pH of 6. Therefore, these carbons can function as reducing agents (Mc Dougall, Lecture Notes).

The aim of this study was to evaluate hazelnut shells, peach and apricot stones as alternative raw materials to coconut shells for the production of activated carbons for usage in the gold metallurgy. Ready and abundant availability of these raw materials in Türkiye makes them attractive source of activated carbons that will be demanded by the gold industry emerging with 12 tons expected gold production capacity in next 5 years. These raw materials despite having very high volatile content and hence, giving low yields in active carbon production , are so inexpensive that the economics involved in their use is favorable (....., 1994).

Since it was intended to produce activated carbons from these raw materials as an alternative raw materials to coconut shells, a comparative approach was followed. The first target was to produce an activated carbon from these raw materials with as much mechanical strength and well developed pore structure associated with high surface area as that from coconut shells. Then, the adsorption characteristics of these carbons were determined.

# CHAPTER II

# LITERATURE REVIEW

## 2.1. Activated Carbon

Activated carbon is a generic term for a family of highly porous carbonaceous materials, none of which can be characterized by a structural formula or by a chemical analysis (Hassler, 1963 and 1974 and Smisek and Cerny, 1970). The elemental composition of activated carbon typically comprises 87 % C, 0.5 % H, 0.5 % N, 1 % S and 5 % O, the balance of 6 % representing inorganic (ash) constituents (Mc Dougall, Lecture Notes). The volume of the pores in activated carbons is generally defined as being greater than 0.2 ml/g, and the internal surface area is generally larger than 400 $m^2/g$ as measured by Nitrogen BET method. The width of pores varies from 3 A° to several thousand angstroms, and the pores are generally classified for convenience in terms of their diameters (Bailey, 1986 and Mc Dougall, 1991):

| | |
|---|---|
| Macropores | 500 to 20.000 A ° |
| Transitional pores (meso pores) | 100 to 500 A ° |
| Micropores | 8 to 100 A ° |

The pores are observed, in cross - section, to be cylindrical or rectangular in shape, but can also appear in a variety of irregular shapes.

Macropores which generally contribute very little to the total internal surface area of the product, depend mainly on the nature of the carbonaceous raw material

employed and the preliminary manufacturing process, viz. grinding and agglomeration of the raw material. Their major function is to serve as transport arteries that make the internal parts of the carbon granules readily accessible to the molecules being adsorbed.

The transitional pores account for about 5 per cent, and the micropores for about 95 per cent of the internal surface area. The micropores are largely the product of activation process(Mc Dougall, 1991).

Activated carbons are commercially available in numerous forms; powders, granular chips in various size ranges and shaped or molded products extruded into rod-like shapes, which are commonly 0.8 to 6 mm in diameter by 3 to 10 mm in length, and available at different prices e.g. 2.250 $ mt (-25 %) for granular coconut and 3.505 $ mt for norit peat-based active carbons which are commonly used in gold metallurgy (Norit Carbon Brochure; Gold Recovery with Norit Activated Carbon).

### 2.1.1. Physical Structure

Carbonization and activation processes that will be detailed in latter sections produce active carbons with extended internal surface area and well developed pore system. The basic structural character of thermally activated carbon (steam activated) is closely approximated by the structure of pure graphite (Hassler, 1963; Mantell, 1968; Bokris, 1969; and Mc Dougall 1991).

Ideal graphite as shown in Figure 1, consists of layers of fused hexagons held approximately 3.35 A ° apart by Van der Waals forces, so that the carbon atoms in any one plane lie above the centers of the hexagons in the layer immediately below it. The lattice is of the A B A B type.

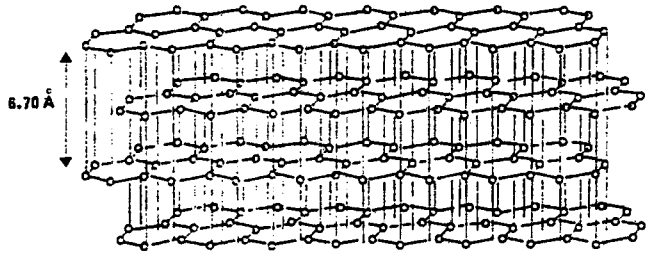


**Figure 1. Schematic representation of the structure of graphite; the circles denote the positions of carbon atoms, while the horizontal lines represent carbon-to-carbon bonds (after Bocris, 1969 )**

The structure of thermally activated carbon differs somewhat from that of graphite as shown in Figure 2. The carbon is believed to be composed of tiny graphite - like platelets (microcrystalline regions of order that have graphite-like structure), only a few carbon atoms thick and 20 to 100 A ° in diameter, which form the walls of open cavities of molecular dimensions, i.e. the pore system. However, the hexagonal carbon rings many of which have undergone cleavage are randomly oriented, and lack the directional relationship with one another that is present in single graphite crystals. The overall structure is therefore very disordered, and is often referred to as "turbostratic" (Mc Dougall, 1991). Furthermore, the separation between the layers is greater than found in graphite, 3.60 A °.

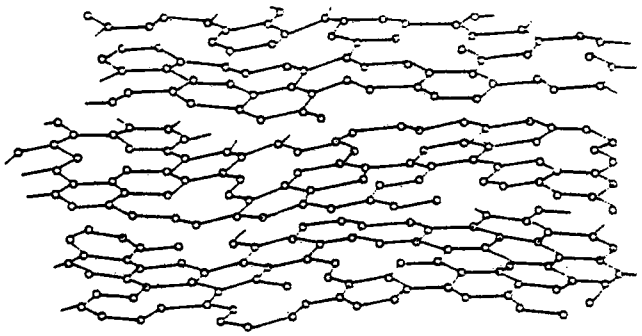

**Figure 2. Schematic representation of the proposed structure of activated carbon;oxygen-containing functional groups are located at the edges of broken graphitic ring systems ( after Bocris, 1969 )**

### 2.1.2. Chemical Structure

Activated carbon can be classified into two broad categories as H and L-type carbons (Hassler, 1963 and Faust and Aly, 1983). The former, H-type, is formed at temperatures exceeding 700 ° C (generally 1.000 ° C) and is characterized by taking up acid on immersion in water. Commercial active carbon used in gold recovery processes can also be classified as H-type due to the high temperature production, > 700 ° C (Garten and Weiss, 1957 and Mc Dougall, 1991). The latter, L-type, is formed at temperatures well below 700 ° C (generally around 300 to 400 ° C) and is characterized by taking up base on immersion in water. It is found that two properties of them are completely inter convertible (Snoeyink and Weber, 1967 and Weber, 1972). Heating the H-type active carbon at low temperatures will produce an L-type active carbon. Another interesting important aspect in the production of both types is that oxygen is irreversibly adsorbed by the carbons on exposure and only comes off again at high temperatures as CO and $CO_2$ which shows the chemical bound of it to the surface as all-important surface oxides of the carbon .

Eventhough the surface oxides are found to play an important role in the chemical nature of the carbon, at the moment, by no means their identification can be well established. This can be attributed to the respective temperatures at which the gases are evolved upon out-gassing samples of carbon under vacuum which correspond with the temperature ranges involved in the production of H and L- type carbons (Mc Dougall, 1980). It is proposed that the surface oxides evolved as $CO_2$ at lower temperature are responsible for the physico-chemical behavior of L-carbons and those evolved as CO at higher temperatures are responsible for H-carbon behavior (Puri, 1962 and 1966 and Mc Dougall, 1980). Most often suggested groups identified by Internal-Reflection Infrared Spectroscopy (IRS), Electronspin Resonance and Nuclear Magnetic Resonance (NMR) techniques are given in Figure 3 (Mattson and Mark, 1971). It is remarked after this sophisticated technical studies that the low-temperature oxides appear to be carboxylate in nature, whereas those formed at higher temperatures, as in carbon recovery processes, appear to be phenolic or some derivative of this group, such as

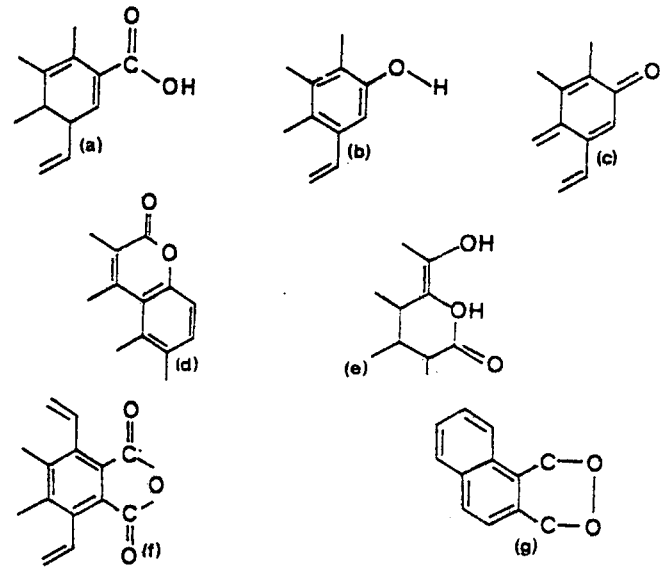

**Figure 3. Structure of some surface oxides ; (a) carboxylic acid (b) phenolic hydroxyl (c) quino-type carbonyl groups (d) normal lactone (e) fluorescein-type lactones (f) carboxylic acid anhydres (g) cyclic peroxides( Mc Dougall, 1991).**

lactones. The importance of these groups probably lies in their ability to alter the hydrophobic versus hydrophilic properties of the carbon surface.

### 2.1.3. Characterization

Activated carbons produced from many different kinds of raw material under various conditions can be distinguished from one another only by reference to certain physical and chemical properties. Among the most important properties, the number and size distribution of the pores, bulk density, dry impact hardness, wet abrasion resistance and particle size distribution can be cited ( Mc Dougall, Lecture Notes).

As far as the chemicals are concerned, different active carbons are compared on the basis of their ability to adsorb various selected substances from the gaseous phase; benzene, $CCl_4$ and $N_2$, as well as from the aqueous phase; iodine, molasses, phenol, methylene blue and tannin (Hassler, 1974).

The Nitrogen BET value expresses the surface area in square meters per gram of active carbon that can be covered by nitrogen in a monomolecular layer. Activated carbons typically have surface area of 400 to 1.500 $m^2/g$, the former and the latter values show that of low activity and high activity carbons respectively.

However, surface area dimensions of active carbons are, alone, insufficient to characterize the carbon product because the nitrogen molecule is very small (surface area: 16.2 $(A^o)^2$ / molecule) and can ,therefore, penetrate into pores that are not accessible to other larger molecules.

The degree of adsorption of selected molecules by the carbon gives an indication of the distribution of the internal accessible volume among the pores of different size. Hence, the small iodine molecule is adsorbed in pores down to 10 A ° in diameter so that the iodine number is an indication of the surface area of the pores in that size range. On the other hand, molasses, a large polysaccharide molecule, is adsorbed only in pores larger than about 30 A° in diameter, indicating the number of pores in that size range (Mc Dougall, 1991).

In order to characterize the active carbons of coconut origin that is most commonly employed in gold industry, some important physical and chemical properties are tabulated in Table 1 ( Mc Dougall, 1991 ). Typical values in the table show high

**Table 1. Physical properties and chemical adsorption characteristics of a thermally activated coconut shell carbons typical of those employed in gold recovery processes (Mc Dougall, 1991)**

| | | |
|---|---|---|
| **1.** | **Physical Properties** | |
| | Particle Density | 0.80-0.85 g/ml |
| | Apparent Density | 0.48-0.54 g/ml |
| | Pore Volume | 0.70-0.80 ml/g |
| | Hardness | 97-99 |
| | Particle Size | 1.18-2.36 mm |
| | Ash | 2-4 % |
| | Moisture | 1-4 % |
| **2.** | **Chemical Characteristics** | |
| | Surface Area ($N_2$, BET) | 1,050-1,200 $m^2/g$ |
| | Iodine Number | 1,000-1,150 $m^2/g$ |
| | $CCL_4$ Number | 60-70 % |
| | K - Value | 32 mg. Au/g |
| | R - Value | 0.075 |

activity coconut shell carbon which is activated thermally using steam and which is commonly employed in gas-phase applications and in processes for recovery of gold from cyanide leach liquors.

## 2.2. Manufacture of Activated Carbon

Active carbon can be manufactured by the carbonization and activation of carbonaceous materials, almost exclusively of vegetable origin, such as wood, coal, peat, coconut shells, fruit stones and shells. Charcoal, the product of simple carbonization, that is the pyrolysis of the starting material with the exclusion of air and without the addition of chemical agents, is practically an inactive material with surface area, essentially external, of the order of several $m^2$ /g, that is insignificant when compared to that of granular activated carbon, typically 1.000 $m^2$/g. A carbon to be used in gold metallurgy with a highly developed porosity and therefore extended internal surface area can only be obtained by activating the carbonized material with steam, $O_2$ or $CO_2$ at temperatures from 700 to 1.000 ° C (Smisek and Cerny, 1970).

During carbonization most of the non-carbon elements, $H_2$ and $O_2$ are first removed in gaseous form by pyrolytic decomposition of the starting material and the freed atoms of elementary carbons are grouped into organized crystallographic formation known as microcrystallites. The mutual arrangement of the crystallites is irregular so that free interstices remain between them and apparently, as a result of deposition and decomposition of tar ( a by product from source material) and disorganized amorphous carbon these become filled or at least blocked (Agrawal et al., 1983 and Agrawal, 1988).The resulting product, charcoal, has a very small adsorption capacity. A carbon with a large adsorption capacity, then, can be produced by activating the carbonized product with steam, $O_2$ or $CO_2$. Activation takes place in two stages (Smisek and Cerny, 1970). In the initial stage, disorganized carbon is burnt out preferentially, and the closed and clogged pores between the crystallites are freed. In the second stage, however, carbon of the crystallites is burnt and high level structural disordering in activated carbon leads, at the broken edges, many reaction with activating agents, so that the surface is composed of oxygen - containing functional groups (Section 2.1.2)( Matson and Mark, 1971).

Active carbon can also be prepared by another process.This process involves the use of activating agents such as $ZnCL_2$, $H3PO_4$ and salts of sodium and potassium etc. These chemicals act as dehydrating agents and may restrict the formation of tar during carbonization. However, the final product has lower adsorption capacity due to the presence of residual chemicals that block the entries of pores. (Smisek and Cerny, 1970 and Hassler, 1974).

### 2.2.1. Chemical Manufacturing

Chemical activation, a wet single stage process, is employed for carbons produced from materials of recent origin of cellulosic materials such as wood. The activating agents used influence the pyrolytic processes so that the formation of tar is restricted to minimum and the amount of the aqueous phase in the distillate (acetic acid, methanol etc.) is also less than in normal carbonization. The yield of carbon in the carbonized product is increased accordingly. Furthermore, a respectively lower temperature is needed for pyrolysis in the process. The most widely used activating agents are zinc chloride, phosphoric acid, sulfuric acid, sodium carbonate, sodium, calcium and potassium hydroxide and chloride salts of magnesium etc. (Bevla et al., 1984; Richard, 1988 and Laine et al., 1989).

The process involves mixing the raw material and chemical agent which dehydrates the structure into paste which was then dried and carbonized at between 200 °C to 600 ° C. The impregnated chemicals dehydrate the raw material, resulting in charring and aromatization of the carbon skeleton, with the concomitant creation of a porous structure and extended surface area (Mc Doughall, 1991). The process generally yields a product with lower adsorption capacity due of the blockage of the opened pores by residual chemicals. If a granular product is desired, after the impregnation of chemical with granular raw material, simple carbonization without air is employed. However, this granular active carbon is unfortunately soft unless they are manufactured from the powder after suitable pelletization or extrusion with a appropriate coking binder such as coal tar pitch (Mc Dougall, 1991).

After the carbonization, the activating agents are usually recovered and recycled for economic reasons. However, it should be taken into consideration before final decision of employment that all the commonly used chemicals impose several constraints mainly on the overall activation process, the equipment employed and on the quality and field of application of product.

### 2.2.2. Thermal Manufacturing

Thermal manufacturing of activated carbon constitutes two stages. The first step is carbonization followed by activation of carbonized product with suitable oxidizing agents such as steam, $O_2$ and $CO_2$.

Carbonization is essentially accomplished by heating of the source material in an inert atmosphere such as flue gas to a temperature that must not exceed 700 ° C to control effectively the dehydration and devolatization of many of the carbon atoms. On heating the lignocellulasic materials, typical of vegetable origin in a nonreactive atmosphere, they decompose to various pyrolysis products. Depending on their volatility, these products can be grouped into three classes; charcoal, gases and tars (Hassler, 1963 and 1974; Browning, 1963; Smisek and Cerny, 1970; Mc Dougall, 1980 and 1991 and Agrawal, 1988). Char is a carbon rich nonvolatile solid residue, usually constituting approximately 15-20 percent yield. Gas phase products include all lower molecular weight products (CO, $CO_2$, $CH_4$, $H_2$ etc.) including water. Usually, gas phase products are constituting 20-25 percent of the total products of pyrolysis. Tars are any of several high molecular weight products that are volative at carbonization temperature but readily condense into any surface near room temperature. Tars are comprising approximately 60-65 percent of the products.

The main purpose of carbonization in practical aspect is to reduce the volatile content of the source material in order to convert it to a suitable form for activation. After carbonization, carbon content of product should reach to 80 per cent (higher values are desirable) and carbon atoms rearranges into graphite - like structure.

Carbonized product consequently is activated to have the pores developed and surface area extended internally at temperatures between 700-1,000 ° C in the presence of a suitable oxidizing agents such as steam, air and $CO_2$. The active oxygen in the activating agent burns away the more reactive components of the carbon skeleton as CO and $CO_2$, depending on the oxidizing agent employed.

The basic reactions of carbon with steam and $CO_2$ are endothermic whereas the reaction involved in air activation is exothermic. The stoichiometric equations can be written for steam and $CO_2$ in the form:

$$C + H_2O \rightarrow CO + H_2 \quad (\Delta H = 29 \text{ kcal}) \qquad (2.1)$$

$$C + CO_2 \rightarrow 2CO \quad (\Delta H = 39 \text{ kcal}) \qquad (2.2)$$

This reaction of steam with carbon is accompanied by the secondary reaction of watergas formation which is catalyzed by the carbon surface as:

$$CO + H_2O \rightarrow CO_2 + H_2 \ (\Delta H = -10\text{kcal}) \qquad (2.3)$$

The reaction of carbon with air (oxygen) is however exothermic and can be written as:

$$C + O_2 \rightarrow CO_2 \quad (\Delta H = -97 \text{ kcal}) \qquad (2.4)$$

and since this reaction is difficult to control, excessive burn-off of the external carbon surface can easily occur which reduces the yield of final product.

As a consequent of reactions mentioned, combustion proceeds for all the cases which results in the development of a large internal surface area and creation of pore structure by preferential etching. The art in the manufacture of activated carbon lies in conducting the activation process in such a way that combustion of the carbonized product proceeds internally and not from the exterior of the granules.

### 2.2.3. Characteristics of Physically and Chemically Produced Activated Carbons

Chemically and thermally activated carbons differ from each other in their pore size distribution and semiconductor properties. Figure 4 represents that chemically activated carbons are characterized by a macroporous pore-size distribution. Therefore, they had high molasses number and comparatively low iodine number

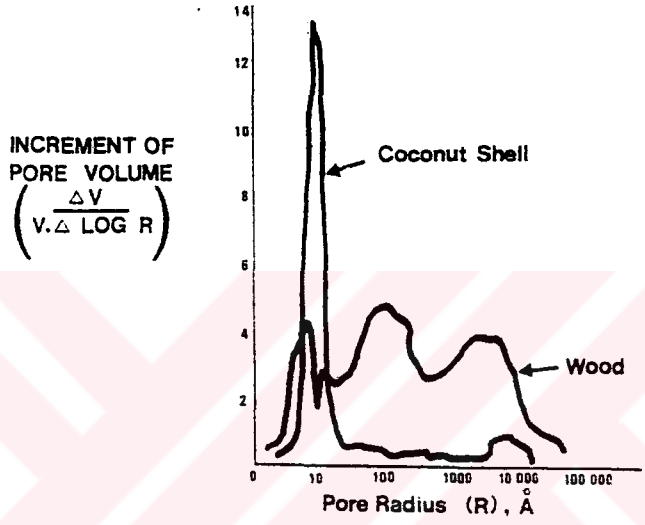


**Figure 4. Pore-size distribution in typical thermally activated coconut-shell carbon and chemically activated wood carbon ( Fornwalt et al., 1963)**

and low nitrogen BET surface area (Fornwalt et al., 1963 and Mc Dougall, 1991). This type activated carbons are used mainly in applications that require the removal of large molecules from solutions, e.g. in the decolorization of sugar syrups. The absence of semi conductor properties in chemically activated carbons almost certainly relates to the fact that the temperature generally employed in the manufacture is too low for creation of graphitic zones in the final product. It is generally accepted that the graphitic zones in the product responsible for the semi-conductor redox properties of thermally activated carbons.

The reduction potential of thermally activated carbons, measured by a graphite-rod technique, has been found to be typically above -014 V versus the saturated calomel electrode at a pH value of 6 (Mc Dougall et al., 1980). Therefore, these carbons can function as reducing agents, and many properties of thermally activated carbons, particularly their redox and catalytic properties, are believed to be related to their semi conductor properties.

Chemically activated carbons have found to be poor in affinity for the adsorption of aurocyanide complex and this finding is attributed to the absence of graphitic zones that are believed to be present in thermally activated carbons ( Adams et al., 1987). Therefore, high adsorptive power for the small aurocyanide complex of thermally activated carbons makes them ideal for applications involving gold recovery processes particularly, in carbon in pulp (CIP) and carbon - in -leach (CIL)

.

## 2.3. Raw Materials

Activated carbon can be obtained from;

a) Coal of various rank (peat, lignite, bituminous coal and anthracite),

b) Fruit stones and shells (coconut shells, nutshells, and olive, peach and apricot stones),

c) Others such as wood, waste tyres, sawdust, cellulose, rice husks, corn cobs, sugar, bones etc (Smisek and Cerny, 1970 and Mattson and Mark, 1971 ).

All the raw materials used in relatively large scale manufacture should be readily available in large quantities to reasonably price the product. Table 2 shows approximate carbon content ( an indication of the yield of final product ) in the

**Table 2. Carbon content of raw materials commonly employed in the manufacture of activated carbon (Mc Dougall, 1991).**

| Material | App. Carbon Content, % |
|---|---|
| Wood, shells and stones | 40 |
| Lignite | 60 |
| Bituminous coal | 75 |
| Anthracite | 90 |

starting material. In the manufacturing, volatile matters are driven off the product. Therefore, an economic relationship should be made between the volatile content of the raw material and the price, availability and quality. In the developing world, trends are towards the manufacture of active carbon from waste materials such as coconut shell and fruit stones. Because, eventhough their high volatile content (Table 2), they are so in expensive that the economics involved in their use are often favorable.

## 2.4. Selection of Activated Carbon For Gold Recovery Processes

Gold adsorption processes require an activated carbon with the capability to adsorb gold which will be released easily in latter process steps. To be suitable for use in gold recovery processes an activated carbon must therefore have :

a) High adsorption capacity,
b) High adsorption rate and
c) High hardness (Faulkner, 1984; Mc Dougall and Fleming, 1987; Calgon Carbon Brochure and Norit Carbon Brochure).

The adsorption capacity which depends on the carbon raw material is generally expressed by the Freundlich constant, K (Gold loading of milled granular carbon in equilibrium with 1 mg/l gold in a standard buffered pH 10 solution) in equation (2.5). (Calgon Test Method 53; Urbenic, Jula and Faulkner, 1985 and Shipman, 1991).

$$x / m = K.C_s^{1/n} \qquad (2.5)$$

Where,

**x** is the mass of the adsorbate

**m** is the mass of the adsorbent

$C_s$ is the equilibrium concentration of solute in the solution

**K** and **n** are constants.

In practice, only a small fraction of the total adsorption capacity of carbons for gold is utilized. It has been shown that in laboratory, gold loading levels as high as 45 mg Au/g of carbon can be achieved whereas the loading of gold on carbon in the first stage of a CIP plant seldom exceeds 10 mg.Au/g of carbon (Faulkner, 1984). Therefore, carbons with gold loading capacities higher than this point are believed to strip most of the gold in solution when sufficient mixing is provided.

The plant performance, design of adsorption tanks and throughput of CIP and to some extent CIL plants mainly depend on the adsorption rate of the carbon (Bailey, 1986 and Shipman, 1991). Activation degree of the carbon, its particle size, agitation efficiency in the adsorption tanks, the viscosity and the pulp density of slurry have bearing effects on adsorption rate and hence on plant performance. Furthermore, low soluble gold losses, in large part, is generally associated with low adsorption rate. Rapid adsorption minimizes soluble loss at low concentration of carbon in the pulp, which in turn can lead to increased gold loading on carbon withdrawn from the circuit. The R-value (Calgon Test Method 1983; Urbanic et al., 1985 and Calgon Carbon Brochure) is a measure of the rate of gold adsorption and determined by exposing a specific particle size granular activated carbon to 5 ppm borate buffered KAu (CN )2 solution. The data obtained are fitted to an equations that yields a straight line in normal cases as illustrated by equation (2.6);

$$t / x / m = (1 / m).t + 1 / R \qquad (2.6)$$

Where;

**t** is time

**x/m** is carbon loading

**m** is the reciprocal of the slope

**R** is the reciprocal of the intercept

The R- value for each carbon under consideration is relative i.e., higher R values indicate faster adsorption under the existing conditions. So, a relative comparison

can be made between the R-value of commercially used coconut carbon, which is typical 0.075 and that of one intended to be used.

The high hardness of the carbon particles insures that the carbon attrition is minimized during agitation and transport within the system. This will further reduce the possibility of gold being lost on under sized carbon particles. The ball-pan hardness test or Ro-tap abrasion test is generally used to measure the hardness number of carbon. This method measures the percentage retention of original average particle size by the resistance of the particles to the action of steel balls. Coconut carbons best suit to the gold recovery processes with their structural firmness that makes the particles resist to highly agitative plant conditions. These carbons have 97-99 hardness number as reported by the worlds leading manufacturers (Calgon Carbon Brochure).

These above mentioned properties enable gold processor to obtain the highest possible yields from ores. Thus, low level of capital investment and energy requirements are also realized.

### 2.1.7. Mechanism of Gold Adsorption by Activated Carbon

It is generally conceded that carbon owes its adsorptive properties primarily to its large internal surface area, as well as its large pore-size distribution, and that the external surface area and the nature of the surface oxides play minor roles (Mattson and Mark, 1971 and Cheremisinoff and Ellerbusch, 1978 ).The size of the pores developed during activation therefore has an important influence on adsorption behavior because the pores act as a screen. This screen prevents the adsorption of large molecules, but promotes the adsorption of an adsorbate that fits snugly into the pores, making the maximum number of contacts with the adsorbed molecule, and thus maximizing $\Delta H$ as defined in equation (2.7):

$$\Delta H = \Delta G + T\Delta S \qquad (2.7)$$

where

$\Delta H$ is the change in free enthalpy,

$\Delta G$ is the change in free energy,

$\Delta S$ is the change in entropy, and

$T$ is the temperature of the system.

The external surface can provide only a certain amount of access to the inner pores, and it is likely that the main role of the surface oxides is to impart a hydrophilic character to the predominantly hydrophobic carbon skeleton. This would account for the affinity of activated carbon for many polar and non-polar organic and inorganic species(Mc Dougall and Hancock, 1980).

Activated carbon functions by adsorption, i.e. by the adhesion of certain substances to the internal surface constituting the walls of the pores. Hence, the greater the adsorption surface available, the better is the adsorption function.

Adsorption occurs as the result of an imbalance of the forces that act upon the carbon atoms constituting the surface of the pore wall. Such an imbalance is inherent in all surface and, in an attempt to rectify it, molecules are adsorbed from the gaseous or aqueous phase, and are attracted and held to the surface. Surface adsorption , regardless of the energy of the interaction, must always proceed with a negative change in free energy($\Delta G$), as well as a decrease in entropy ($\Delta S$), which according to equation (2.7), must result in a negative change in free enthalpy ($\Delta H$). Hence, adsorption is always an exothermic process.

There are two types of adsorption process: physical and chemical adsorption. Physical adsorption involves weak Van der Waals forces (also dipole-dipole interactions and hydrogen bonding), and the processes are generally reversible. Chemical adsorption refers to processes involving homopolar forces ( as in ionic or covalent bonds), and such processes are generally reversible. Nevertheless, in most instances, the adsorption can be classified as being physical in nature.

In general, the factors that influence the adsorptive behavior of activated carbon from aqueous solution are temperature ( adsorption generally decreases with increasing temperature); the pH value of the solution ( carbon generally has a low affinity for ions, particularly those with a high charge-to-surface ratio, and pH can

affect ionicity); the chemical nature of the species present and their relative concentration ; and the nature of the activated carbon and its particle size distribution. For molecules to be adsorbed, they must reach the internal surface of the macropores by diffusion. Therefore, the reaction time will be influenced by the length of the diffusion path, and the kinetics of adsorption will increase with decreasing particle size.

Activated carbon is a very versatile substrate with respect to its interactions with various organic and inorganic compounds. It is able to function as a simple adsorbent that is akin to synthetic polymeric adsorbents, since molecular compounds can be physically adsorbed onto its large internal surface area, and be retained there by forces of the Van der Waals type (Mc Dougall,1991). It can also function as reducing agent or, in the presence of excess oxygen , as an oxidation catalyst (Mattson and Mark, 1971 and Hassler, 1974). As a result, the adsorption of organic and inorganic species onto carbon may occur by several mechanisms, and their identification, particularly in the extraction of certain metal complexes from solution, is extremely difficult (Mc Dougall et al., 1980 and Mc Dougall, 1981).

The adsorption of organic species onto carbon usually occurs by simple mechanisms that are fairly well understood in terms of a balance between hydrogen bonding forces in solution and Van der Waals attraction between the carbon surface and the organic compounds. The driving force for the adsorption of organic molecules onto carbon is similar to that responsible for the salting out of organic materials dissolved in water, where the addition of a simple inorganic salt causes the organic material to separate out from the aqueous phase.

These considerations have given rise to the statement frequently made that adsorption onto activated carbon is a fight against solubility. Applications involving organic materials will therefore be most attractive when the adsorbate has high molecular mass, low polarity, and a low degree of ionization, because these properties generally signify low aqueous solubility. Hence, activated carbons are excellent adsorbents for a considerable number of aliphatic compounds, and particularly for aromatic compounds like those commonly found in pesticides and herbicides.

The simplest mode of adsorption of inorganic compounds onto activated carbon is by reduction mechanisms. This mechanism is operative in the adsorption gold from chloride medium and silver from nitrate solutions. Although gold forms a large number of complexes with various ligands, e.g. thourea (gold 1), thiocyanate (gold I), cyanide (gold I), chloride (gold III ) and thiosulphate (gold I), among others, the interaction between activated carbon and the chloride and cyanide complexes of gold have received almost exclusive attention in the literature (Mc Dougall and Fleming; 1987), probably because of their significance in the hydrometallurgical recovery of gold.

The ability of activated carbon to adsorb various gold complexes follows the sequence (Mc Dougall; Lecture Notes)

$$AuCl_4^- > Au(CN)_2^- > Au(SCN)_2^- > Au(CS(NH_2)_2)_2^+ > Au(S_2O_3)_2^{3-}$$

The standard reduction potentials for these gold complexes to metal from a solution containing gold at $10^{-5}$ M are 0.11 V (versus SCE) for Thiourea, 0.47 V (versus SCE) for Thiocyanite, -0.21 V (versus SCE) for Thiosulphate, 0.76 V (versus SCE) for Chloride and -0.79 V (versus SCE) for Cyanide (Mc Dougall et al., 1980). Carbons prepared by the high-temperature thermal route are characterized by a reduction potential of -0.14 V (versus SCE). Therefore, carbon would reduce the gold chloride and the gold thiocyanate complexes to metallic state on carbon surface, but not the gold thiosulphate complex. The gold thiourea complex is a borderline case and should be reduced to the metal by carbon except at very high thourea concentration. The mechanism by which activated carbon loads gold cyanide, $Au(CN)_2^-$, has interested and puzzled researchers since 1913, and despite the commercial importance of the process, no consensus has been reached as yet regarding the mechanism by which gold cyanide is adsorbed onto activated carbon (Davidson, 1974; Tsuchida et al., 1984; Adams and Fleming, 1989; Adams, 1990; Adams et al., 1992 and Ibrado and Fuerstenau, 1992). To a large extent, the difference in opinion can be ascribed to the fact that activated carbon is not readily amenable to direct investigation by techniques such as Infrared or Ultraviolet (UV) - Visible Spectrophotometry.

The mechanisms of gold cyanide adsorption from cyanide solutions, proposed over the years, can be summarized as following:

a) Reduction of $Au(CN)_2$ to gold metal ,
b) Adsorption of $Ca(Au(CN)_2)_2$ ion-pairs,
c) The initial adsorption of ion-pairs followed by a partial reduction step to $Au(CN)_x$ or cluster-type species.
d) The initial adsorption of ion-pairs followed by an oxidation step in which $Au(CN)_2$ is degraded to AuCN and
e) The latest mechanism appeared in technical report by Hans. E. Van Dam (1993) that the adsorption is chemical reaction rather than physical adsorption.

In spite of all these proposed mechanisms there is very little agreement over whether carbon acts as a reductant or an oxidant and what role air or oxygen plays in the process. However, Mc. Dougall and Hancock (1981) and Mc. Dougall and Fleming (1987) critically reviewed the literature about the subject and concluded that the most likely mechanism of gold loading under typical CIP operating conditions involves the adsorption of aurocyanide without chemical change. Moreover, they suggested that adsorption probably occurred by a mechanism firstly proposed by Kuzminyk and Tyurin (1986), which involved the extraction of ion-pairs of the type $M^{+n}(Au(CN)^-_2)_n$, where $M^+ = Na^+, K^+, Ca^{+2}, Mg^{+2}$, etc., at high pH values, and where $M^+ = H^+$ in acidic solution. They suggested that the loading of $M^{+n}(Au(CN)_2)_n$ onto activated carbon will probably be by adsorption on the large internal surface of the carbon or precipitation of the complex in the pores, with $M^{+n}$ derived from the solution or from the ash content of the carbon, which is accompanied by chemical degradation of the $Au(CN)_2^-$ anions to insoluble AuCN (that is retained in the pores of the carbon). The last step in the mechanism proposed by Mc. Dougall and Hancock is partial reduction of the gold cyanide complex to some compound containing gold atoms in both the 0 and 1 formal oxidation states.

Further experiments carried out at the council for Mineral Technology (Mintek) yielded the results that support the ion-pair mechanism in adsorption of aurocyanide onto activated carbon ( Davidson, 1974).

However, the most recent findings appeared in a technical report by Hans. E. Van Dam (1993) demonstrate that the adsorption is a chemical reaction rather than physical adsorption. Hans. E. Van Dam reported that, during the adsorption by activated carbon, a third chemical bond is formed with gold cyanide existing as a linear complex in which the central gold atom is bonded to two cyanide groups. This bond thought to involve an electron from the activated carbon, that now spends part of its time on the gold atom. The gold atom accommodates this electron using an empty energy level, called the lowest Unoccupied Molecular Orbital. Strong bonding of gold cyanide, by this way, occurs when a part-time electron transfer from the carbon to the gold atom is energetically favorable. In that report, he explains this transfer from activated carbon by an electron available at a relatively high energy level. The highest energy level available is called the Highest Occupied Molecular Orbital. The height of this level depends on carbon structure. In activated carbons, most of the carbon atoms are located in small graphite-like structure ; the basal planes (see section 2.1.1). In a basal plane, each of the atoms contributes one electron to the common pi-electron system. The result is a large number of electrons, more or less spread out over the basal plane, having closely adjacent energy level. The energy at the top level depends on the size of basal planes. He also points that to insure overall electro neutrality positively charged counter-ions (cations), mainly $Ca^{+2}$, are co-adsorbed by carbon. But, the exact structure of the combination cation/gold complex is still unknown. The overall reaction is as follows;

$$2\,(Au\,(CN)_2)^- + Ca^{+2} + Carbon \rightarrow Ca\,(Carbon - Au\,(CN)_2)_2 \qquad (2.8)$$

Factors that affect the kinetics of gold adsorption are the hydrodynamic conditions in the adsorption stages, the particle size and pore size distribution of the carbon, the viscosity and density of the solution or pulp in contact with the carbon, and presence of species that can adsorb onto and poison carbon (Fleming and Nicol, 1984). Plant experience and laboratory investigations have shown that the initial

rate of adsorption of aurocyanide onto carbon is rapid and is controlled by the hydrodynamics in the adsorption contactor. This initial film-diffusion controlled reaction, which involves the adsorption in the macropores and mesopores, result in the establishment of a pseudo-equilibrium 4 to 48 hours. This point generally responds to the 50-70 % of the equilibrium gold adsorption capacity of carbon (Bailey, 1986). Subsequently. gold cyanide continues to be adsorbed onto the carbon almost indefinitely and, in practice, it is difficult to establish a true equilibrium. During this period of pore-diffusion controlled adsorption, gold cyanide diffuses slowly into the micropores of the carbon and as the cross sectional area of micropores approaches that of the aurocyanide ion, the resistance to mass transfer becomes infinite.

From a practical point of view, therefore, the interaction between aurocyanide and carbon can be considered to posses two thermodynamic regimes, the macropore-mesopore equilibrium and the total equiblirium. The pseudo-equilibrium apparently responds to its chemical environment, and is influenced by the thermodynamics of the adsorption reaction in much the same way as a true equilibrium would be. It is not a well defined entity, however, due to the unhomoginity of the pore size distribution from one carbon particle to another and from one batch of carbon to another.

It is apparent that the plant operating parameters should be set in such a way that the carbon loading is maintained within the macropore-mesopore equilibrium range.The rate of extraction is fast and responsible to good mixing efficiency in the contactors. Rate of elution and the ultimate efficiency of elution are also maximized.

# CHAPTER III

# MATERIALS AND METHODS

## 3.1. Materials

Hazelnut shells from Black Sea Region, apricot stones from Malatya and peach stones from Bursa were used throughout the study. The chemical analysis of raw materials are given in Table 3.

**Table 3. Proximate analysis of raw materials**

| | Fixed Carbon(%) | Volatile Matter(%) | Ash(%) | Moisture(%) |
|---|---|---|---|---|
| Hazelnut Shells | 22.8 | 62.0 | 1.2 | 14 |
| Apricot Stones | 25.8 | 63.8 | 0.4 | 10 |
| Peach Stones | 24.6 | 63.5 | 0.9 | 11 |

All the raw materials contained very high volatile matter and hence, had lower fixed carbon which consequently yielded less amount of product after carbonization. Hazelnut shells and stones after freed from their kernel were sized .

### 3.2 Experimental Method

Main parameters of carbonization such as reaction time, temperature and per-cent mass loss to yield chars (or charcoals) with required fixed carbon content, essentially higher than 80 % (Kostorava et al., 1976 and Ermakov et al., 1978), were determined by testing the hazelnut shells that was obtained in respectively larger quantities. All the tests were carried out in a stainless steel reactor in an oxygen free atmosphere obtained by nitrogen flushing.

At the first attempt, hazelnut shells were carbonized at a faster heating by simply exposing the reactor to the furnace temperatures between 500 °C and 700 °C. Fast carbonization was supposed to drive off the smoke quickly which is known as to contain high molecular weight tarry substances from the structure. Therefore, blockage of pores by deposition of these substances was minimized. Then, subsequent carbonization tests were carried out in order to investigate the influence of heating rate and high carbonization temperatures on the characteristics of final product. In these tests, slower heating was applied upto 650 °C using a controlled heating rate of 5 °C $min^{-1}$ while high carbonization temperature was applied by increasing the final temperature of carbonization to 900 °C and residing the reactor at this level for 1 hour.

The reactor in each case, after the carbonization completed, was allowed to cool down to room temperature under nitrogen flushing.

Following the determination of carbonization parameters for hazelnut shells, due to the same carbonaceous origin and hence, similarities in chemical structure (see Table 3), apricot and peach stones were subsequently carbonized by considering these pre-determined experimental parameters.

Charcoals obtained from all raw materials were finally crushed and sized to -7+35 mesh. This portion of size was then analyzed to determine physical properties and chemical characteristics charcoals under suitable ASTM testing condition (ASTM 1762-64, ASTM 2367-70; ASTM 2854-70; ASTM 3037-78 and ASTM 1991 ) and consequently used in the activation experiments.

Activation experiments were carried out in a stainless steel reactor under the flow of steam at a rate of 4 ml. $min^{-1}$ that was kept constant throughout the study. Activation temperatures between 700 °C-1000 °C were tested. In this way, a wide range of burn offs ( the term burn off is used to denote the degree of activation by mass loss of char in percentage ) have been obtained and carbon properties were examined.

Another type of activation, namely " Chemical Activation" was carried out with hazelnut shells using chemical agents such as KOH and ZnCl2 that were known to be most powerful dehydrators (Cerny, 1970; Gonzales et al.,1980 and Bevia, et al. 1984). The crushed raw materials were impregnated with a solution of different concentrations of these agents and dried overnight at 105 °C. Then, they were carbonized at 650 °C and cooled down to room temperature under the flow of nitrogen gas. Finally, charcoals obtained by this way were washed, by acid (dilute HCl) and then by hot water to remove impregnants from the surface.

Since the main aim of this study was to produce activated carbon from hazelnut shells, peach and apricot stones for gold metallurgy as an alternative to coconut shells, a comparative approach was followed in the activation. The first target was to produce an activated carbon from these materials with as much mechanical strength and surface area ($N_2$, BET) as that from coconut shells. Therefore, mechanical strength and surface area of active carbons were ,at first, determined by Hardgrove machine and Micromeritics surface analyzer, respectively. The detailed information about testing procedure for hardness and surface area of carbons are given in Appendix A and B. Then, adsorption characteristic; gold adsorption capacity and rate of gold adsorption of the best activated carbons were determined by Calgon Test Method 53 and Calgon Test Method 1983, respectively.

The gold adsorption capacity of a carbon depends on the carbon raw material and is generally expressed as the Freundlich constant, K, as illustrated in equation (2.5) (Urbanic et al., 1985).

It was experimentally obtained by determining the Freundlich isotherm by exposing the carbons, ground to less than 30 μm or 95% passing 325 mesh, to a 100 ppm gold concentration as K Au $(CN)_2$ in borate buffered solution at pH 10 (Calgon Test Method 53). The detailed procedure about testing is given in Appendix C. The K-value was then measured from the isotherm as the carbon gold capacity in mg Au $g^{-1}$ of carbon at 1 ppm residual gold concentration.

Rate of gold adsorption (hence, gold adsorption kinetics) was studied by obtaining R-values of the best carbons from gold adsorption data since this value is generally accepted as a measure of rate of gold adsorption (Urbanic et al., 1985). It was determined by Calgon Test Method 1983 as exposing the 1 gr. of a specific particle size fraction (-7+14 mesh) of the activated carbon sample to 1.7 L of a borate buffered 5-ppm K $Au(CN)_2$ solution at pH 10. The exposure took place in a glass reaction vessel. The reaction vessel was magnetically stirred at a rate that the particles were continually suspended in the solution. The gold concentration of the solution was measured periodically over an eight hour exposure by Atomic Absorption Spectrophotometer (AAS) at a wavelength at 242,8 nm. The experimental procedure for R-value determination is given in Appendix D. Data obtained were then fitted to the equation (2.6) that yields a straight line in normal cases. R-value was the reciprocal of the intercept at zero time when the time divided by loading on carbon was plotted against time.

The analysis of gold in cyanide solution by AAS formed one of the most important aspects of the rate and loading capacity tests since carbon loading were derived from a balance of the gold concentration in solution (Shipman, 1994). Therefore, gold concentrations in solution were measured directly by a AAS using background correction (Ludquist, 1940; Greaves,1963; Olson, 1965; Simmons, 1965; Tindall, 1965; Strelow et al., 1966; Gupta, 1977; Hall, 1979 and Mallett et al., Research Report No:24). Calibration graphs were obtained from the standard solution (borate buffered at pH 10) in the normal manner ( Weast, 1974) and the gold concentrations in the test solutions determined from these graphs. However, in some case, dilution of the test solutions before analysis became necessary not to ruin the calibration of the machine.

### 3.3. Reagents and Chemicals

All the reagents used were of analytical grade. A stock solution of the 1000 ppm $KAu(CN)_2$ in borate buffer at pH 10 was prepared by dissolving 1 gr. of pure gold metal (99,9%) in dilute KCN solution. The solution was, then, completed to 1L by borate buffer. Iodine solutions used in iodine number determinations were prepared in accordance with ASTM 1991 standards.

# CHAPTER IV

# RESULTS

## 4.1. Carbonization

### 4.1.1. Effect of Temperature on the Mass Loss Attained in Carbonization

Tests were carried out with hazelnut shells to investigate the effect of temperature on mass loss attained in carbonization. The results are plotted in Figure 5. As seen in the figure, the weight loss that corresponds to the carbonization temperatures from 500 °C to 700 °C were in the range of 31.9 - 72.2 % at 7 minutes, 61.8 - 73.4 at 13 minutes and 68.8 - 74.1 at 24 minutes, respectively. The maximum weight loss observed in the tests was 74.1 % at 700 °C carbonization for 24 minutes.

The weight loss increased sharply upto 650 °C with an increase in the carbonization time but very little change was observed thereafter.

### 4.1.2. Effect of Mass Loss in Carbonization on Fixed Carbon Content of Charcoals

Tests were carried out with hazelnut shell charcoals to examine the effect of weight loss on the fixed carbon content (hence degree of appropriateness to subsequent steam activation) of carbonized product. The results are plotted in Figure 6. As seen from the figure, the fixed carbon content of charcoals carbonized at 500 °C and 600 °C were sharply increased as the carbonization proceeded from 7 minutes

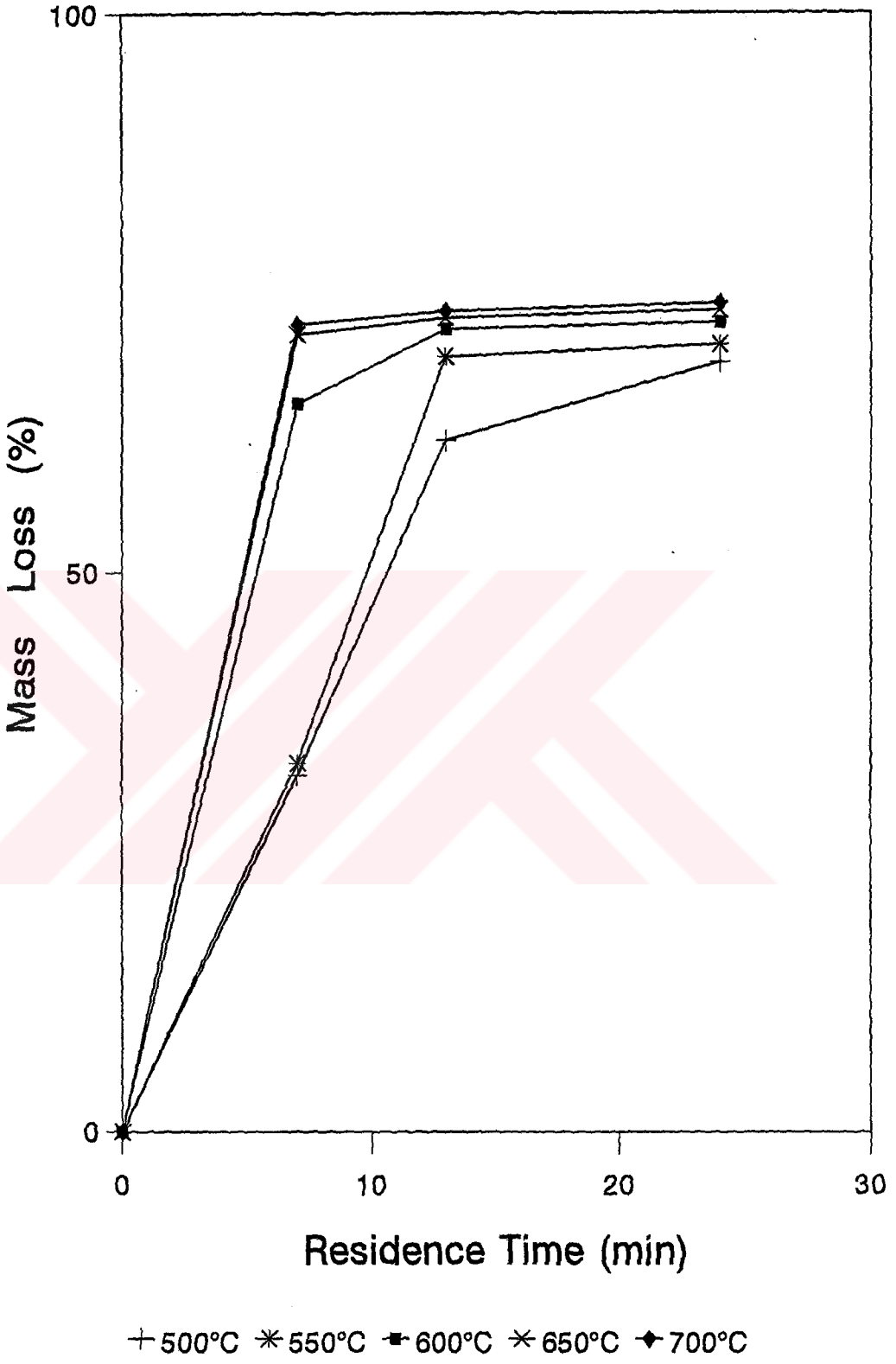


Figure 5.Relationship between mass loss observed in raw material and residence time in the reactor at various temperatures (Hazelnut Shells)

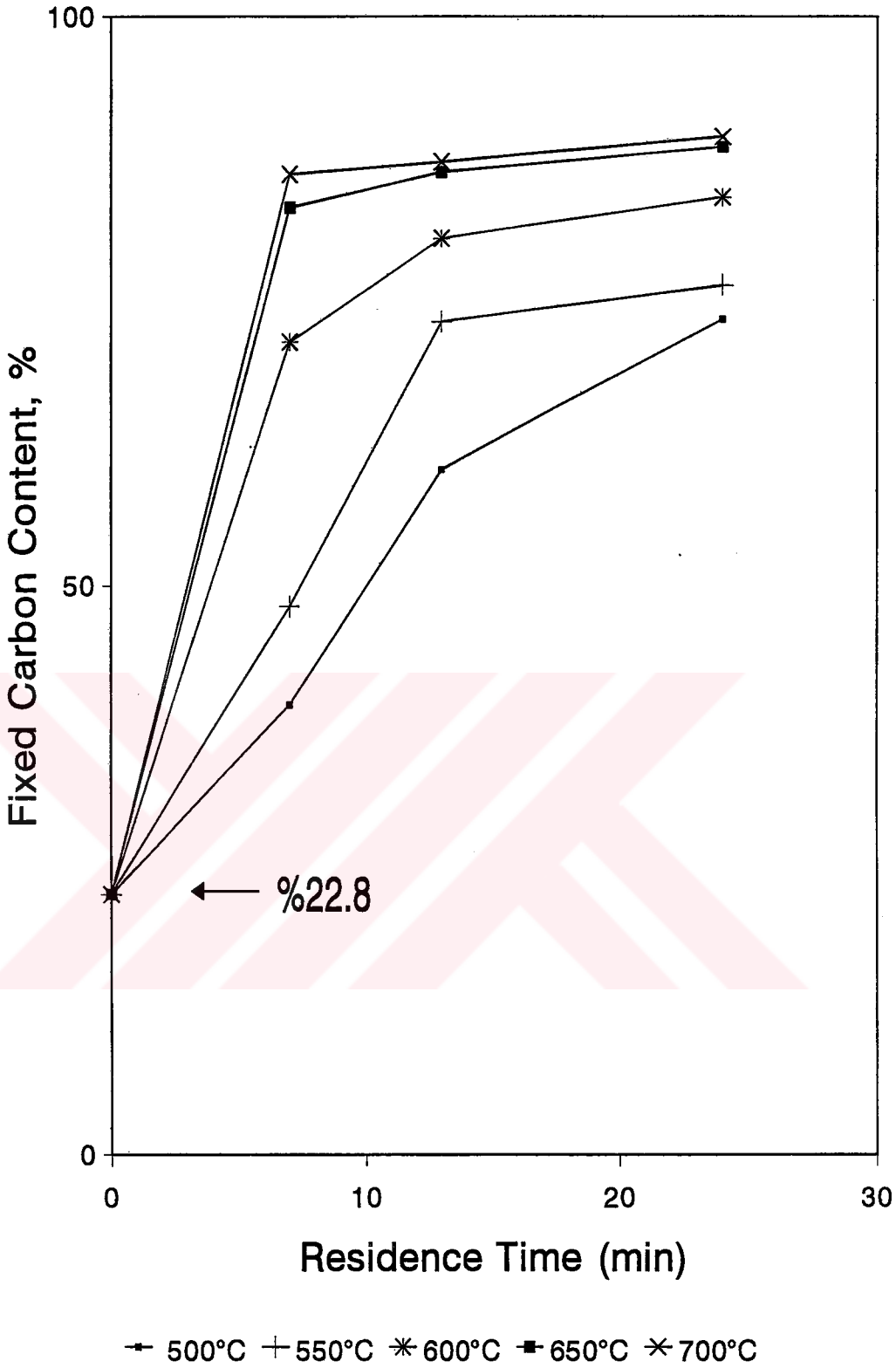


Figure 6. Relationship between fixed carbon content of charcoals and residence time in the reactor at various temperatures (Hazelnut Shells)

to 24 minutes. The observed values were in the range of 34.5-73.4 % and 71.4-84.1 %, respectively. On the other hand, charcoals carbonized at higher temperatures had fixed carbon that did not vary significantly as the carbonization continued. On this basis, charcoals carbonized at 650 °C and 700 °C had fixed carbon in the range of 83.2 - 86.1 % and 88.5 - 89.4 %, respectively, the former and latter values representing the 7 and 24 minutes of carbonization period.

The changes in fixed carbon content were not significant after 650 °C and values obtained were higher than 80 % that is essentially required in the charcoal for a successful activation process.

### 4.1.3. Effect of Carbonization at 650 °C on the Structural Contents of Charcoals

The previous two sections comprised the results of tests for optimization of carbonization condition for hazelnut shells. These showed that hazelnut shells could be carbonized at 650 °C to yield a suitable charcoal for subsequent steam activation. Since hazelnut shells, apricot and peach stones are all of the same origin ( cellulosic materials) and hence have similarities in chemical structure (see Table 3), apricot and peach stones were also carbonized at 650 °C and the products were analyzed for their structural contents. The result are given in Table 4; the results previously obtained from hazelnut shells are also included in the table for comparison purposes.

**Table 4. Proximate analysis of charcoals ( dried overnight at 105 °C)**

| | Wt loss in carbonization % | Yield % | Fixed Carbon % | Volatile Content % | Ash % |
|---|---|---|---|---|---|
| Hazelnut Shells | 70.3 | 29.7 | 88.5 | 8.0 | 3.5 |
| Peach Stones | 72.0 | 28.0 | 88.0 | 9.0 | 3.0 |
| Apricot Stones | 74.3 | 25.7 | 88.0 | 11.0 | 1.0 |

As seen in the table, the weight loss attained in carbonization was 70.3 % for hazelnut shells and 72.0 % and 74.3 % for peach and apricot stones, respectively. Fixed carbon contents of charcoals were almost the same, being 88.5 % for hazelnut shells and 88 % for peach and apricot stones. Hazelnut shell had the highest ash value with 3.5 % that was followed by peach stones with 3.0 % while the smallest value was obtained from apricot stones with 1.0 %. Carbonization removed most of the volatile matter but, some still resided in the structure requiring higher temperature to be driven off. Thus, charcoals still contained residual volatile matter in the range of 8 - 11 %, the former and latter representing the hazelnut shells and apricot stones, respectively.

### 4.1.4. Effect of Heating Pattern in Carbonization on Structural Contents of Charcoals

Carbonization tests were carried out to investigate the effect of elevated temperature and rate of heating on chemical properties of charcoals. Elevated temperature was applied to the preliminary carbonized product by increasing the final temperature upto 900 °C for 1 hour while a lower heating rate was adopted by increasing the temperature upto 650 °C by 5 °C/min. The results are tabulated in Table 5. As seen in the table, carbonization of raw materials at elevated temperature increased the weight loss upto 73.4 % for hazelnut shells and 80 % for apricot stones. As a result of increase in the weight loss due of removing much

**Table 5. Proximate analysis of charcoals ( dried overnight at 105 °C)**

| | | Wt loss in carbonization % | Yield % | Fixed Carbon % | Volatile Content % | Ash % |
|---|---|---|---|---|---|---|
| Hazelnut Shells | a | 70.0 | 30.0 | 89.0 | 7.5 | 3.5 |
| Hazelnut Shells | b | 73.4 | 26.6 | 94.0 | 2.0 | 4.0 |
| Peach Stones | a | 73.0 | 27.0 | 88.5 | 9.5 | 2.0 |
| Apricot Stones | a | 75.0 | 25.0 | 88.0 | 11.0 | 1.0 |
| Apricot Stones | b | 80.0 | 20.0 | 92.0 | 6.0 | 2.0 |

a. Slow carbonization upto 650 °C

b. Elevated temp. carbonization at 900 °C for 1 hour.

higher amount of volatile matter, charcoals contained lower volatile matter content in the range of 2-6 %. Fixed carbon contents of charcoals increased accordingly to 94 % for hazelnut shells and 92 % for apricot stones. Ash values were also increased due to the same reason. Charcoals from slow carbonization of hazelnut shells contained 89 % fixed carbon, 7,5 % volatile matter and 3.5 % ash when 70 % of original weight was lost, while 73 % and 75 % of original weight were lost for peach and apricot stones, respectively. These charcoals had 88.5 - 88 % fixed carbon, 9.5-11 % volatile matter and 2-1.0 % ash in the structure, the former and latter values belonging to peach and apricot stones, respectively.

### 4.1.5. Effect of Carbonization on the Physical and Chemical Properties of Charcoals

Charcoals carbonized under different conditions mentioned previously were analyzed to identify their physical and chemical properties. The results are given in Table 6. As seen in the table, charcoals from hazelnut shells and apricot stones had 40 and 60 $m^2/g$ surface area, 0.53 and 0.59 $g/cm^3$ apparent density, 82.6 and 93 relative hardness numbers, 445 and 409 iodine numbers, respectively when carbonized at a slow rate of heating of 5 °C / min. The charcoals had 34 and 80 m2/g surface area 0.50 and 0.56 g/cm3 apparent density, 89 and 92.7 hardness number and 466 and 431 iodine numbers, respectively when they were carbonized at a faster rate. Carbonization at 900 °C for 1 hour increased surface area and hardness of these charcoals. Hazelnut shells had 141 $m^2/g$ surface area and 114.5 hardness number while charcoals from apricot stones had 140 $m^2/g$ surface area and a slightly higher hardness number of 135.4. There were no significant change observed in apparent density and iodine numbers of charcoals.

Peach stones yielded charcoals with slightly higher surface area values of 170 and 180 $m^2/g$ and lower apparent densities of 0.48 and 0.44 $gr/cm^3$ for slow and fast carbonizations, respectively. However, no significant change was observed in their

**Table 6. Physical and chemical properties of charcoals (- 7 + 14 mesh size)**

| | Carbonization | Surface Area m2/g, BET | Apparent Density g/cm3 | Hardness Number | Iodine Num. mg/g |
|---|---|---|---|---|---|
| Hazelnut Shells | a | 40 | 0.53 | 82.6 | 445 |
| Hazelnut Shells | b | 34 | 0.50 | 89.0 | 446 |
| Hazelnut Shells | c | 141 | 0.53 | 114.5 | 466 |
| Apricot Stones | a | 60 | 0.59 | 93.0 | 409 |
| Apricot Stones | b | 80 | 0.56 | 92.7 | 431 |
| Apricot Stones | c | 140 | 0.57 | 135.4 | 556 |
| Peach Stones | a | 170 | 0.48 | 84.2 | 431 |
| Peach Stones | b | 180 | 0.44 | 90.0 | 440 |

a. Slow carbonization upto 650 °C (5 °C/min.)
b. Fast Carbonization at 650 °C
c. Elevated temperature carbonization at 900 °C for 1 hour.

in their hardness and iodine numbers as compared to those obtained from hazelnut shells and apricot stones.

Generally, charcoals were observed to be poor in activity as deduced from low $N_2$ BET values and had highly increased hardness values when carbonized at an elevated temperature. Thus, substantial steam activation became essential to impose high surface area and gold adsorption properties to the final products.

## 4.2. Activation

### 4.2.1. Effect of Temperature and Burn off on the Surface Area and Hardness of Activated Carbons

#### 4.2.1.1. Hazelnut Shells

Charcoals produced from hazelnut shells were poor in activity as deduced from very low N2 BET values and iodine numbers in the previous section (see Table 6). Thus, they were activated by steam to various burn off levels at temperatures

ranging from 700 °C to 1.000 °C. The effect of temperature and burn off observed in the particles on the surface area and hardness of final product were investigated in this tests.The results are plotted in Figures 7 and 8.

As seen in Figure 7, carbons activated of 700 °C had 43 $m^2/g$ surface area at 6.6 % burn off, that increased to 626 $m^2/g$ at 48 % burn off and no change was observed upto 55 % burn off. In the case of activation at 800 °C, surface area of active carbons increased sharply upto 49.5 % weight loss and had the highest value at this point with 823 $m^2/g$. The surface area of carbons diminished there after down to 800 $m^2/g$ and 738 $m^2/g$ at 55 % and 59.8 % burn offs, respectively. On the other hand, carbons activated at 900 °C and 1.000 °C followed a different pattern. The largest surface area occurred at slightly higher levels of activation, but the values were lower than that obtained at 800 °C. On this basis, carbons had the maximum surface area values as 709 m2/g at 900 °C and 771 $m^2/g$ at 1.000 °C when they were activated to 79.4 and 56.8 % burn offs, respectively . The surface area were observed to decline down to lower values as the activation further continued to higher burn offs.

Figure 8 represents the change in hardness of activated carbons with respect to temperature and degree of activation. It can be noticed from the figure that hardness of the products increased with increasing temperature and this increase was much more marked between 15 and 35 % burn offs. The increase in hardness replaced by a decline after nearly 35 % burn off such that gold hydrometallurgical requirements for hardness (essentially > 97) could not be satisfied any more. As a result, the hardest carbons would only be produced when they were activated upto 32.1 % burn off at 700 °C, 35 % at 800 °C while 15.4 % and 29.8 % burning were eventually required for 900 °C and 1.000 °C activations, respectively. These carbons had 95.6, 98.3, 102 and 103 hardness in the respect of increasing temperature from 700 °C to 1.000 °C.

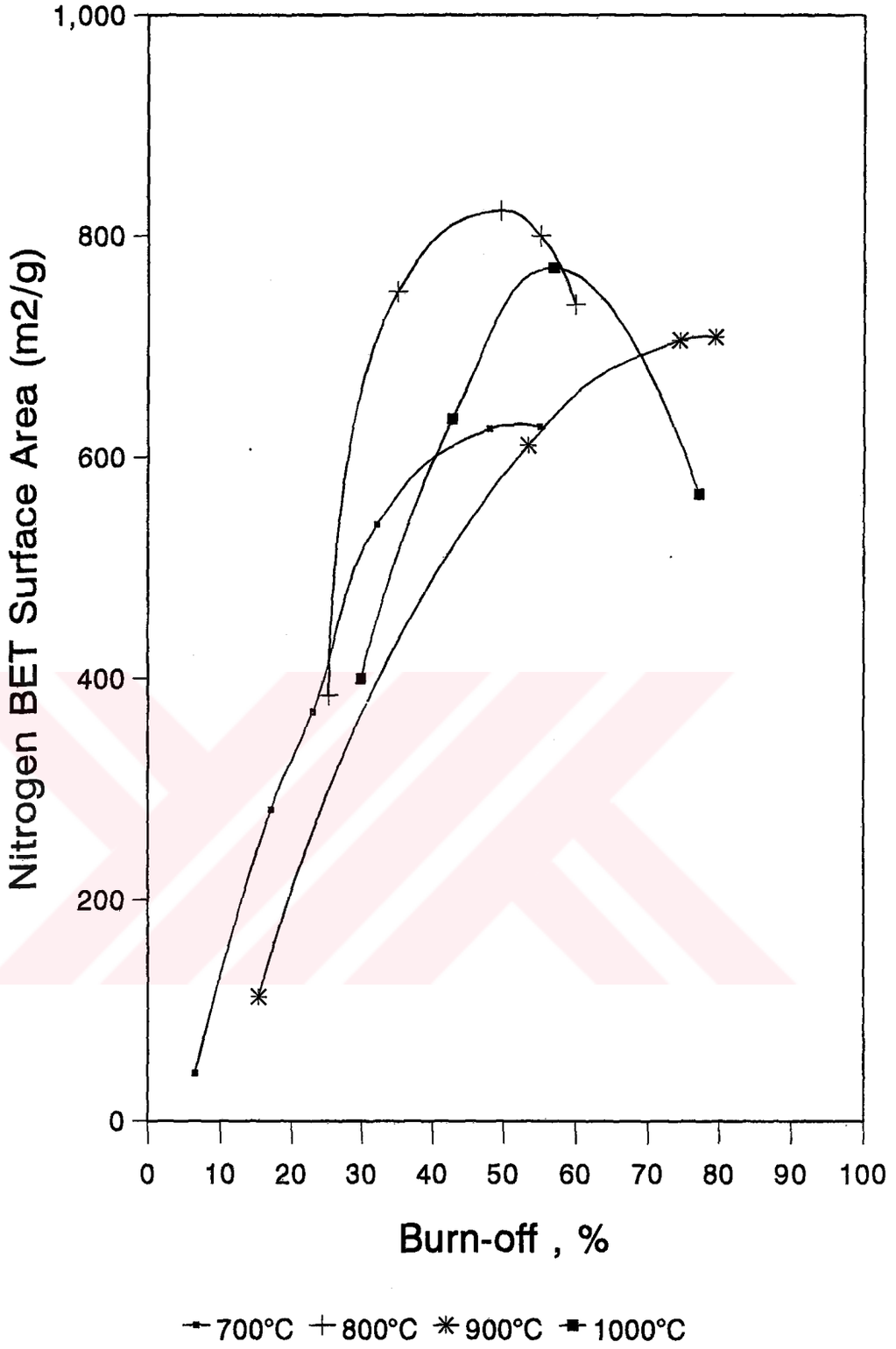


Figure 7.Relationship between Nitrogen BET surface area and mass loss in activation at various temperatures (Hazelnut Shell Carbons)

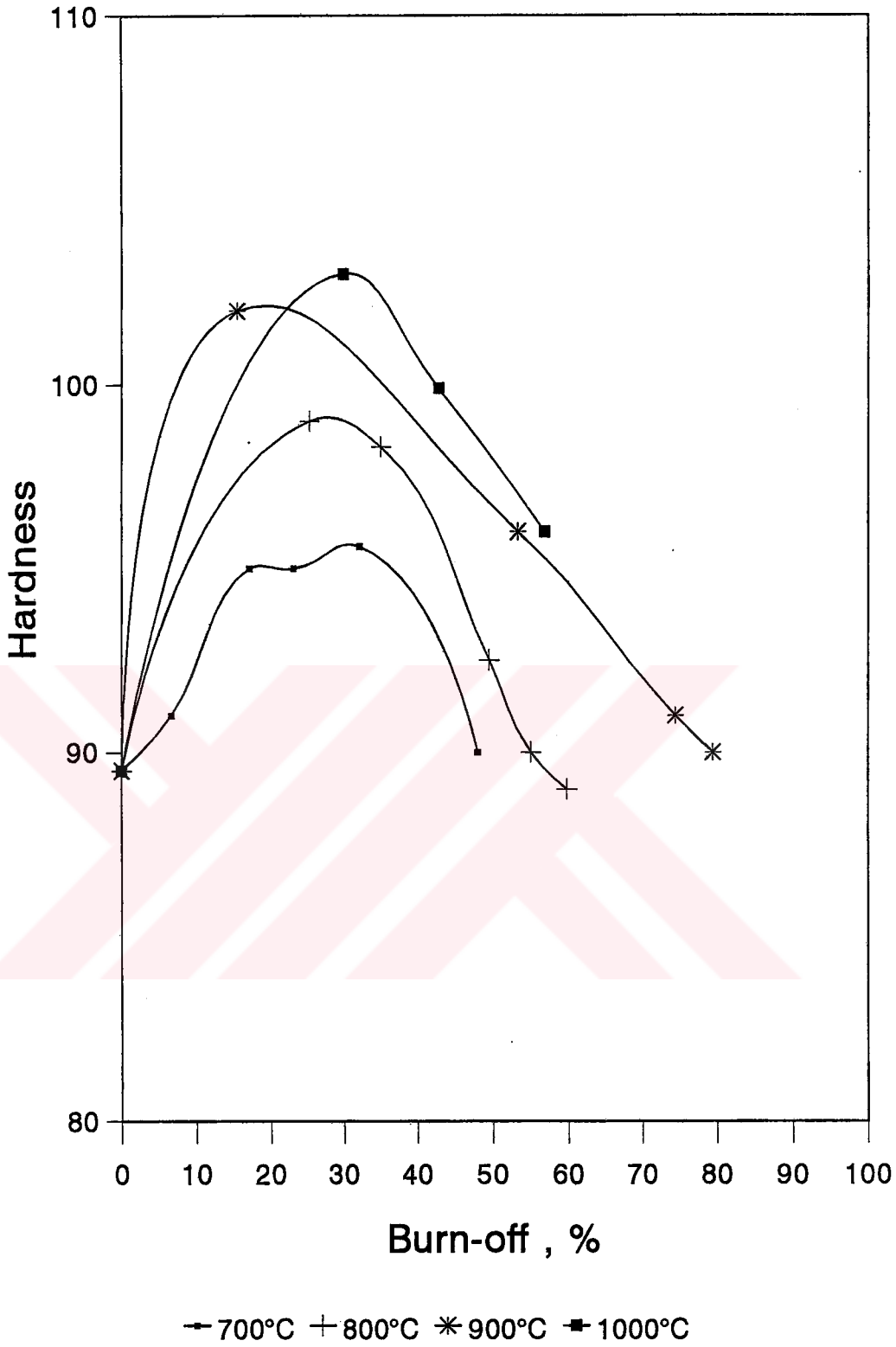


Figure 8. Relationship between hardness of activated carbons and mass loss in activation at various temperatures (Hazelnut Shell Carbons)

#### 4.2.1.2. Apricot Stones

Activation tests were continued to investigate the effect of activation temperature and burn off under the action of steam on the surface area and hardness of activated carbons produced from apricot stones that were carbonized at faster rate heating at 650 °C. Those carbons from elevated temperature and slow carbonization were also activated but will be given in the section (4.2.2.2). The results obtained from the activation of fast carbonized products are plotted in Figures 9 and 10.

The results showed in Figure 9 that the general trend was an increase in surface area with an increase in burn of upto 50 % at any activation temperature except 1.000 °C at which a sharp increase was observed in surface area at any level of burn offs. However, the increase in surface area upto 50 % burn off was then replaced by a reduction as the activation further proceeded. The largest surface area in the carbons was obtained as 760 $m^2/g$ at 700 °C, 840 $m^2/g$ at 800 °C and 896 $m^2/g$ at 900 °C with corresponding burn offs at 43.8 %, 56.7 % and 49.5 % respectively However, contradicting to the previous results, the highest surface area at 1.000 °C activation was obtained at higher levels of burn off (70.5 %) with 905 $m^2/g$.

Generally, highest surface area values were obtained at between 40 -60 % burn off as observed in the case of hazelnut shells in previous section. Further increase in degree of activation, in fact, decreased the surface area of carbons.

As shown in Figure 10, the maximum hardness values were obtained in the initial period of activation. Carbons had 109.2 hardness at 700 °C 108.9 hardness at 800 °C, 110.3 hardness at 900 °C and 109.6 hardness at 1.000 °C. The corresponding burn offs were 11.2 %, 8.4 %, 12.7 %, and 30.9 %, respectively. This showed that the structure is slightly reacted by the action of steam in the initial period of activation and high temperature application compacted the structure; thus hardness values appeared very high. On the other hand, carbons were qradually exposed to the strong action of steam as activation increased and hence, a reduction in hardness of carbons was also observed.

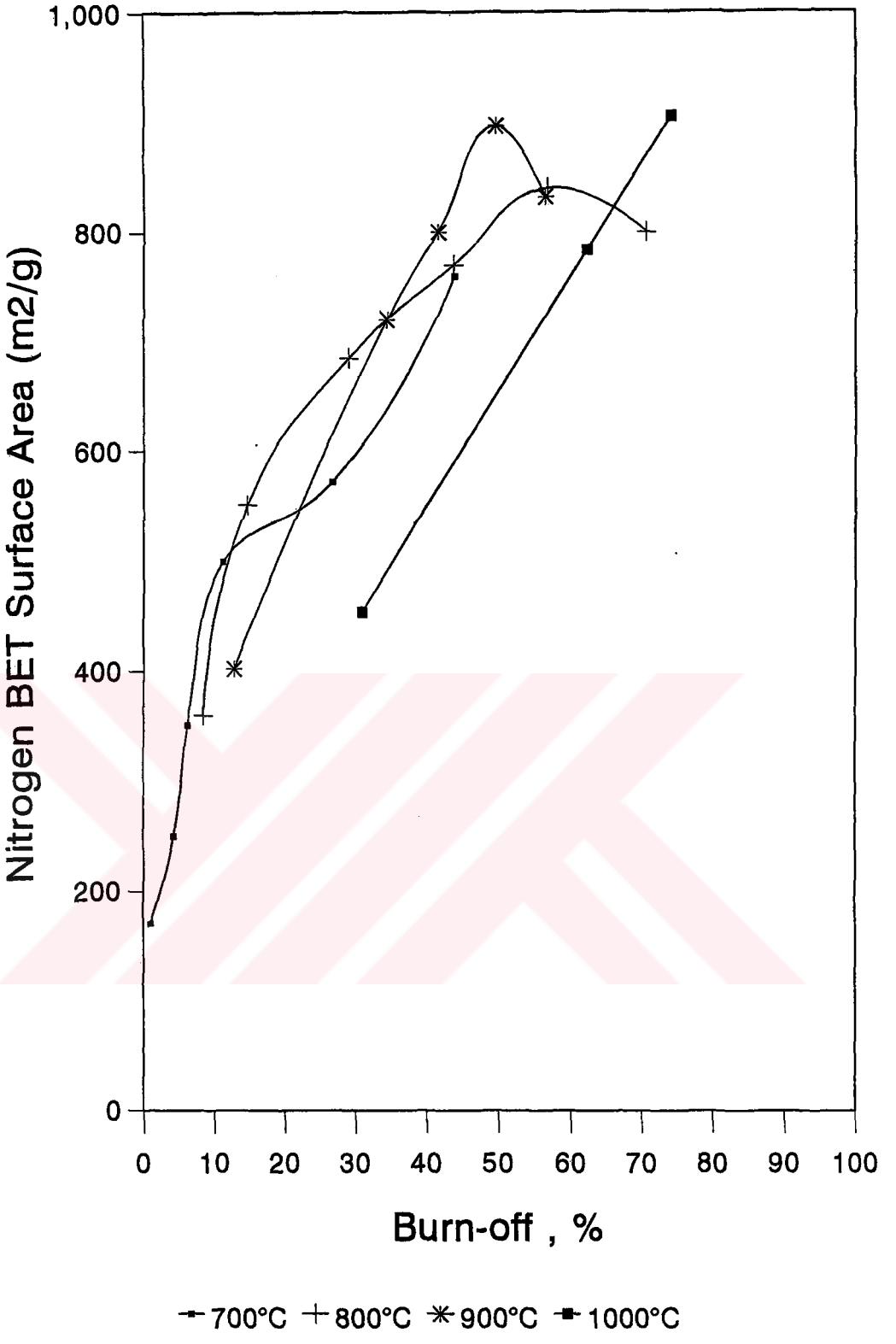


Figure 9.Relationship between Nitrogen BET surface area and mass loss in activation at various temperatures (Apricot Stone Carbons)

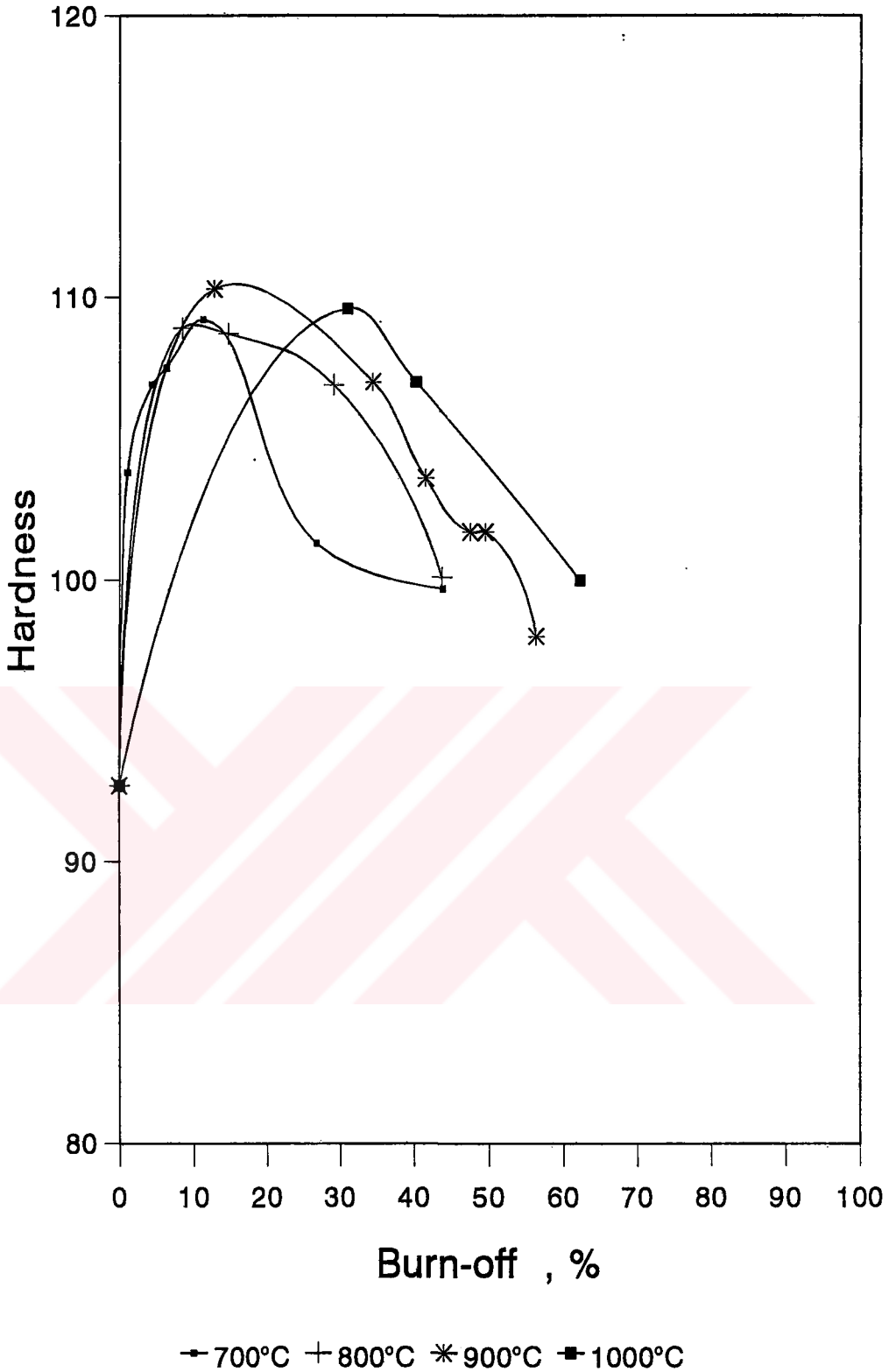


Figure 10. Relationship between hardness of activated carbons and mass loss in activation at various temperatures (Apricot Stone Carbons)

It was deduced that eventhough reductions in hardness values were observed, the values were still very high even the activation proceeded to obtain good product to about 60 % burn off. On this basis, carbons had 99.7 hardness at 700 °C and 43.8 % burn off, 100.1 hardness at 800 °C and 43.7 % burn off, 103.6 hardness at 900 °C and 41.5 % burn off and at 1,000 °C they acquired 107 hardness at 40.2 % burn off.

Commercial active carbon originating from coconut shells have generally hardness values not lesser than 97; thus, these carbons are considered to have practical and industrial significance in active carbon production for gold metallurgy.

#### 4.2.1.3. Peach Stones

Final series of steam activation tests were carried out with peach stones. In the first place, the influence of activation temperature and burn off (hence degree of activation) on the surface area and hardness of carbons was investigated by activating the charcoals carbonized by fast heating. Effect of slow heating in carbonization on the surface area and hardness of activated carbons will be given in section (4.2.2.3). The results are given in graphical form in Figures 11 and 12.

As illustrated in Figure 11, the surface area of carbons increased sharply to 760 $m^2/g$ at 700 °C and 911 $m^2/g$ at 800 °C. The corresponding burn offs were 27.7 % and 44.3 %, respectively. As the activation continued to further burn offs, little change was observed for 700 °C activation but, the values diminished to 797 $m^2/g$ at 50.23 % burn off in the case of 800 °C activation. The largest surface area was obtained at relatively higher levels in activation of peach stones at 900 °C. In this sense, peach stone carbons with a surface area of 950 $m^2/g$ were obtained at 79 % burn off. Therefore, Activation of peach stones at 900 °C was also supposed to yield active carbon with very high $N_2$ BET values as that obtained at 800 °C, but somewhat larger amounts had to be burnt out.

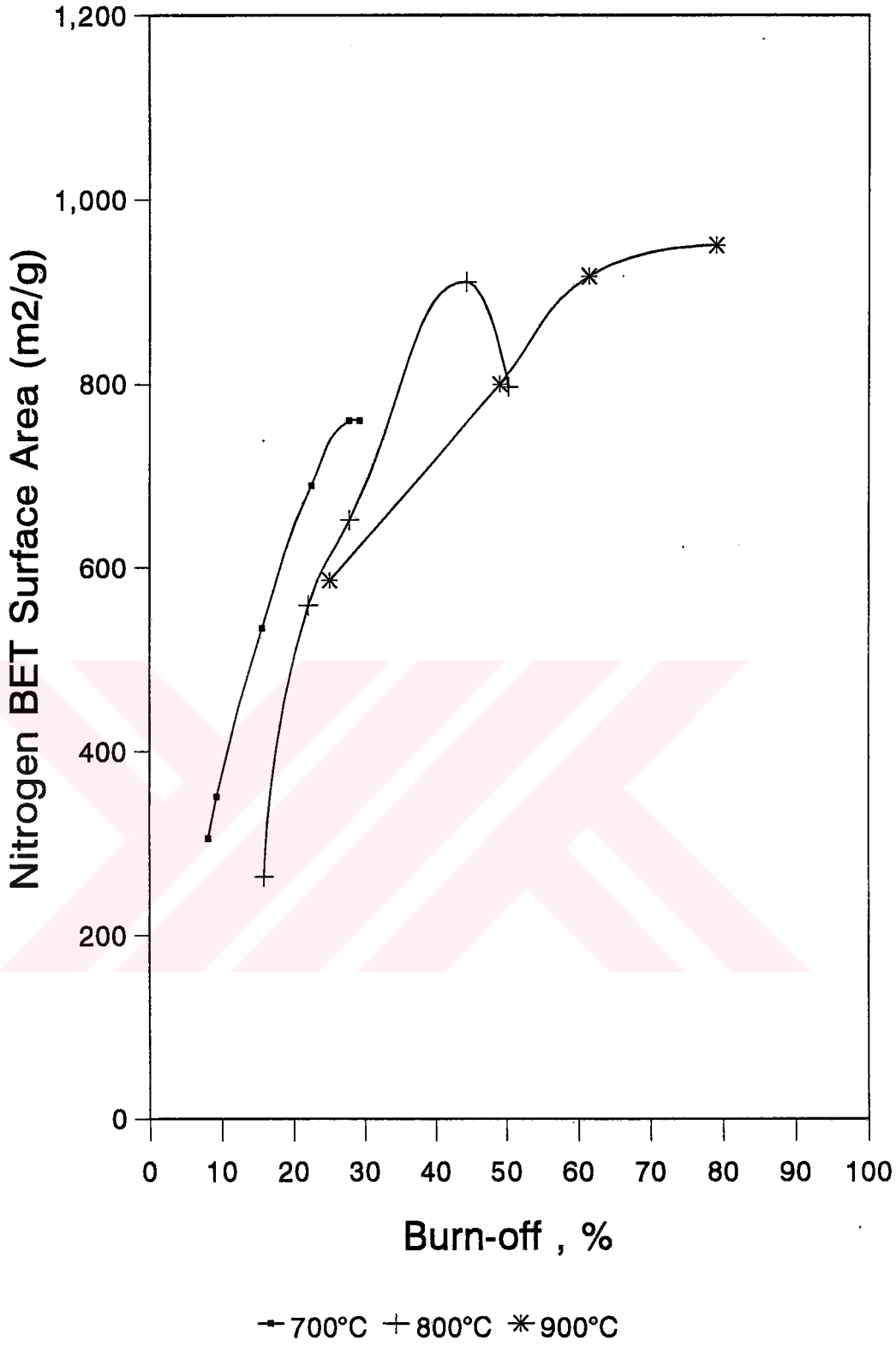


Figure 11. Relationship between Nitrogen BET surface area and mass loss in activation at various temperatures (Peach Stone Carbons)

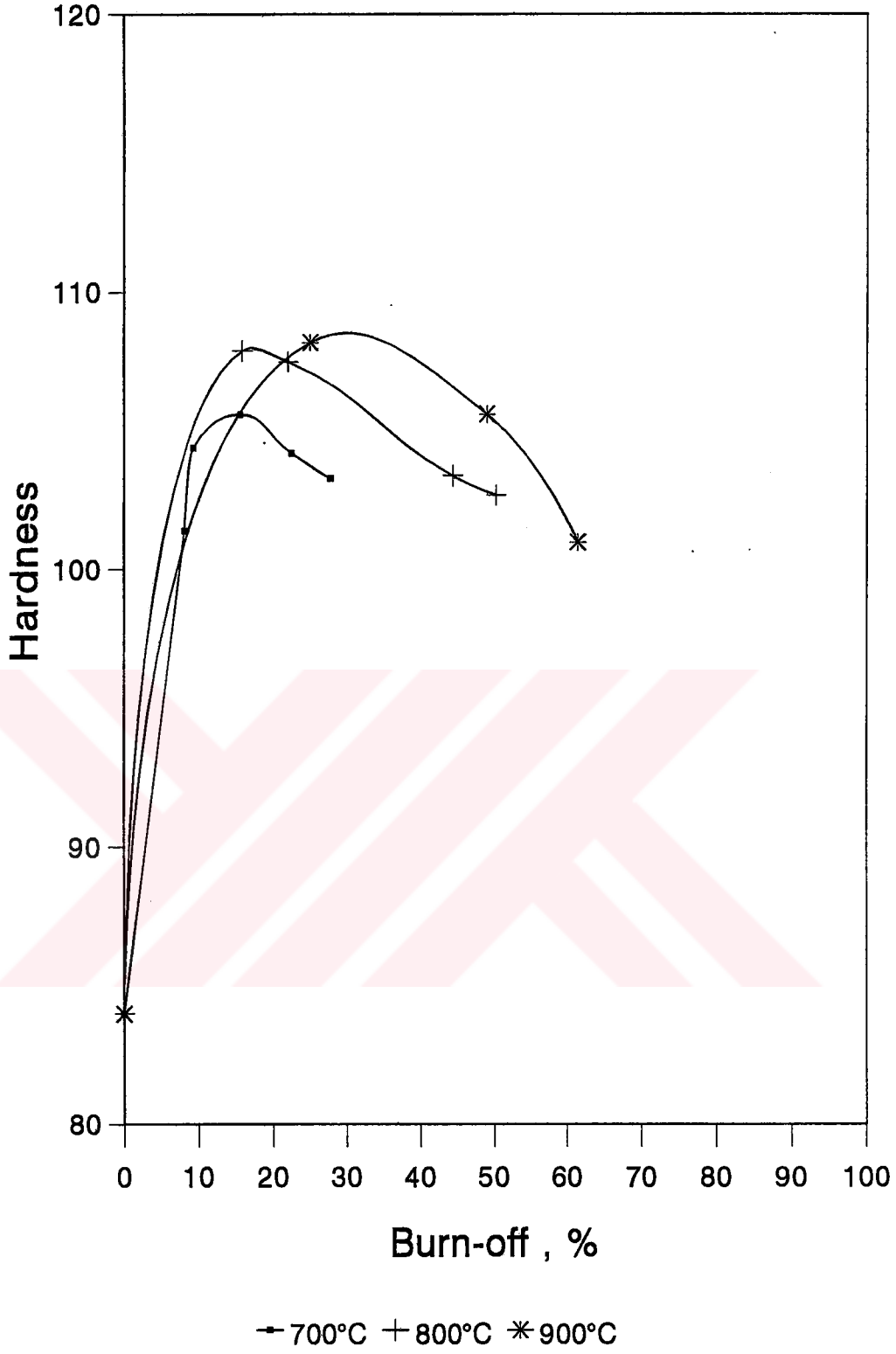


Figure 12. Relationship between hardness of activated carbons and mass loss in activation at various temperatures (Peach Stone Carbons)

The manner of development of surface area in peach stone carbons under activation conditions seemed to be similar to those obtained from previous two raw materials, but higher surface areas were developed in peach stones carbons at especially 800 °C activation than hazelnut shells and to some extent, apricot stones when the activation was limited to between 40 and 60 % burn off.

The changes in hardness of activated carbon with respect to activation temperature and burn off are given in Figure 12. As seen in the figure, the hardness of the carbons increased to maximum values; being 105.6 for 700 °C, 107.9 for 800 °C and 108.2 for 900 °C, at relatively low degree of activation (< 25 % burn off). It was seen that hardness values of the carbons have been drastically reduced down to 103.3 at 27.7 % burn off for 700 °C and 102.7 and 100.98 for 800 °C and 900 °C at 50.23 % and 61.4 % burns off, respectively. As seen from these results, peach stones yielded very hard carbons; especially at 900°C activation so that they were also considered to have industrial and practical significance for active carbon production.

### 4.2.2. Effect of Heating Pattern in Carbonization on the Surface Area and Hardness of Activated Carbons.

#### 4.2.2.1. Hazelnut shells

Effect of heating pattern in carbonization on the surface area and hardness of activated carbons were examined by the tests carried out at 800 °C. This temperature appeared in section (4.2.1.1) as the best activation temperature. In this sense, charcoals were at first produced by carbonizing the hazelnut shells at slower and faster heating at 650 °C and at elevated final temperature of 900 °C and then activated by steam to various levels of burn off. The results are plotted in Figures 13 and 14.

As seen in Figure 13, the largest surface area occurred at 55 % burn off for slow carbonized products with 832 $m^2/g$ and at 49.5 % for fast carbonized products with 823 $m^2/g$ while exactly half of original weight had to be burnt out to yield carbon

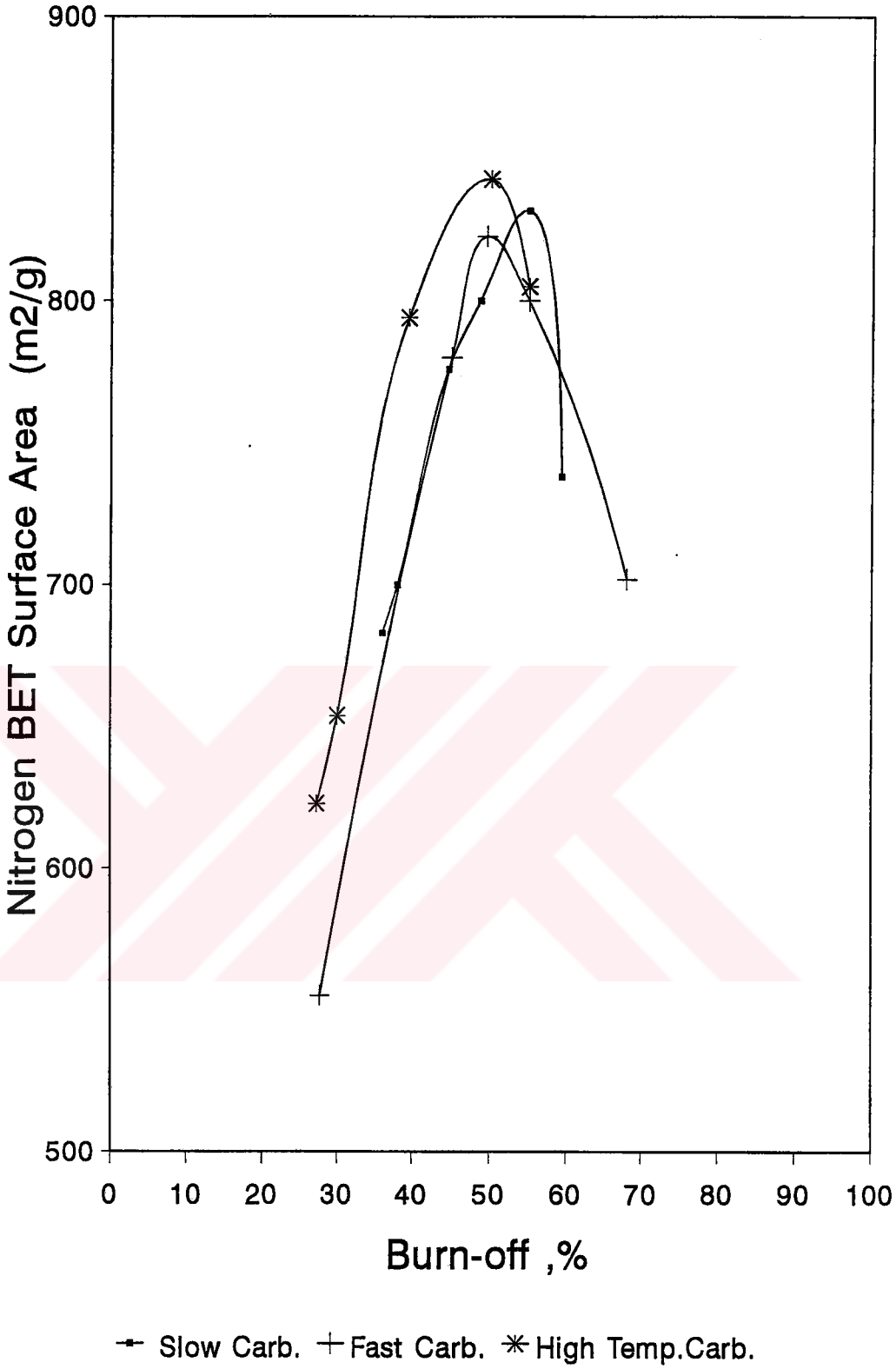


Figure 13. The effect of heating pattern in carbonization on Nitrogen BET surface area of carbons activated at 800°C (Hazelnut Shell Carbons)

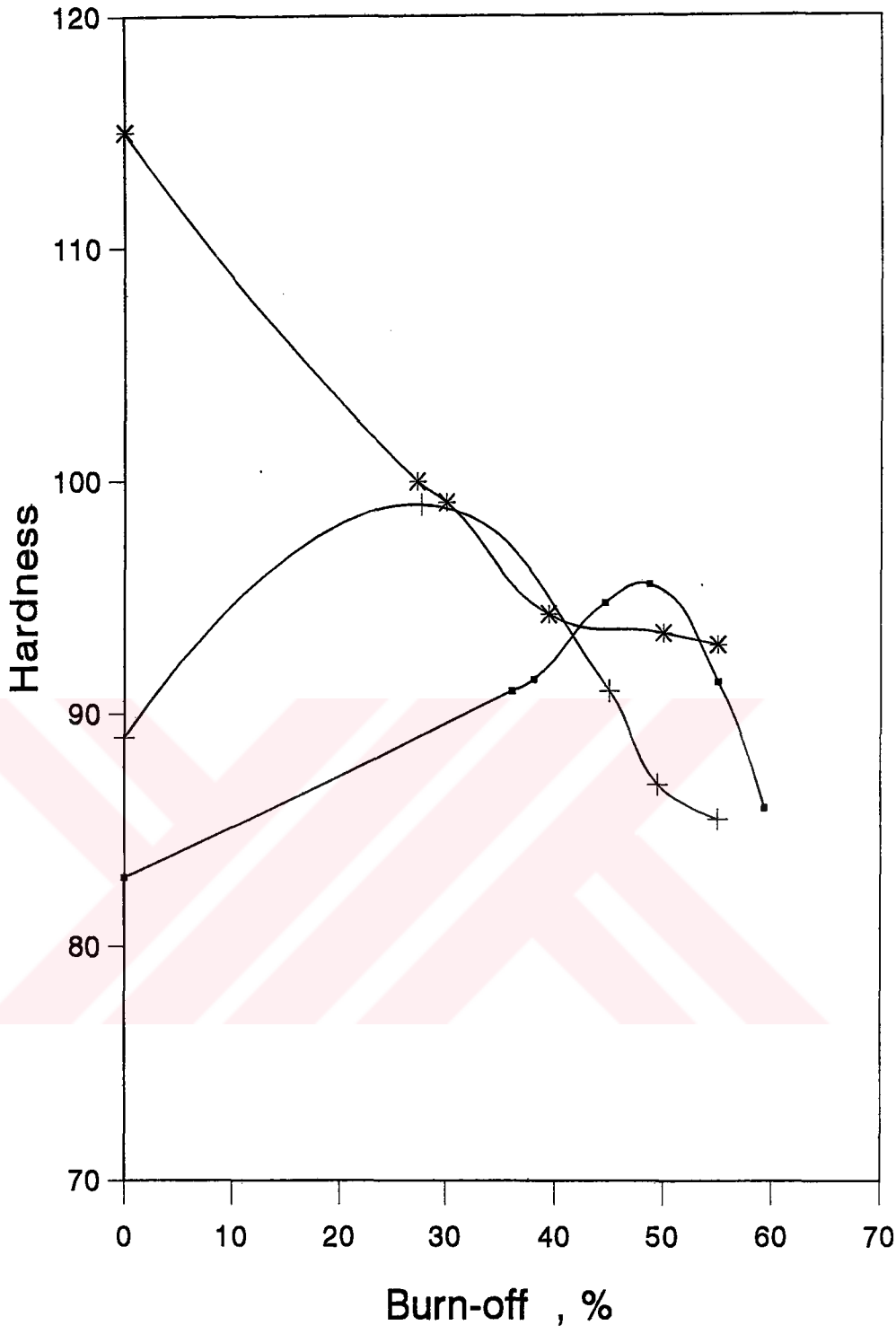


Figure 14. The effect of heating pattern in carbonization on hardness of carbons activated at 800°C (Hazelnut Shell Carbons)

with highest surface area of 843 $m^2/g$ from high temperature carbonized products. Commonly, surface area of carbons sharply increased with an increase in the level of burn off (hence, degree of activation) upto nearly 50 % after which further activation resulted a decrease in the surface area values and it was observed that this decrease was more marked beyond 60 % burn off.

Figure 14 represents the changes in the hardness of active carbons with respect to degree of activation at 800 °C. As seen in the figure, the hardness of the carbons gradually increased upto 95.6 for carbons from slow carbonized products and 99 for carbons from fast carbonized products at 48.7 % and 27.7 % burn offs, respectively. The increase was then replaced by a drastical decrease indicating the damage in the structure by the strong action of steam. On the other hand, those carbons produced at elevated temperature previously had extremely high hardness values in the initial times of activation (114.5; at a burn off < 5%) but it was followed by a reduction down to 100 and 99.1 hardness values as the activation proceeded to 27.3 % and 30 % weight loss, respectively. The lowest value was then obtained at 55 % burn off as 95.

#### 4.2.2.2. Apricot Stones

Tests were carried out to investigate the effect of slower carbonization at a heating rate of 5 °C/min and carbonization at elevated temperatures such as 900 °C on the surface area and the hardness of active carbons produced from apricot stones. In these tests, charcoals carbonized at such different conditions were steam activated at 900 °C that seemed the optimum activation temperature in section (4.2.1.2). The results are given graphically in Figures 15 and 16. The results obtained from the activation of fast carbonized product at 900 °C were also plotted in the figures for a comparison purpose.

As seen in Figure 15, activation of charcoals from elevated temperature and slow carbonization yielded more active carbons; those obtained from elevated temperature carbonization being the most active than obtained from the activation of products carbonized by fast heating. Active carbons gained activity as the

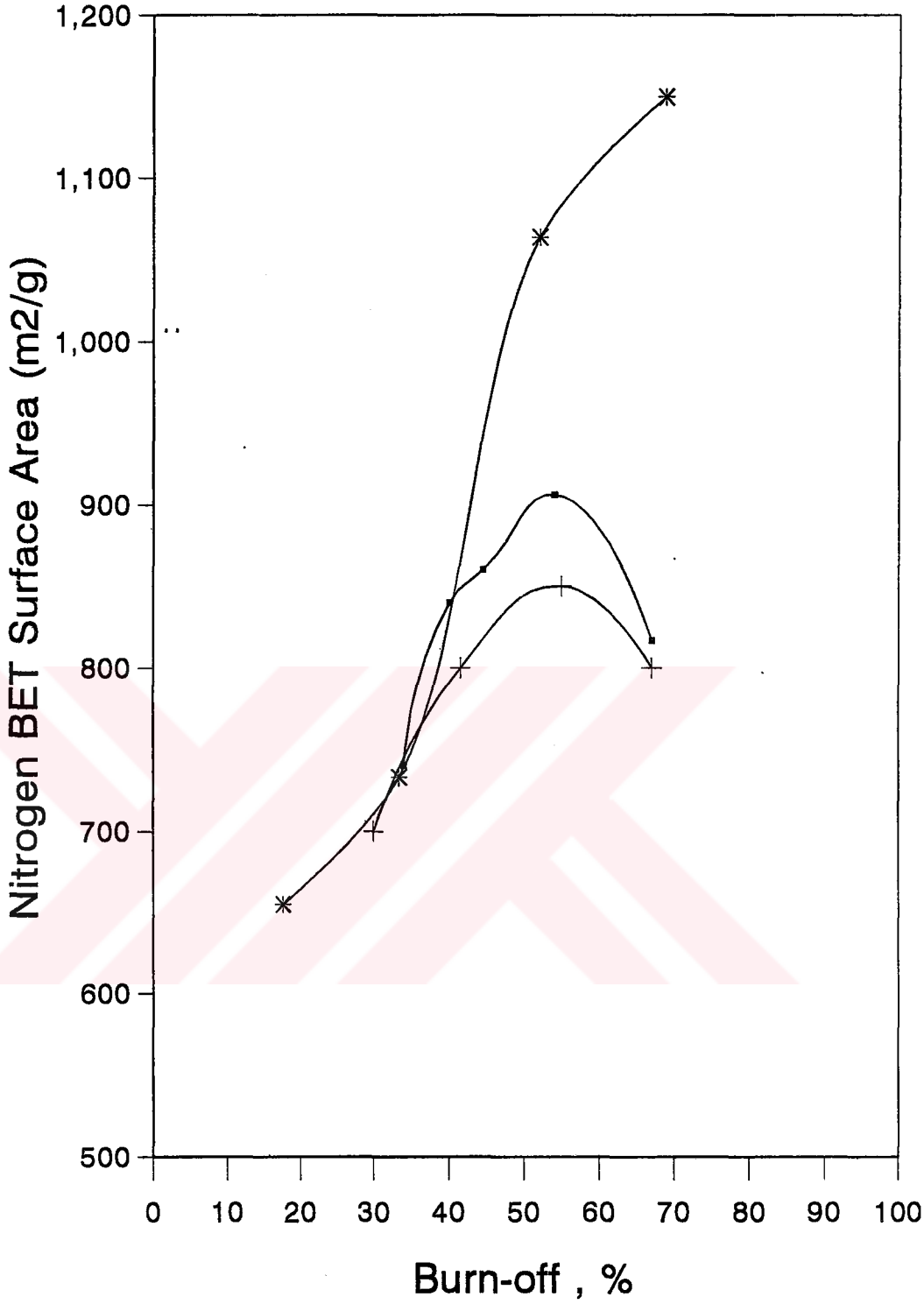


Figure 15. The effect of heating pattern in carbonization on Nitrogen BET surface area of carbons activated at 900°C (Apricot Stone Carbons)

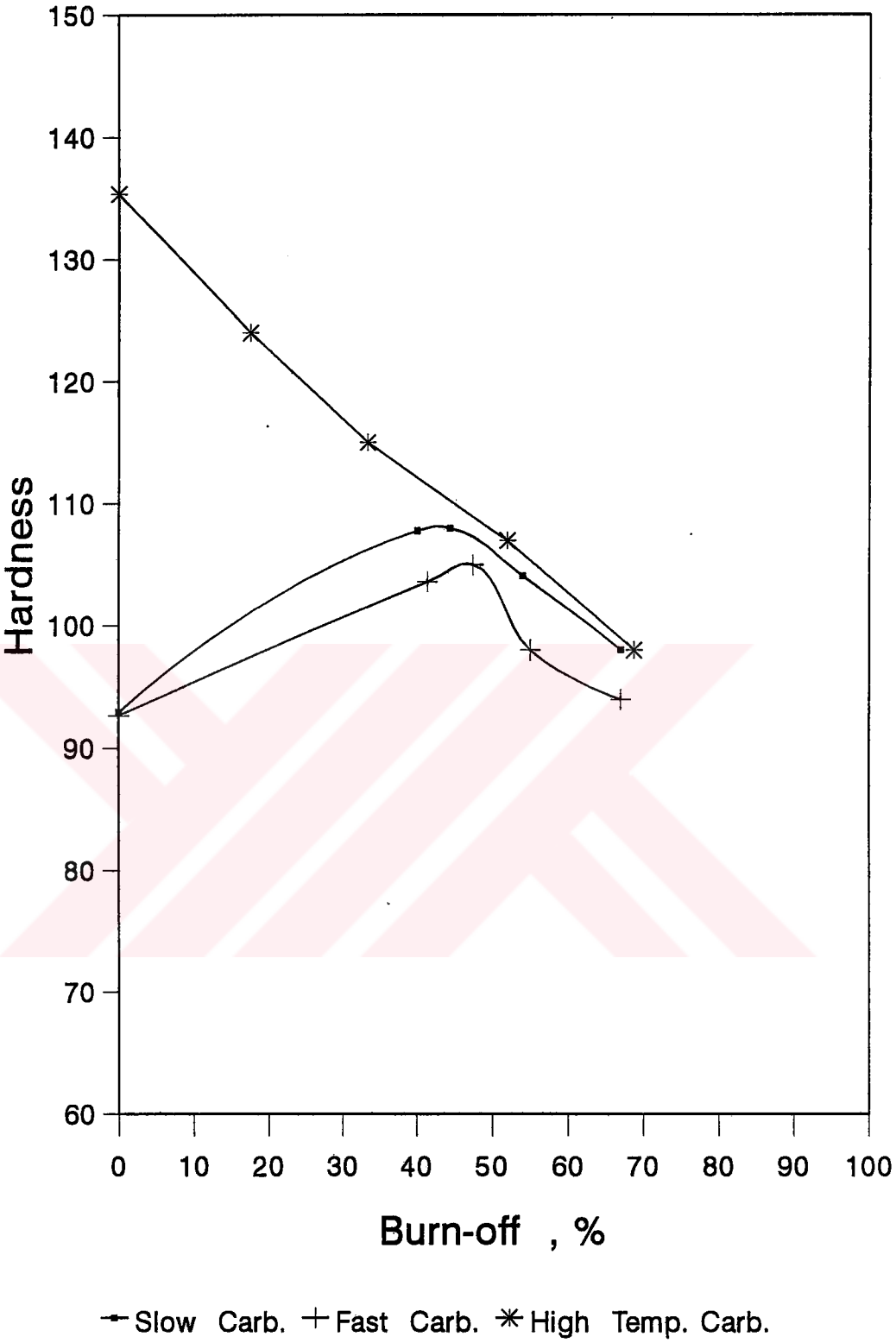


Figure 16. The effect of heating pattern in carbonization on hardness of carbons activated at 900°C (Apricot Stone Carbons)

surface area increased by selective oxidation or etching of steam that resulted weight loss in the particles. This led to the maximum development of surface area as being 1.150 $m^2/g$ for carbons from elevated temperature carbonization and 850 $m^2/g$ and 906 $m^2/g$ for carbons from fast and slow carbonization, respectively, at corresponding burn offs of 68.8 %, 55 % and 54 %. This showed that nearly half of the original weight should be burnt out to yield active carbons with surface area higher than 850 $m^2/g$. It was also seen in the same figure that activation of carbons beyond 50 % burn off resulted reductions in surface area values for carbons from fast and slow carbonization, while only lowered the rate of increase in surface area for carbons from elevated temperature carbonization. On this occasion, carbons had lower surface area values with 817 $m^2/g$ and 800 $m^2/g$ at 67 % burn off in the case of activation of fast and slow carbonized products, respectively and the surface area obtained from elevated temperature carbonization was 1.150 $m^2/g$ at 68.8 % burn off.

Figure 16 shows the change of hardness of active carbons with respect to burn off attained in activation. It was seen in the figure that the curves representing the changes in hardness of carbons were typical for each carbonization condition and similar to those obtained from hazelnut shell carbons in previous sections; however, the values were higher. In the case of activation of slow and fast carbonized products, carbon acquired higher hardness values in the range of 93-108 and 92.7-105, respectively; the former values represent the hardness of charcoals and the latter values represent the maximum values at 44.5 % and 47.5 % burns off, respectively. However, these values were replaced by lower values when activation was further proceeded beyond the point where nearly half of the original weight was burn out. Fortunately, It seemed that apricot stones could yield very stiff carbons with hardness values similar to that of coconut shell carbons. Hardness of activated carbons from elevated temperature carbonization started from extremely high levels, being 135.4 in the initial period of activation; then, it gradually decreased to 124, 115 and 107 as activation proceeded towards 50 % weight loss. The value attained at higher burn offs such as 68.8 % was 98, still being very high. As a result, it appeared that apricot stones could yield very hard active carbon even the activation was continued to nearly 50 % mass loss that was

previously appeared as optimum activation level to obtain carbon with highest surface area.

#### 4.2.2.3. Peach Stones

Tests were continued with peach stones to investigate the effect of heating types on the surface area and hardness of activated carbons. In these tests, charcoals carbonized at slower and faster heating at 650 °C were steam activated at 800 °C. This temperature appeared to be optimum activation temperature in section (4.2.1.3). The results are given in Figures 17 and 18.

As seen from the Figure 17, the manner of surface area development were alike for both processes. The maximum values were obtained at 44.3 % and 52.6 % burn offs with 911 $m^2/g$ and 962 $m^2/g$ for fast and slow carbonized products, respectively. Eventhough a decrease in surface area values dominated after 50 % burn off for fast carbonized carbons, slow carbonized carbons had slightly increasing values at this level of activation. Consequently, it appeared that peach stone carbons with 911-962 $m^2/g$ surface area could be very well comparable to coconut shell carbons with nearly 1000 $m^2/g$ surface area.

When the hardness values were considered in Figure 18, it was noticed that carbons have acquired mechanical strength in the initial period of activation and thus, hardness values increased rapidly. But, as the activation proceeded toward 50 % mass loss, this increase was replaced by a reduction in hardness values. However, the values obtained at this level of activation was extremely higher than that of coconut shell carbons; being 102,7 and 103 for fast and slow carbons, respectively. As a result, peach stones appeared to yield carbons acquiring high mechanical strength with enough resistance to oxidation condition resulted by active oxygen in steam.

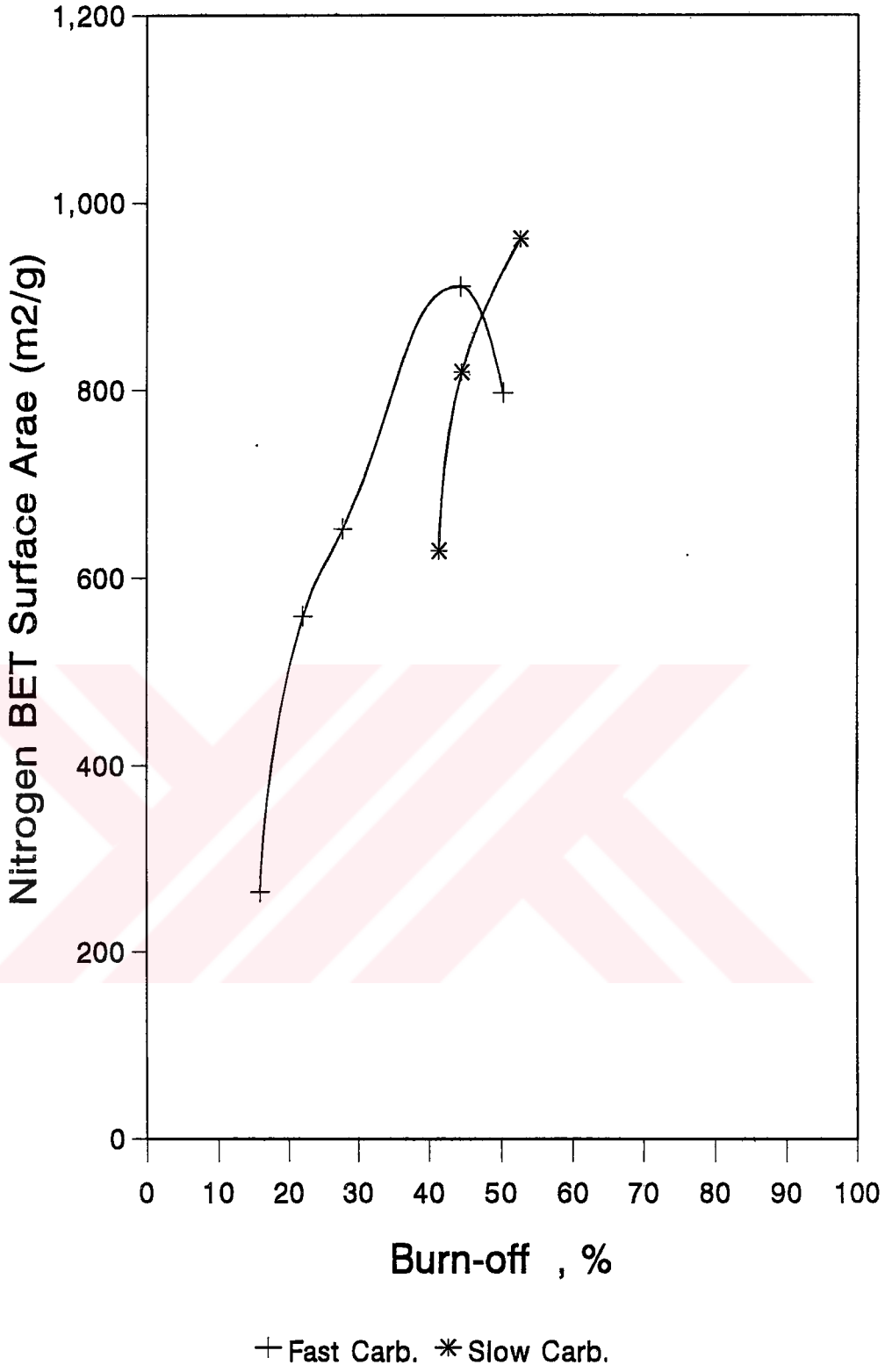


Figure 17. The effect of heating pattern in carbonization on Nitrogen BET surface area of carbons activated at 800°C (Peach Stone Carbons)

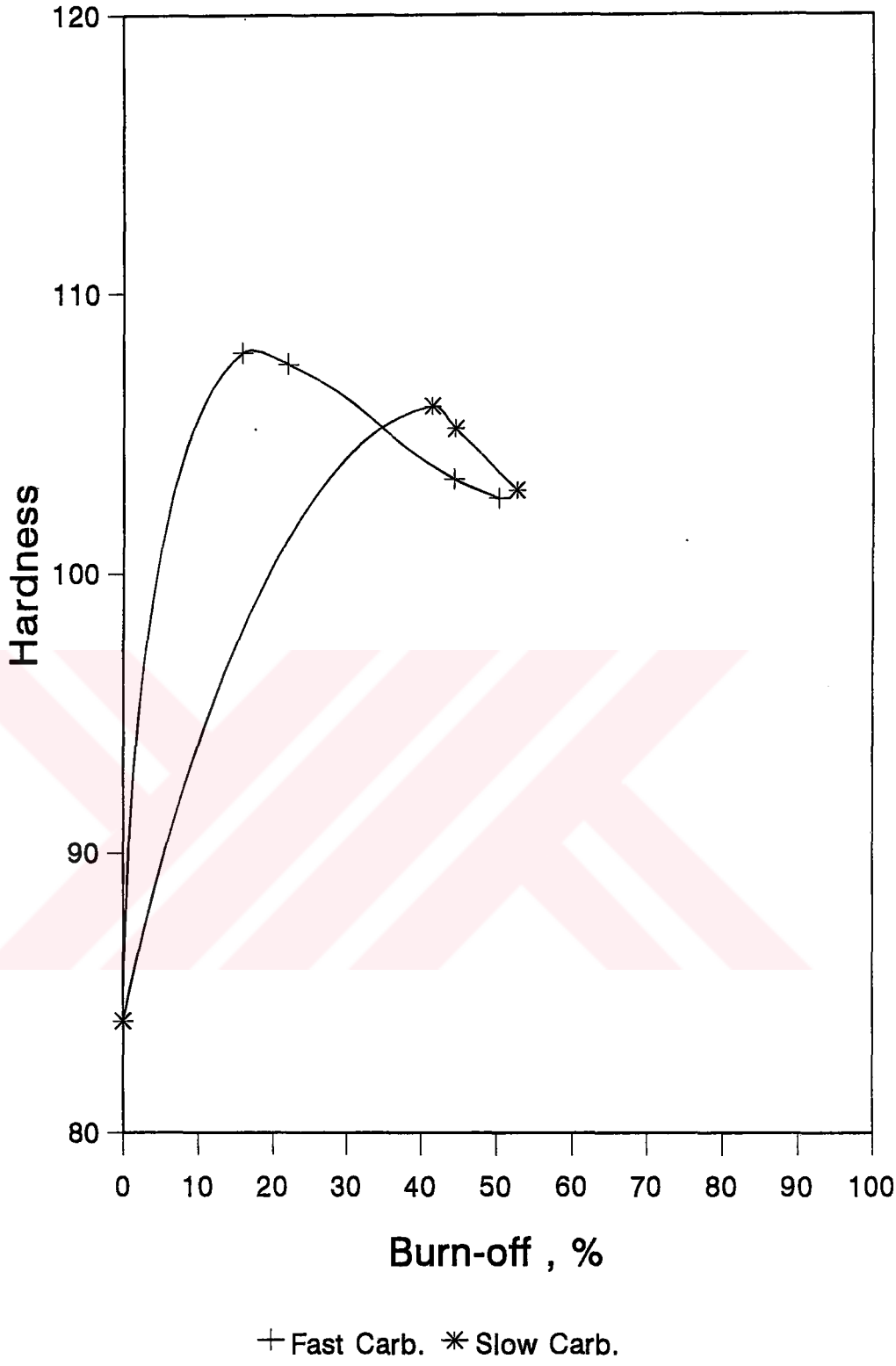


Figure 18. The effect of heating pattern in carbonization on hardness of carbons activated at 800°C (Peach Stone Carbons)

## 4.3. Chemical Activation

### 4.3.1. Effect of Impregnant Agent Concentration on the Surface Area of Activated Carbons

Another type of activation; namely chemical activation, was also carried out with hazelnut shells. KOH and $ZnCl_2$ known as the most powerful activators were used in these tests. This chemicals dehydrated the raw materials so that carbons acquired surface area. The results are given in Table 7.

**Table 7. Chemical activation of hazelnut shells at 650 °C**

| Agent | Concentration W/W | Weight Loss % | Yield % | Surface Area m2/g |
|---|---|---|---|---|
| KOH | 5 | 66.5 | 33.5 | 12 |
| KOH | 10 | 67.8 | 32.2 | 22 |
| KOH | 20 | 74.7 | 26.3 | 118 |
| $ZnCl_2$ | 5 | 62.2 | 37.8 | 44 |
| $ZnCl_2$ | 20 | 56.5 | 43.5 | 215 |
| $ZnCl_2$ | 80 | 54.0 | 46.0 | 852 |

The results in the table showed that the surface area in the case of KOH impregnation increased from 12 $m^2/g$ to 118 $m^2/g$ with an increase in the concentration from 5 w/w to 20 w/w. However, this values have no significance for a particular uses in hydrometallurgy. In the case of $ZnCl_2$, surface area increased to 852 $m^2/g$, only at extremely high level of impregnation (80 w/w). It was noticed in the same table that, contradicting the results obtained from KOH, $ZnCl_2$ increased the yield of activation from 37.8 % to 46.0 %. This was so expected since $ZnCl_2$ is known to restrict the formation of tarry substances. Therefore, the amount of material removed from the structure was minimized.

### 4.3.2. Effect of Steam Activation on the Surface Area and Hardness of Chemically Activated Carbons

The carbons produced by KOH impregnation at 5/100 (w/w) level (others not tested due to the soft forms of the products) and $ZnCl_2$ impregnation at 5/100 and 80/100 levels were steam activated at 800 °C to various burn offs to see the changes in surface area development and hardness under the action of steam. The results are given in Table 8.

**Table 8. Steam activation of chemically activated carbons**

| Agent | Burn off % | Surface Area m2/g | Hardness |
|---|---|---|---|
| KOH | 31.0 | 632 | a |
| KOH | 67.8 | 840 | a |
| KOH | 88.9 | 980 | a |
| $ZnCl_2$(5/100) | 16.9 | 207 | 92.6 |
| $ZnCl_2$(5/100) | 19.9 | 604 | 91.4 |
| $ZnCl_2$(5/100) | 40.8 | 568 | 90.4 |
| $ZnCl_2$(80/100) | 21.7 | 976 | 69.7 |
| $ZnCl_2$(80/100) | 23.0 | 1,237 | 67.0 |
| $ZnCl_2$(80/100) | 46.0 | 1,098 | 65.0 |

a: Not measured due of very soft product.

As seen in the table, steam activation increased the surface area of carbons in the range of 632-980 $m^2/g$ for KOH impregnation and 207-568 $m^2/g$ and 976-1.098 $m^2/g$ for $ZnCl_2$ at 5/100 (w/w) and 80/100 (w/w) impregnation levels, respectively. This showed that steam activation is much more effective than chemical activation. Extreme results were obtained with 980 $m^2/g$ and 1.237 $m^2/g$ for KOH and $ZnCl_2$ when activation was carried out to 88.9 % and 23 % burn off, respectively. Unfortunately, all the products obtained by this way were so soft that some of them could not be tested. This was so expected since structure was exposed to the strong action of both chemicals and steam sequentially and damaged very much accordingly.

### 4.4. Carbon Adsorption Characterization

This part of the study comprised the characterization of coconut shell carbon and best selected carbons from hazelnut shells, peach and apricot stones in previous sections. Carbon characterization studies were carried out in two parts. In the first part, gold loading capacities of these carbons were determined. For the purpose of evaluation of testing method, coconut shell carbon was firstly investigated. The results obtained hereby were then used in the comparison of results obtained from tested raw materials. In the second part, gold adsorption kinetics of these carbons were investigated. The results were evaluated and used in the comparison in the same way.

#### 4.4.1. Gold Loading Capacity of Coconut Shell Carbons

Since the main aim of this study was to produce activated carbons from indigenous raw materials with as much mechanical strength and gold adsorption properties as much as required in gold hydrometallurgy as an alternative to coconut shells, gold loading capacity of coconut shell carbon, expressed by K-value (gold loading of milled granular carbon in equilibrium with 1 mg/L gold in a standard borate buffered pH 10 solution ), were primarily determined. It was then used in a comparison to those obtained from tested raw materials.

On this basis, K-value expressing the gold loading capacity at room temperature was determined from the Freundlich isotherms (see section 2.4) at 1 ppm residual gold concentration in the test solution. The results are plotted in logarithmic form in Figure 19 and K-value in mg Au/g measured from this figure is given in Table 9.

**Table 9. Gold loading capacity of activated carbons of coconut shells**

| Carbon | K-Value mg Au/gr | Slope | Max. Capacity mg Au/g |
|---|---|---|---|
| Coconut Shell | 31.6 | 0.266 | > 100 |

The slope of isotherm and maximum loading capacity attainable by the carbon are also included in the table for comparison purposes. The values of maximum loading capacity express the loading capacity of carbon at equilibrium with 100 ppm gold concentration in solution. Hence, it could be interpreted as the loading capacity at strong concentrations.

As seen in the figure, the isotherm approximated a straight line in accordance with equation (2.5). It was so expected since Freundlich equation is widely accepted to successfully express the adsorption from liquids. K-value appearing in the table was very high, being 31.6 mg Au/g with a steep slope of 0.266.

Hence, carbon acquired very large maximum attainable capacity (> 100 mg Au/g). It was noticed from these results that K-value given in data sheet of manufacturer (Le Carbons, France) being 31 mg Au/g was satisfactorily measured in laboratory.Thus. It further appeared that the methodology used in this study was suitable to characterize the active carbons for gold loading capacity. As a result, carbons from indigenous raw materials were characterized in the same manner and the results were discussed in sections henceforth.

### 4.4.2. Gold Loading Capacity of Hazelnut Shell Carbons

Since the first target of this study was to produce active carbons with as much mechanical strength and surface area as coconut shells have and then to characterize them for gold adsorption capacity, carbons with best properties were selected and characterized. The physical and chemical properties of selected carbons are given in Table 10.

**Table 10. Physical and chemical properties of selected carbons from hazelnut shells ( steam activated at 800 °C)**

| Carbon | Carbonization | Burn Off % | Ash % | App. Density g/cm$^3$ | Hardness | BET m$^2$/g |
|---|---|---|---|---|---|---|
| A | Slow upto 650 °C | 49.59 | 7.0 | 0.36 | 95 | 785 |
| B | Fast at 650 °C | 50.04 | 7.0 | 0.35 | 97 | 820 |
| C | High Temp. at 900 °C | 52.71 | 8.4 | 0.40 | 93.6 | 825 |

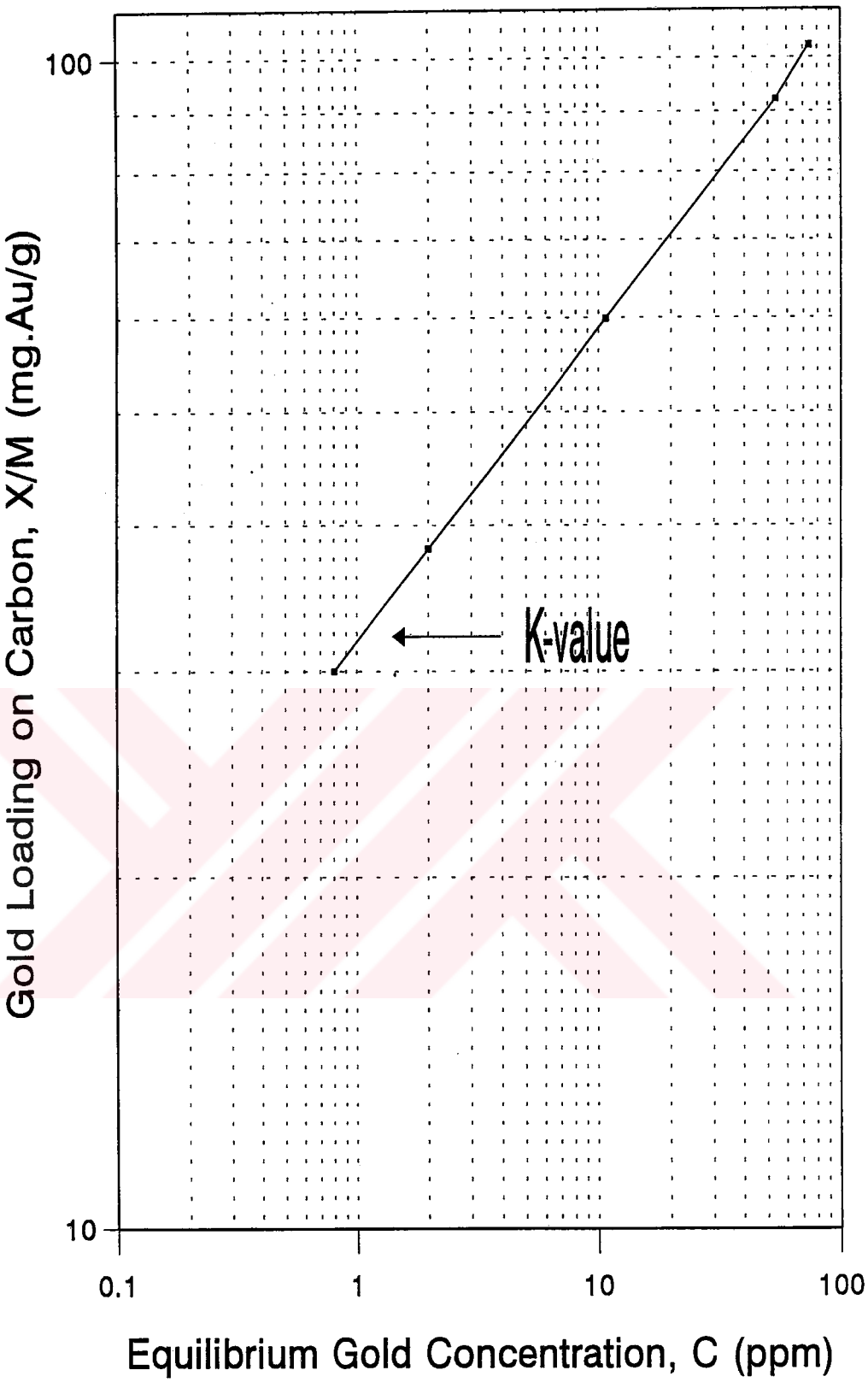


Figure 19. Isotherm of aurocyanide adsorption on coconut shell carbon

It was seen from the table that hazelnut shells should be activated to nearly 50 % weight loss for best carbon. These carbons even had appreciable internal surface area, they are classified as weak carbon for gold hydrometallurgy because of very low hardness values. Apparent densities of carbons were lowered from nearly 0.50 $g/cm^3$ ( density of charcoal ) to approximately 0.40 $g/cm^3$ as a result of internal burning under the action of steam. Carbon had very high ash content in the range of 7.0-8.4 % because of the high inclusions in the raw material.

The results from characterization studies of these carbons for loading capacity in Table 10 are plotted in logarithmic form to set a series of Freundlich isotherms in Figure 20. K-values obtained from this figure at 1 ppm residual gold concentration are tabulated in Table 11.

**Table 11. Gold loading capacity of activated carbons of hazelnut shells.**

| Carbon | K-Value mg Au/gr | Slope | Max. Capacity mg Au/g |
|---|---|---|---|
| A | 19.5 | 0.35 | 90 |
| B | 24.0 | 0.23 | 70 |
| C | 30.7 | 0.14 | 62 |

As illustrated in the figure, the isotherms approximated a straight line in accordance with equation (2.5) and Table 11 showed that carbon from high temperature carbonization had K-value very close to that of coconut shell carbon but, had relatively gentle slope of 0.14.This lead to very low maximum capacity of 62. Carbon from slow carbonization had the lowest K-value (19.5 mg Au/g) with steep slope of 0.34. Thus, this carbon had very high maximum capacity of 90 mg Au/g. Carbon from fast carbonization, on the other hand, had 24.0 K-value with a slope of 0.23. The maximum capacity of this carbon appeared to be 70 mg Au/g in the same table.

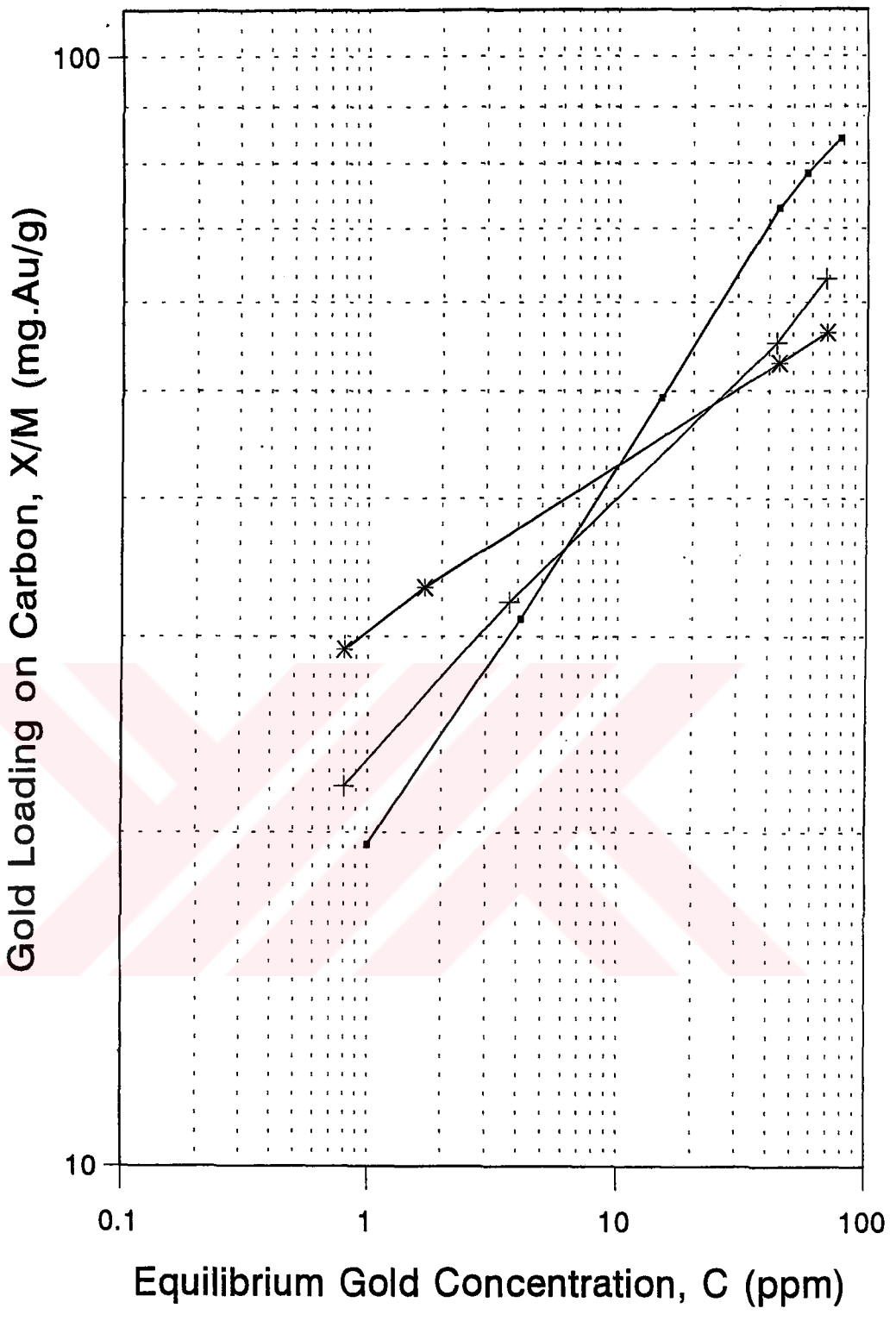


Figure 20. Isotherms of aurocyanide adsorption on hazelnut shell carbons

### 4.4.3. Gold Loading Capacity of Apricot Stone Carbons

In the same sense, activated carbons with best values in surface area and hardness were selected from apricot stone carbons and tested to determine the gold loading capacity. The physical and chemical properties of these carbon are given in Table 12. The isotherms obtained from these carbons are plotted in Figure 21 and K-values measured from this figure are given in Table 13.

**Table 12. Physical and chemical properties of selected carbons from apricot stones ( steam activated at 900 °C)**

| Carbon | Carbonization | Burn Off % | Ash % | App. Density g/cm$^3$ | Hardness | Surface Area BET m$^2$/g |
|---|---|---|---|---|---|---|
| A | Slow upto 650 °C | 48.53 | 2.0 | 0.42 | 107 | 890 |
| B | Fast at 650 °C | 52.70 | 2.1 | 0.38 | 99.5 | 850 |
| C | High Temp. at 900 °C | 44.49 | 2.0 | 0.41 | 114 | 970 |

**Table 13. Gold loading capacity of activated carbons of apricot stones**

| Carbon | K-Value mg Au/gr | Slope | Max. Capacity mg. Au/g |
|---|---|---|---|
| A | 25.8 | 0.26 | 84 |
| B | 26.4 | 0.17 | 60 |
| C | 27.5 | 0.22 | 79 |

As seen in Table 12, apricot stones had to be activated at 900 °C to nearly half of original weight loss to obtain carbons with surface area in the range of 890-970 m$^2$/g. Apparent densities of carbons decreased from 0.56-0.59 gr/cm$^3$ ( density of charcoals ) to 0.38-0.42 gr/cm$^3$ as a result of internal burning. Apricot stones yielded very hard active carbons as deduced from high hardness values in the range of 99.5-114, the former and the latter representing the hardness of carbons from fast and high temperature carbonization, respectively. They had very little amount of ash in their structure in the range of 2.0-2.1 % because of low inclusions in raw material.

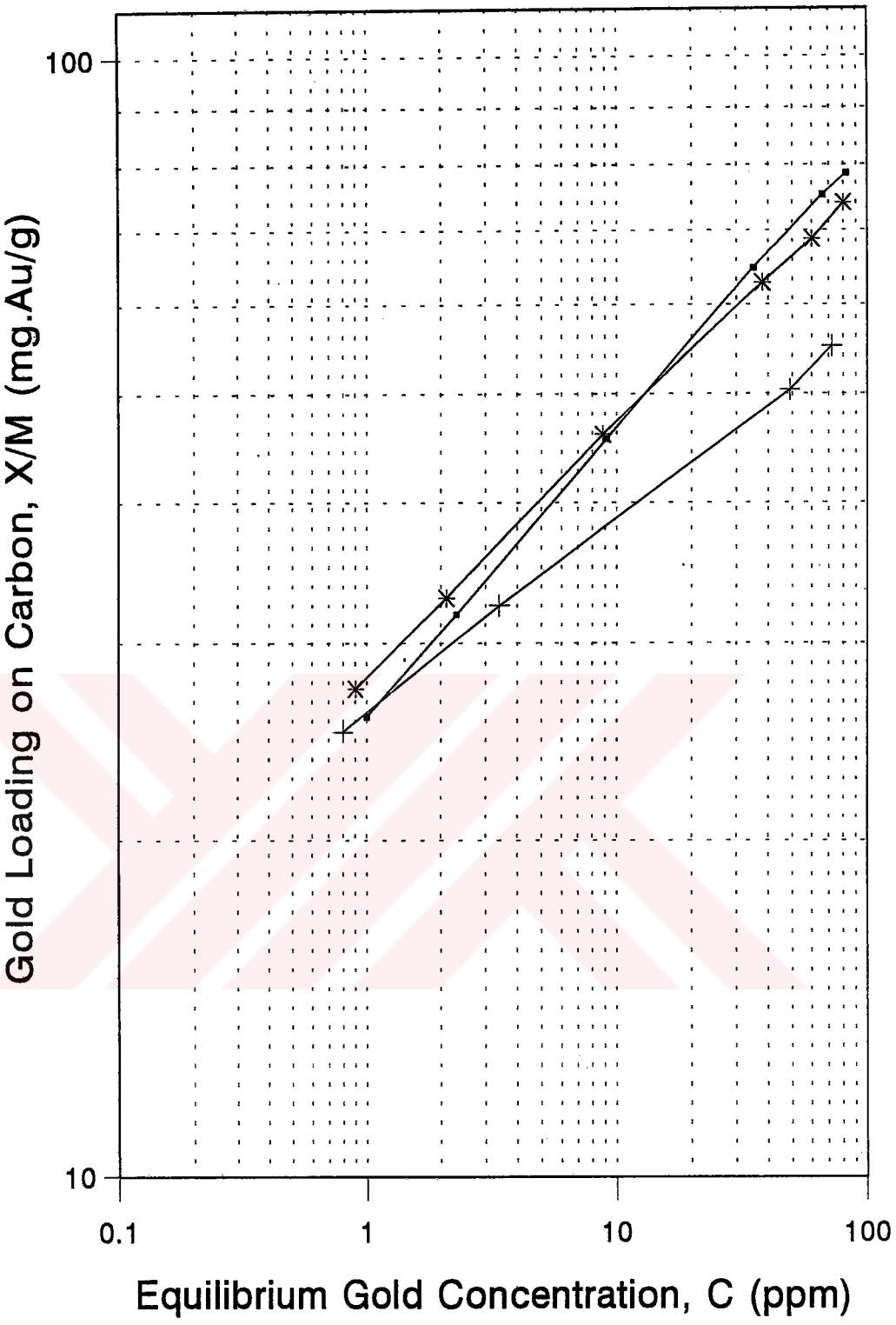


Figure 21. Isotherms of aurocyanide adsorption on apricot stone carbons

Adsorption data plotted in Figure 21 approximated a straight line. This showed the adsorption data under consideration to be expressed by Freundlich equation (2.5). It was noticed from Table 13 that K-values of carbons did not differ significantly from each other.But, the results seemed somehow smaller than that obtained from coconut shell. However, this values fell in the range of K-values of carbon used in industry (Shipman, 1981; Urbanic et al., 1985 and Calgon Carbon Brochure).

### 4.4.4. Gold Loading Capacity of Peach Stone Carbons

Characterization studies were continued with best selected peach stone carbons that have high hardness associated with high surface area. The physical and chemical properties of these carbons are given in Table 14.

**Table 14. Physical and chemical properties of selected carbons from peach stones (steam activated at 800 °C)**

| Carbon | Carbonization | Burn Off % | Ash % | App. Density g/cm$^3$ | Hardness | Surface Area BET m$^2$/g |
|---|---|---|---|---|---|---|
| A | Slow upto 650 °C | 50.0 | 4.0 | 0.35 | 104.0 | 923 |
| B | Fast at 650 °C | 47.1 | 3.5 | 0.37 | 103.5 | 884 |

As seen from the table, peach stones had to be activated at 800 °C to 50 % and 47.1 % burn off for slow and fast carbonized carbons, respectively. These carbons had 884-923 m$^2$/g $N_2$ BET value, 103.5-104 hardness, 0.37-0.35 gr/cm$^3$ apparent density and 3.5-4.0 % ash; the former and the latter values indicate fast and slow carbonized carbons, respectively.

The adsorption data were plotted in Figure 22 to determine K-values that are given in Table 15. The isotherms obtained from peach stone carbons approximated a straight line as observed in the case for hazelnut shells and apricot stones. This was so expected since they were of the same origin and had similarities in chemical structure (see Table 4). K-values obtained from the figure are tabulated in Table 15. As seen from the results in the table, peach stone carbons had very

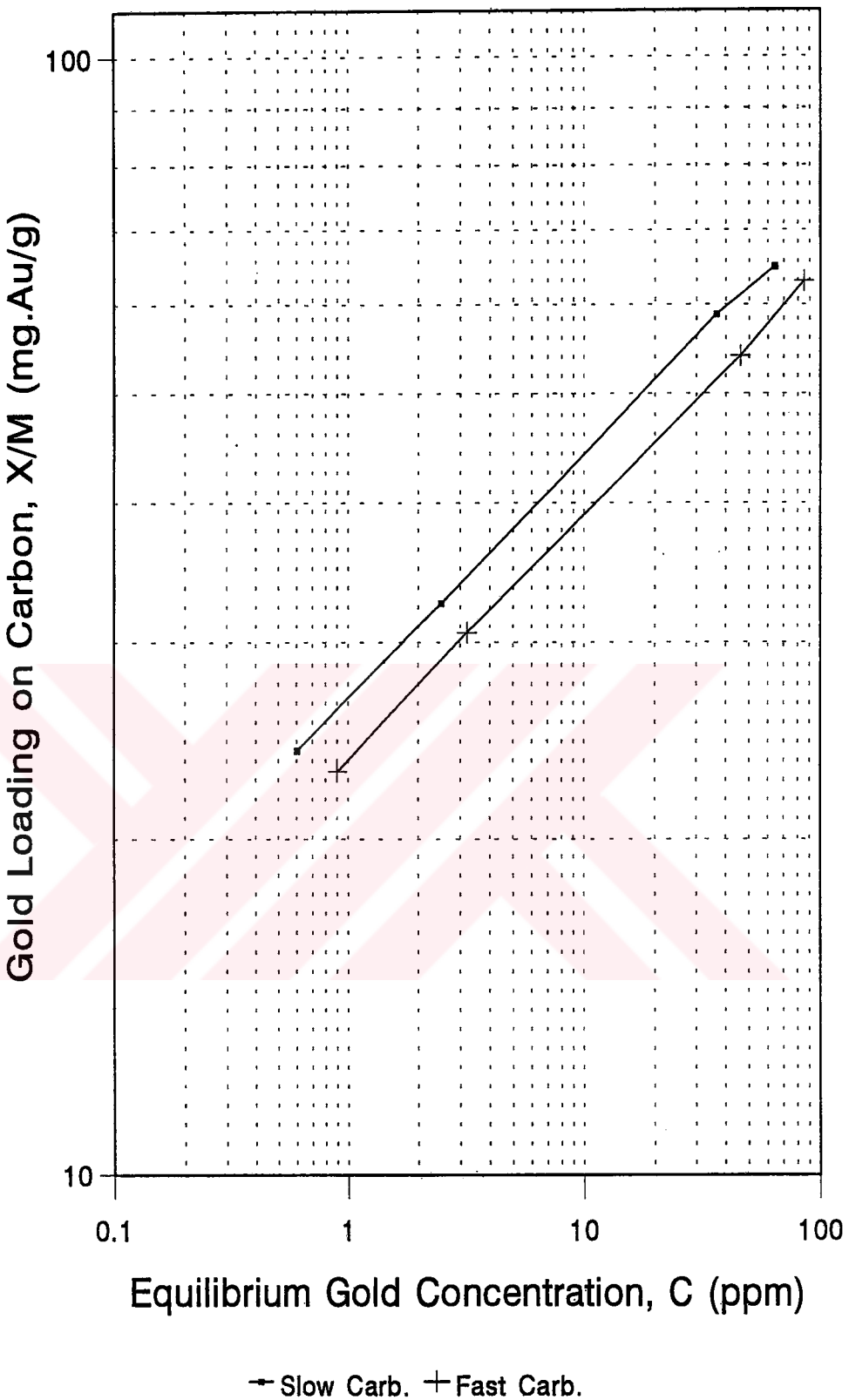


Figure 22. Isotherms of aurocyanide adsorption on peach stone carbons

similar K-values, being 27 and 24 mg Au/g for slow and fast carbonized products, respectively. Furthermore, slope and maximum capacity of carbons seemed proximating to each other. Although the results obtained from peach stones were lower than coconut shell, they fell in the range of K-values of carbon used the industry. Thus, peach stone carbons also had industrial significance and could be considered as a valuable source of raw material for activated carbon production.

**Table 15. Gold loading capacity of activated carbons of peach stones**

| Carbon | K-Value mg Au/gr | Slope | Max. Capacity mg Au/g |
|---|---|---|---|
| A | 27.0 | 0.21 | 73 |
| B | 24.0 | 0.21 | 65 |

### 4.4.5. Gold Adsorption Kinetics of Coconut Shell Carbons

Tests were continued to investigate the gold adsorption kinetics of best selected carbons (mentioned in previous sections; 4.4.2 - 4.4.4) and carbon from coconut shells. This section comprised second part of characterization studies for coconut shell carbons.

In the tests, R-values that expressed the rate of gold adsorption of carbons were determined by exposing 1 gr of -7+14 mesh size fraction of activated carbon to 1.7 L of a borate buffered 5 ppm $KAu(CN)_2$ solution at pH.10. While the reaction took place, the gold concentration of the solution was measured periodically over an eight hour exposure by AAS. The change in the adsorption of gold with respect to time are plotted in Figure 23. The gold adsorption data were then plotted in Figure 24 for R-value determination in accordance with equation (2.6). Figure 24 was consequently used to determine 1/R value at zero time, which was later converted to R-value and tabulated in Table 16. Time required to lower Au concentration by 50 % and residual gold concentration after 1 hour exposure were also included in the table as $t_{50}$ and $C_s$ at 1 hour values for comparison purposes.

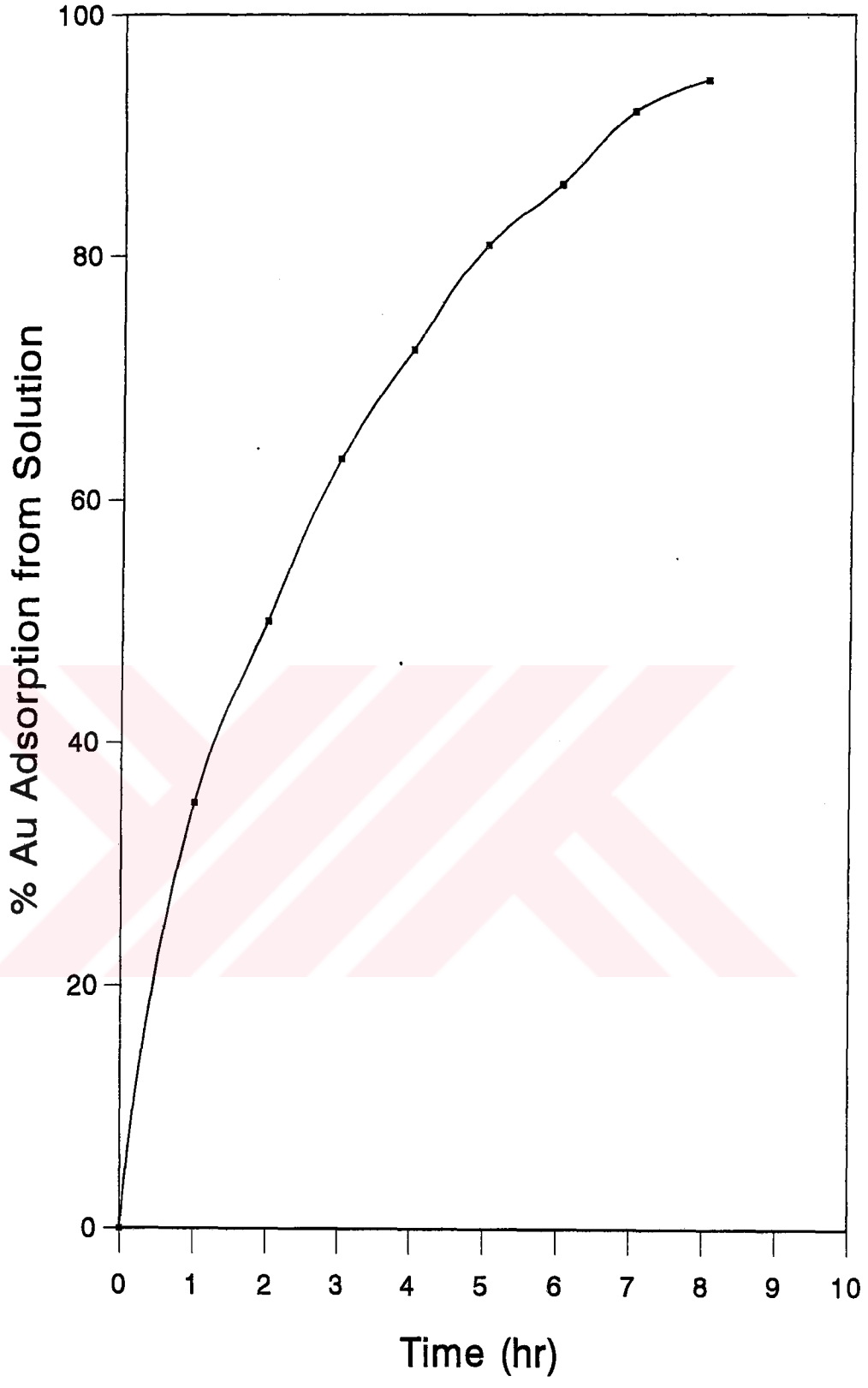


Figure 23. Kinetics of gold adsorption on coconut shell carbon

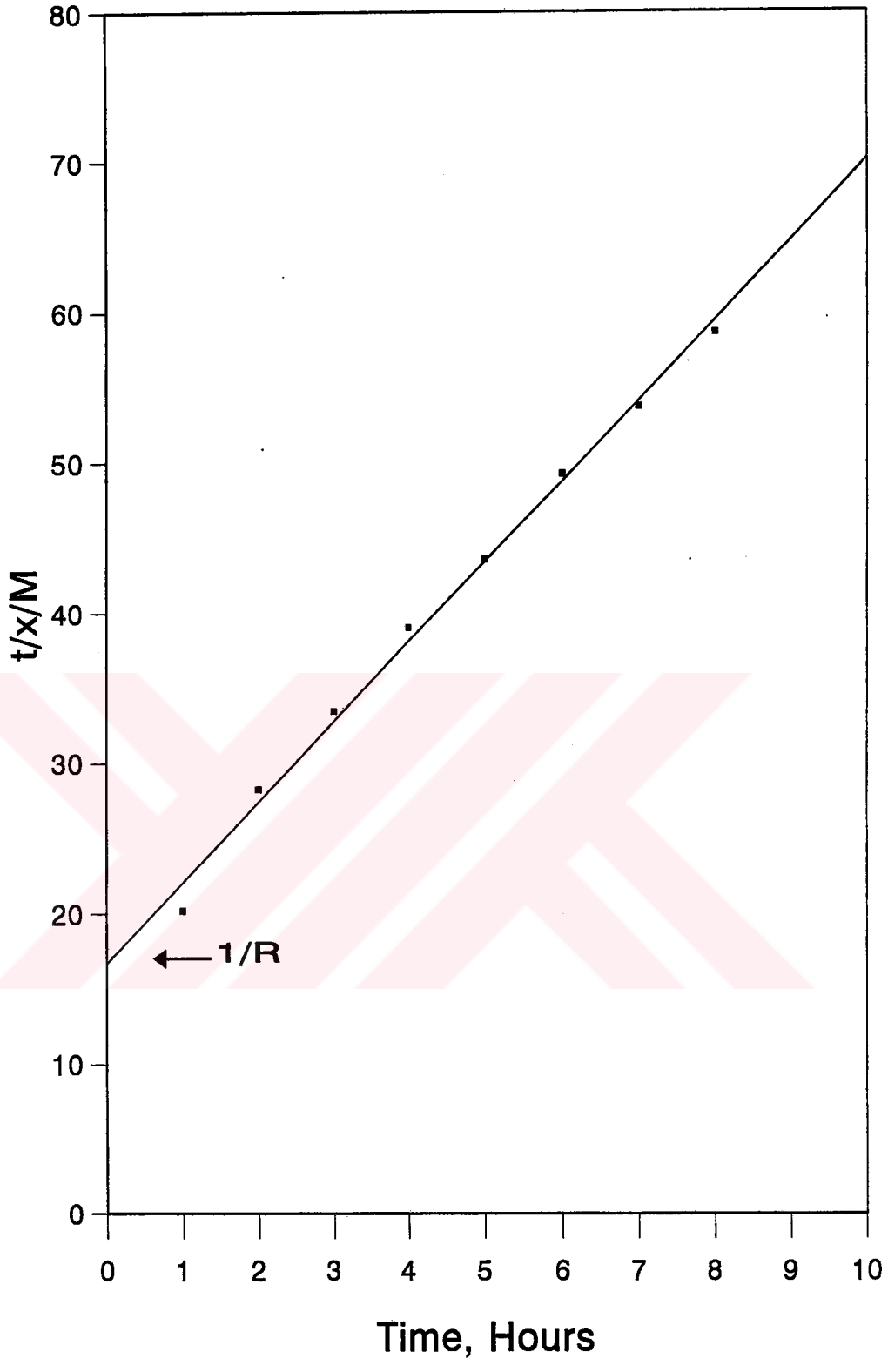


Figure 24. Gold adsorption data plotted for R-value determination (Coconut Shell Carbon)

**Table 16. Rate of gold adsorption by coconut shell carbons**

| Carbon | 1/R | R-Value * | $C_s$ 1 hr | $t_{50}$ * |
|---|---|---|---|---|
| Coconut Shell | 17 | 0.059 | 3.25 | 120 |

It is seen in Figure 24 that experimental points showed a linear variation of experimental data with respect to the reaction time. This showed that gold adsorption data for this carbon could successfully expressed by the empirical equation (2.6). When the results in Table 16 were considered, coconut shell carbon had 0.059 R-value and 3.25 $C_s$ and 120 minutes $t_{50}$ values.This indicated that the results obtained from coconut shell carbon were consistent with that presented in data sheet of carbon (Calgon Carbon Brochure).

### 4.4.6. Gold Adsorption Kinetics of Hazelnut Shell Carbons

Kinetic Tests were continued with previously selected Hazelnut Shell carbons (see Table 10) in a way that was proved with the results obtained from coconut shell carbons. The change in the adsorption of gold with respect to time are plotted graphically in figure 25. The gold adsorption data are then plotted in Figure 26 for R-value determination in accordance with equation (2.6). R-values obtained for each carbon from the figure are tabulated in Table 17. $t_{50}$ and $C_s$ at 1 hr values are also included for a comparison purposes in the same table.

As seen in Figure 26, adsorption data under consideration approximated a straight line shoving a linear variation of data with respect to the time of reaction for all the carbons. Table 17 includes the data obtained from Figure 25 and data obtained from the intercept of this line at zero time in Figure 26. It was seen from the table that carbons from slow carbonization and high temperature carbonization had 0.051 and 0.050 R-value with 130 and 150 min. $t_{50}$ values respectively, while carbon from fast carbonization had slightly higher R-value of 0.057 with 140 min $t_{50}$ value.

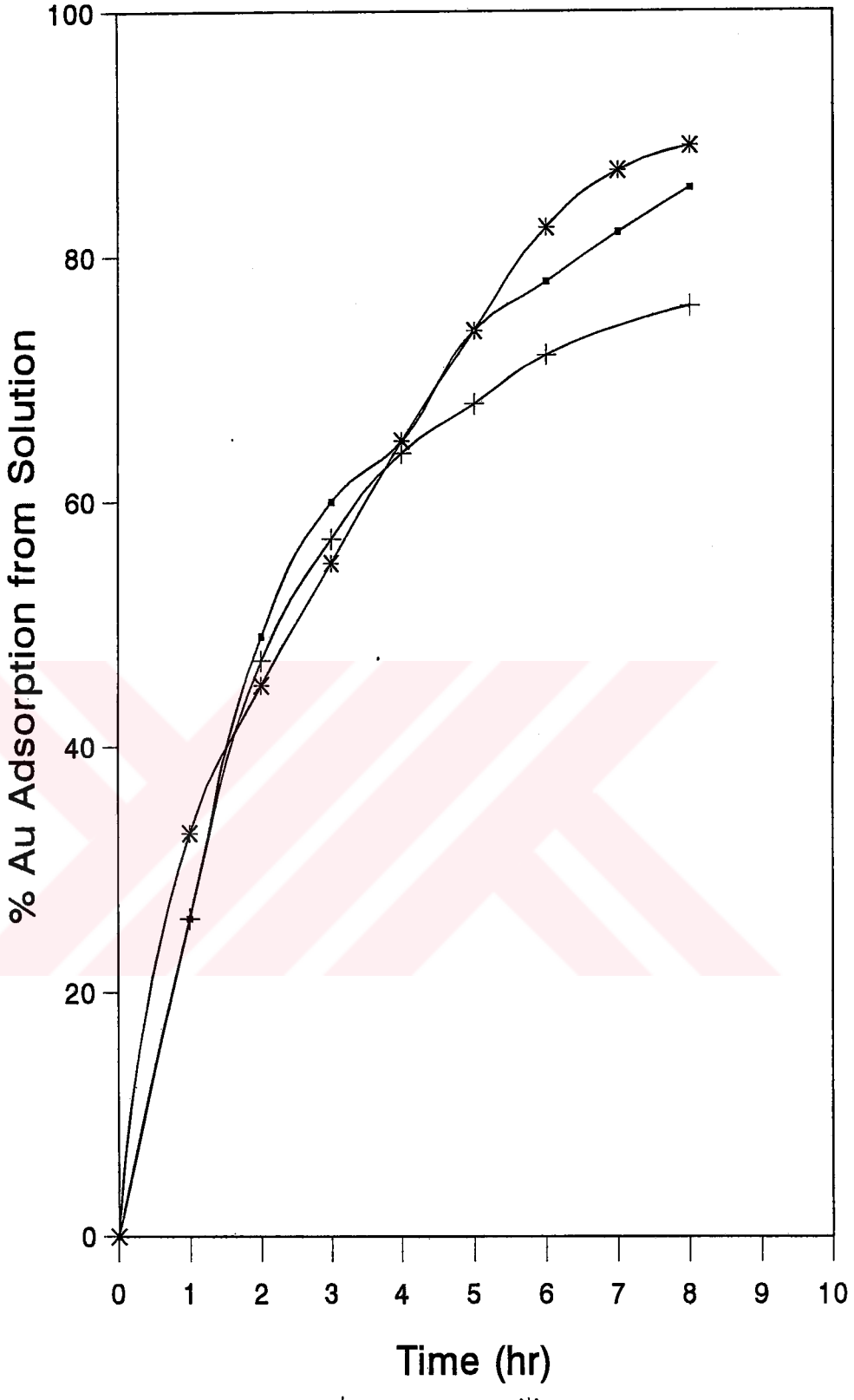


Figure 25. Kinetics of gold adsorption on hazelnut shell carbons

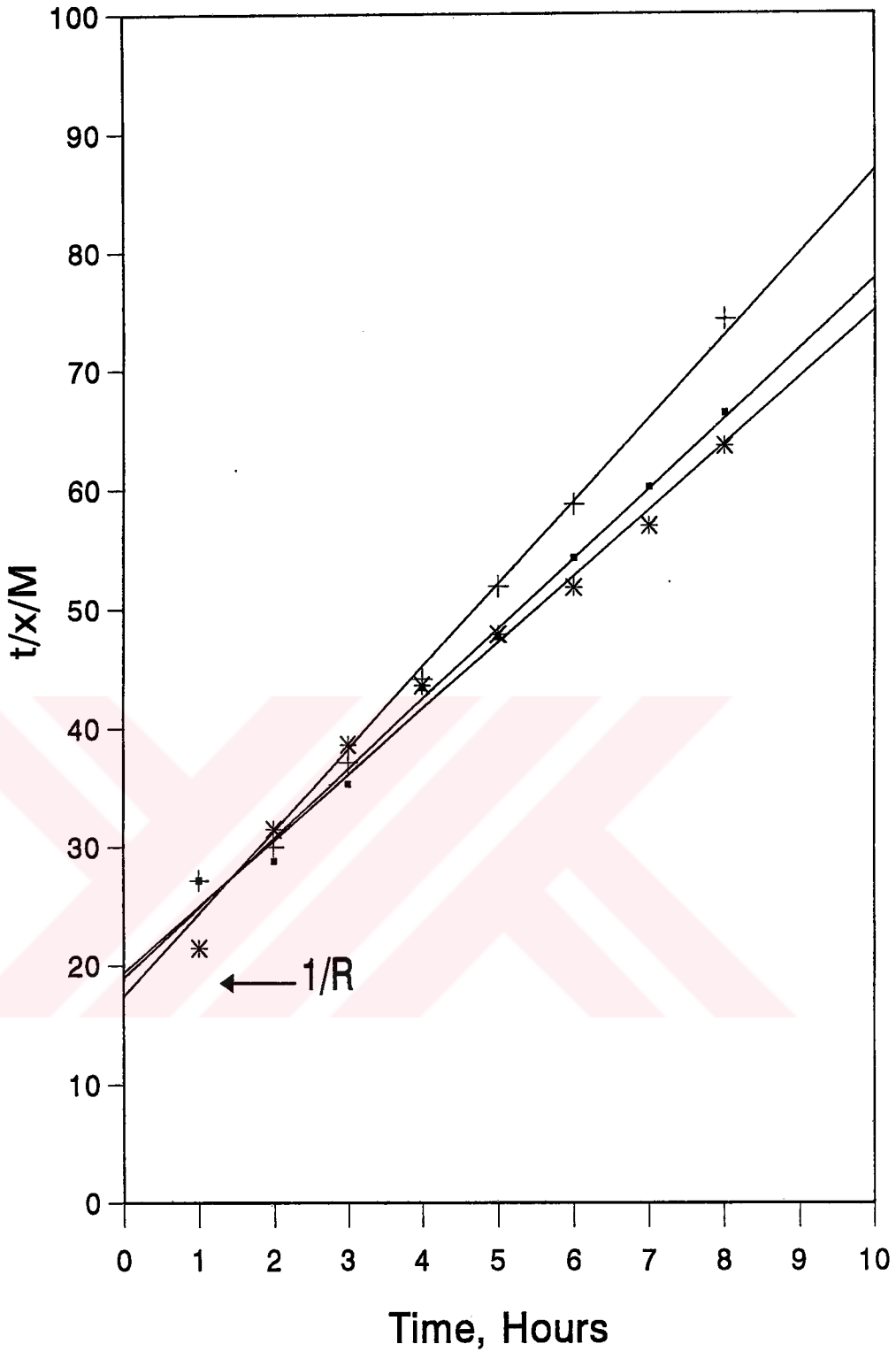


Figure 26. Gold adsorption data plotted for R-value determination (Hazelnut Shell Carbons)

**Table 17. Rate of gold adsorption by hazelnut shell carbons**

| Carbon | 1/R | R-Value | $C_s$ at 1 hr ppm | $t_{50}$ * min |
|---|---|---|---|---|
| A | 19.5 | 0.051 | 3.70 | 130 |
| B | 17.5 | 0.057 | 3.73 | 140 |
| C | 20.0 | 0.050 | 3.35 | 150 |

A : Slow carbonized upto 650 °C

B : Fast carbonized at 650 °C

C : High Temperature carbonization at 900 °C for 1 hour.

* : Measured in Figure 25.

It was also seen from the table that for hazelnut shell carbons, nearly two and a half hours was required to lower the Au concentration by 50 % and this resulted in increase in $C_s$ values in the table, accordingly.

Consequently, hazelnut shell carbons had almost the same adsorption rate as coconut shell carbons with 0.059 R-value, but, $C_s$ and $t_{50}$ values appeared slightly higher.

### 4.4.7. Gold Adsorption Kinetics of Apricot Stone Carbons

The adsorption data obtained from apricot stone carbons selected for characterization experiments (see Table 12) are plotted graphically in Figure 27. The data are further used in Figure 28 for R-value determination.The results are given in Table 18, together with $t_{50}$ and $C_s$ at 1 hr values.

As seen from the table carbon from fast and slow carbonization with R-values of 0.054 and 0.060, respectively and $t_{50}$ of 120 minutes had the same adsorption rate as coconut shell carbons had with 0.059 R-value and 120 minutes $t_{50}$ value. Carbon from high temperature had slightly lower R-value indicating poor adsorption kinetics. $t_{50}$ and $C_s$ values of this type carbon appeared higher, accordingly.

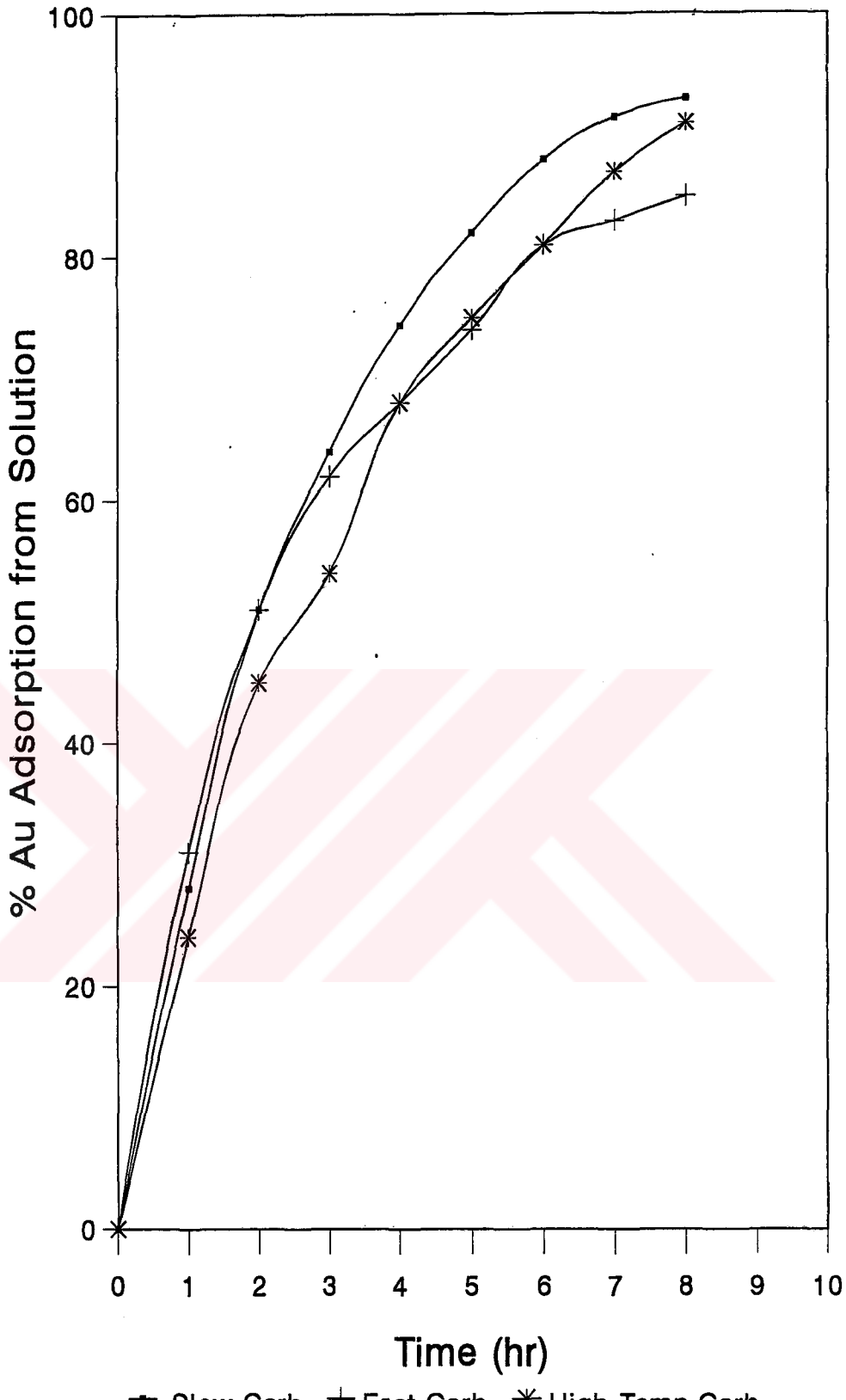


Figure 27. Kinetics of gold adsorption on apricot stone carbons

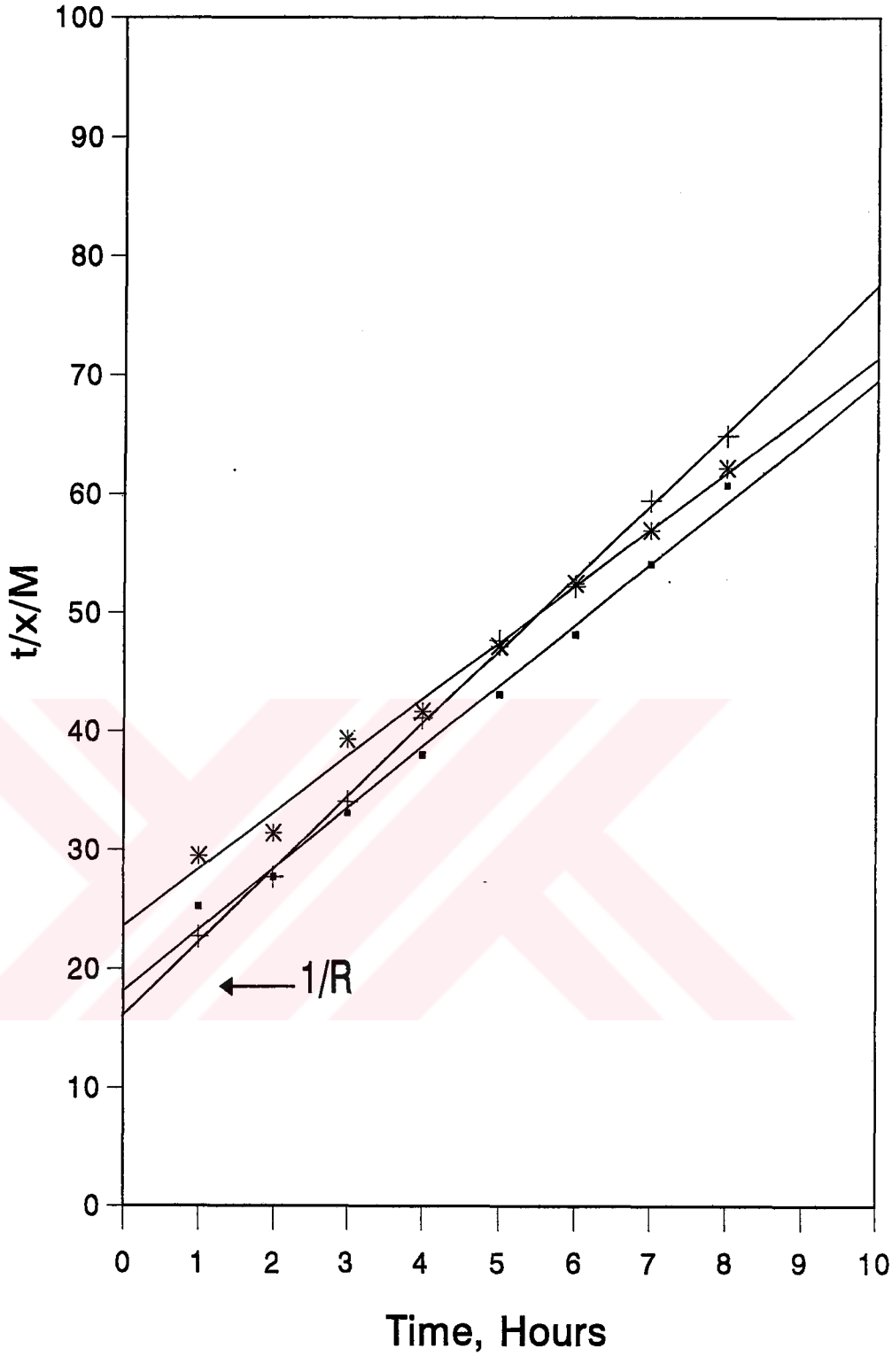


Figure 28. Gold adsorption data plotted for R-value determination (Apricot Stone Carbons)

**Table 18. Rate of gold adsorption by apricot stone carbons**

| Carbon | 1/R | R-Value | $C_s$ at 1 hr ppm | $t_{50}$ min |
|---|---|---|---|---|
| A | 18.5 | 0.054 | 3.60 | 120 |
| B | 16.6 | 0.060 | 3.45 | 120 |
| C | 23.5 | 0.043 | 3.80 | 160 |

A : Carbon from slow carbonization
B : Carbon from fast carbonization
C : Carbon from high temperature carbonization.

Thus, it was recognized that apricot stones could yield active carbon with desired level of activity under steam oxidation of fast and slow carbonized charcoals. As mentioned in previous sections comprising the results of K-values for apricot stones, this type carbon had also very high gold adsorption capacity, nearly approaching to that of coconut shell carbons. Hence, apricot stones appeared as a valuable source of raw material for activated carbon production.

### 4.4.8. Gold Adsorption Kinetics of Peach Stone Carbons

Last series of tests were carried out with selected peach stone carbon (see Table 14). R value of these carbons were determined by adsorption experiments in a similar manner. The adsorption data are plotted in graphical form in Figure 29, that is further used in Figure 30 for R value determination. The adsorption data plotted in Figure 30, in accordance with equation (2.6) were then used to determine 1/ R value which was later converted to R value and tabulated in Table 19.

**Table 19. Rate of gold adsorption by peach stone carbons**

| Carbon | 1/R | R-Value | Cs at 1 hr ppm | $t_{50}$ min |
|---|---|---|---|---|
| A | 23.0 | 0.043 | 3.70 | 210 |
| B | 22.0 | 0.045 | 3.65 | 160 |

A : Carbon from fast carbonization
B : Carbon from slow carbonization

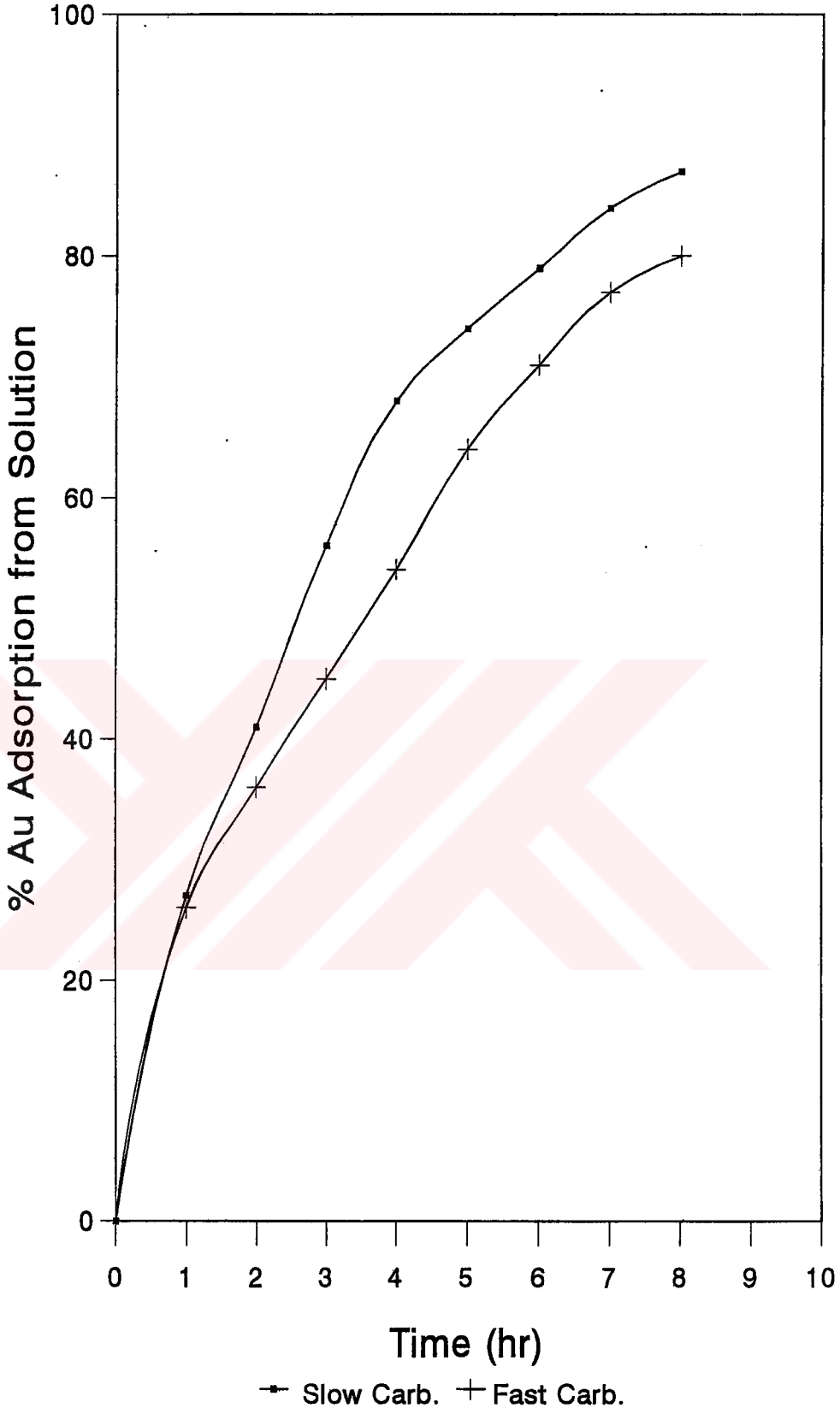


Figure 29. Kinetics of gold adsorption on peach stone carbons

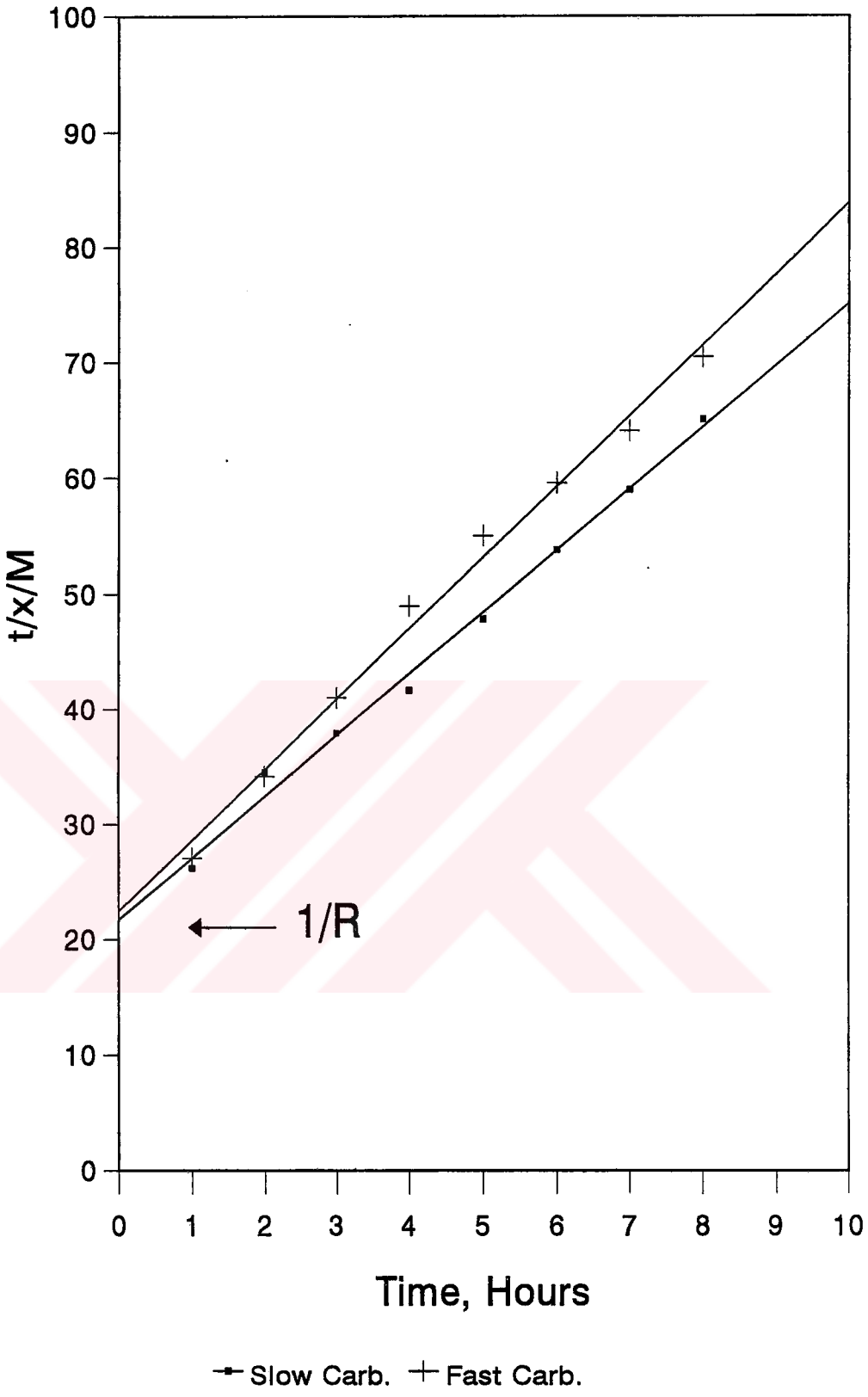


Figure 30. Gold adsorption data plotted for R-value determination (Peach Stone Carbons)

As seen from the results in the table, peach stone carbons were considered as poor in gold adsorption with lower R-value in the range of 0.043 - 0.045, the former indicating the fast carbonized products. $C_s$ at 1 hour values appeared very high with 3.65 ppm and 3.70 ppm for slow and fast carbonized carbons, respectively and thus, larger amount of gold resided in the solution after a particular contact time, accordingly. In the same respect, time required to lower the gold concentration by 50% increased, consequently.

# CHAPTER V

# DISCUSSION

## 5.1. Carbonization

### 5.1.1. Effect of Temperature on the Mass Loss Attained in Carbonization

As indicated in Figure 5, a sharp increase in the weight loss was observed at carbonization temperatures upto 650 °C. It was so expected since hazelnut shells as in the case of other cellulosic materials are known to contain, depending on their degree of volatility, combustible or non-combustible all lower molecular weight gases (CO, $CO_2$, $CH_4$, $H_2$, $O_2$ etc.) including water, high molecular weight tarry products and carbon rich solid residue (namely charcoal). Usually, gas phase matters are constituting 20-25 % of total product of carbonization and have a boiling point below 300 °C. Tars constituting approximately 60-65 % of the product are of high molecular weight products; hence they have a boiling point higher than 300 °C. The solid residue rich in carbon constitutes the rest of raw material (20-30 %). The main purpose of carbonization is to increase the carbon content to at least 80 % in the solid residue for effective subsequent activation by steam.

As a result, gases and to a very great extent tars, were driven off the structure, charcoal constituting nearly 30 % of the original raw material remained in place. The amount of mass loss attained after 650 °C did not change significantly with respect to time. This indicated the completion of dehydration and devolatilization after removing nearly all the volatile matters from the structure.

Thus, carbonization of hazelnut shells at 650 °C was accepted as the optimum carbonization temperature.

### 5.1.2. Effect of Temperature on Fixed Carbon Content of Charcoals of Hazelnut Shells.

As illustrated in Figure 6, the fixed carbon content of charcoals exhibited a sharp increase upto 650 °C at all carbonization times. It was so expected since charcoals enriches in mostly non-volatile carbon after giving off volatile substances as carbonization proceeded. It was also appearing in the figure that the fixed carbon content of charcoals produced at 650 °C attained higher than 83.2 % in the product even in the initial period of carbonization and very little change was observed thereafter. Since the main purpose of carbonization is to increase the fixed carbon content to higher than 80 % in the product, carbonization of the hazelnut shells at 650 °C would be defined as optimum carbonization condition to convert it to suitable form for activation. Because of having similarities in their chemical structure, all the raw materials investigated were carbonized at 650 °C.

### 5.1.3. Effect of Carbonization at 650 °C on the Structural Contents of Charcoals

As deduced from Table 4, all raw materials resulted with very low yields after carbonization at 650 °C. This was so expected since these materials contained very large amount of volatile water which were driven off, together with water, from the structure. Thus, weight lost increased accordingly, that eventually resulted low yields after carbonization.

It was also deduced from Table 4 that fixed carbon contents in the charcoals from all raw materials were around 88 % which were higher than desired levels for a successful activation by steam. Furthermore, these values came out very close for each raw material. This finding was attributed to the fact that they were of the same "cellulosic" origin and that they have similarities in chemical structure. (see

Table 3). On the other hand, charcoals contained some residual volatile matter in the range of 8-11 % which were thought to be driven off the structure only at higher temperatures than 650 °C. Moreover, it was supposed that this residual volatile matters (mostly tars) enclosed or at least partly blocked the entries of pores by decomposition and filling the pores. Thus, while freed atoms of elementary carbons were grouped into organized crystallographic formation known as elementary graphitic crystallites, the interstices between them closed and clogged so that charcoals were presumably supposed to have low surface area and hence low activity.

### 5.1.4. Effect of Heating Pattern in Carbonization on Structural Contents of Charcoals

As depicted in Table 5, an increase in the final temperature of carbonization resulted charcoals with fixed carbon contents reaching to 94 % and 92 % for hazelnut shells and apricot stones, respectively. This was expected since that were hard to drive off at lower temperatures, larger amounts of volatile matter were removed from the structure. This was deduced from lower volatile matters contents of charcoals with 2 % and 6 % for hazelnut shells and apricot stones respectively. As the final carbonization temperature increased to 900 °C, many of the hydrogen atoms or hydrocarbon groups (mainly tars) were driven off (as indicated by low volatile matter contents in Table 5), leaving a structure with much more open porosity . These pores had been clogged previously by residual tarry substances. Furthermore, the more deeply the process of compaction of the material took place under high temperature and stronger became the granules. Thus, this type of charcoals were expected to have high hardness value and high surface area as measured by $N_2$ BET value. It was also depicted in the same table that chemical properties of charcoals carbonized by slower heating did not differ very much from the same properties of charcoals of fast heating carbonization. This was so expected since the rate of rise of the temperature in carbonization was of little importance in driving off the same amount of volatile matter at the same final carbonization temperature used in fast carbonization. However, the effect of this factor was assumed to be great on the formation of porous structure of final

product. Thus, the higher the rate of heating of the raw material, the greater is the foaming of structure formed through the rapid evolution of volatile products and the greater is the total pore volume of carbonized products .

Consequently, different carbonization conditions were supposed to have great influence on the final properties of active carbons after activation by steam.

### 5.1.5. Effect of Carbonization on the Physical and Chemical Properties of Charcoals

As seen in Table 6, charcoals produced at elevated temperature (900 °C) had the greatest surface area in their series; being 141 $m^2/g$ and 140 $m^2/g$ for hazelnut shells and apricot stones, respectively, Besides, they had the highest hardness values for all the testing conditions. In this sense, hazelnut shells and apricot stones yielded charcoals with 114.5 and 135.4 hardness, respectively. This was so since most of the volatile materials (mainly tars) that were initially blocking the entries of pores were driven off the structure leaving open porosities to the penetration of $N_2$ molecules and leaving a structure enriched in carbon element mostly. This together with the compaction effect of high temperature on the layers of microcrystallites of charcoals increased the hardness of granules. To some extent, all the other charcoals produced at relatively lower temperatures also acquired mechanical strength while because of this enrichment of carbon element in the structure; but, the values were lower. It must also be mentioned here that since nitrogen and iodine molecules are as small the size of micropores (~ 16 °A vs 8-10 °A) in the product, the $N_2$ BET and iodine numbers represented the presence of micro porosity in the charcoals. Meanwhile, the difference between the values for each charcoal indicated the differences in the structure and in the distribution of pores. On the other hand, lower values of these numbers indicated poor activity since activity of carbons for gold adsorption was directly related to the BET surface area of carbons.

## 5.2. Activation

### 5.2.1. Effect of Temperature and Burn-off on the Surface Area and the Hardness of Activated Carbons

#### 5.2.1.1. Hazelnut Shells

It appeared from the carbonization results that charcoals of any kind had very low surface area; hence low activity for gold adsorption. Thus, the process of oxidation by steam; namely activation by which the carbonized product develops an extended surface area and a porous structure of molecular dimension was essentially required. The results of steam activation of fast carbonized charcoals from hazelnut shells are plotted in Figures 7 and 8.

Figure 7 showed that the surface area of the carbons sharply increased in the initial period of activation with an increase in the percentage of burn off. This was expected to result by the action of active oxygen in the activating agent. Active oxygen in the steam burnt away the more reactive portions of the carbon skeleton as CO and $CO_2$ in consequence with equation 2.1. As combustion proceeded to further burn offs, a preferential etching occurred. This resulted in the development of a large internal surface area with nearly 823 $m^2/g$ $N_2$ BET number at 49.5 % burn off for 800 °C activation and the creation of a pore structure with micropores in majority. The art of the manufacturing active carbon lies in the fact that the activation process must be conducted in such a way that combustion of the carbonized raw material occurs internally. This was supposed to be occurred at 700 °C and 800 ° C. However, higher activation temperatures ( 900 ° C and 1000 °C ) burnt the exterior parts of the granules. At these high temperatures, the reaction of active oxygen in steam with carbon surface was faster than the diffusion of active oxygen through the particles and mostly the exterior parts of the granules were burnt away. This offset any more increase in the surface area of the final product.

Eventhough the activity of the products as measured by $N_2$ BET value is known to be approximately proportional to the degree of burn off, this appeared to be true in the same figure upto a certain point. This point corresponded to the formation of micropores, where further burn off in fact resulted in a reduction in the $N_2$ BET surface area values. Commonly, this occurred in between 50-60 % burn offs. This phenomenon was related to the conversion of micropores into mesopores and macropores by burning away of pore walls entirely. A concomitant loss in structural strength of the product wall also expected presumably at this point to result. Considering all these, activation at 800 °C was selected as the optimum temperature for surface area development in the active carbons. The active carbons produced at 800 °C had 823 $m^2/g$ BET surface area and nearly half of the original weight of charcoal was burnt away internally in majority.

Figure 8 shows the change in the hardness of activated carbons produced from hazelnut shells. As indicated in the figure, the hardness of the products sharply increased in the initial period of activation as the activation temperature increased from 700 °C to 1000 °C. This was so because it was previously emphasized that the higher the temperature particles were exposed to, the further the processes of compaction of micro crystallites take place and the stronger become the particles. For all the temperatures of activation, the hardness of the particles was found to be proportional to the degree of burn off upto a point where further increase in burn off indeed resulted in a reduction in the hardness and carbons become weakened gradually. This was related in case to the weak action of active oxygen in the initial period of activation. It was mainly used in a process of removing the residual tarry products and disorganized carbon. The corresponding points were 25 % burn off for 1,000 °C and 15-20 % burn off for other temperatures. The cleaned surface of the elementary crystallites were then exposed to the strong action of active oxygen in steam. Consequently, the structure of carbon weakened as the activation continued. It must also be mentioned that the rate of chemical reaction rised considerably faster than diffusion through the particles and the process begin to be limited by the supply of oxidizing agent within the particles. Under this condition, the concentration of oxidizing agent fell in the direction towards the center of the granule. Thus, a well oriented pore structure and extended surface area did not develop. This was deduced from the lower surface area values in the initial period

of activation in Figure 7. Hardness of particles declined after these points and when the activation was allowed to proceed upto nearly 50 % burn off to yield active carbon with highest surface area (see Figure 7), hazelnut shell carbons acquired lower mechanical strength with hardness values in the range of 90-95, the later indicating the hardness of the carbon produced at 1,000 °C, than the desired value for coconut shell carbons.

#### 5.2.1.2. Apricot Stones

As shown in Figure 9, the surface area of active carbons produced from apricot stones charcoals that were carbonized by fast heating was observed to increase rapidly upto approximately 50 % burn off. This point was expected to represent a pore structure with micropores in majority. However, a sharp decrease after this point was observed in surface area of the carbons activated at temperatures especially between 700 and 900 °C . Widening or shrinkage of pores by volume increase as observed in activation of hazelnut shells was expected to result in the particles. This diminished the surface area of carbons by pore transformation from micropores to pores with larger open area. Those carbons produced at 1,000 °C, however, had their surface area developed in a different way under oxidation by steam such that pore transformation was not observed even when the burn off reached 70.5 %. Thus, it was noticed that this temperature was too high for preferential etching and activation proceeded in such a way that combustion of carbonized raw material occurred from the exterior of the granules, not internally that was intended to proceed in a controlled activation process.

Considering the results obtained from the activation of fast and slow carbonized charcoals, apricot stones and hazelnut shells had the largest surface area when the activation proceeded upto nearly 50 % burn off and for both, further oxidation reduced the surface area. As emphasized above, this was attributed to pore transformation in the structure. However, apricot stones appeared with larger surface area than hazelnut shells for all the activation conditions. As a final consideration of surface area results of apricot stone carbons activation of carbons

at 900 °C to about 49.5 % burn off was evaluated as optimum activation condition. Carbon produced at this level of oxidation had 896 $m^2/g$ BET surface area.

The change of hardness of apricot stone carbons with respect to the degree of activation was also considered and the results are plotted in Figure 10. As indicated in Figure 10, the hardness of the granules increased rapidly upto 109.2 at 700 °C, 108.9 at 800 °C, 110.3 at 900 °C and 109.6 at 1,000 °C in the initial period of activation. However, a drastical reduction in hardness values of carbons were observed there after. This result was attributed to the same finding as previously discussed for hazelnut shell carbons that the two mechanisms, namely compaction by heat and chemical reaction (oxidation) by steam were competing with each other during activation. At lower levels of burn off (< 15 %), the granules acquired mechanical strength due to the layer compaction by heat and power of oxidative steam was used in the burning out the disorganized or amorphous carbon and residual hydrocarbons; mainly tars; hence the surface of the layers of microcrystallites was not subjected to oxidation effect of steam. As the activation proceeded with further burn offs, the cleaned surface of layers of microcrystallities and thereby, vertical distance between these layers became exposed to the strong action of steam which led to the formation new pores, mainly micropores by selective etching the more reactive carbons in these regions. Consequently, a point reached after which further oxidation of the granules lowered the hardness values, indicating the structural damage due of pore transformation.

In preceding part of this section, it was recognized that the granules enriched in microporosity when nearly half of the original weight was burnt out. As indicated in Figure 10, very stiff active carbons with hardness values of 99.7 at 700 °C (43.8 % burn off), 100.1 at 800 °C (43.7 % burn off), 101.7 of 900 °C (47.5 % burn off) and 107 at 1,000 °C (40.2 % burn off) could be produced at this level of oxidation. Furthermore, these values were very high as compared with coconut shell carbons. Therefore, apricot stones appeared as a good raw material for carbon production.

#### 5.2.1.3. Peach Stones

It is evident from Figure 11 that 800 °C activation of peach stones to about 44.3 % burn off seemed the optimum condition such that particles were expected to be burnt internally that yielded active carbon with 911 $m^2/g$ surface area. Lower activation temperatures yielded poor carbon with lower surface area while nearly 15 % excessive burn off needed at 900 °C activation to yield carbon acquiring as much surface area as obtained at 800 °C activation. The maximum surface area obtained at 800 °C being 911 $m^2/g$ was very well comparable to the surface area of coconut shell carbons with 1,000 $m^2/g$. Furthermore, peach stones yielded very stiff carbon at 800 °C and 900 °C activation temperature with hardness values all above 100 under oxidation of particles to 50 % burn off as indicated in Figure 12. This showed that peach stones could be a another valuable source of raw material after apricot stones for active carbon production.

### 5.2.2. Effect of Heating Pattern in Carbonization on the Surface Area and the Hardness of Activated Carbons

#### 5.2.2.1. Hazelnut Shells

As deduced from Figure 13, the surface area of active carbons produced by the activation of charcoals at 800 °C sharply increased to approximately 850 $m^2/g$ in a proportionality to the degree of burn off. At this point, nearly 50 % of the original weight was burnt away due to the action oxidizing agent. Further increase in burn off resulted in the transformation of micropores that was dominated in the particle to mesopores and macropores by shrinkage in pores and hence removed pore walls entirely. Consequently, a drastical reduction in surface area values were observed.

It was also deduced from the same figure that carbonization conditions did not affect significantly the surface area occurrence in the final products. All carbons had highest values at nearly 50 % weight loss. Although these values being 832 $m^2/g$ for slow carbonized products and 823 $m^2/g$ and 843 $m^2/g$ for fast carbonized

and elevated temperature carbonization, respectively, were significantly lower than that of commercial active carbon with 1,000 $m^2/g$ surface area, they were in the range of acceptable limits.

Figure 14 shows the change in the hardness of active carbons produced by activating the hazelnut shell charcoals at 800 °C with respect to the degree of burn off. It was recognized that the hardness of carbons previously carbonized at elevated temperature started from a very high value of 115 (hardness of charcoal) in contrast to 89 and 82.6 hardness values of fast and slow carbonized products, respectively, and it decreased down to 90 as the activation continued to 40 % burn off. But, very little change was observed thereafter. This was attributed to the high temperature compaction of microcrystallites of carbon in carbonization. However, this type of charcoals were expected to have a equally resisting property as activated carbon to oxidation due of graphitization process that occured at this level of temperature. Thus, during subsequent selective oxidation, it became very difficult to develop a micropore structure by burning out of the reactive carbon elements in the interstices between the micro crystallites and partial burning out of basal planes of micro crystallites without extensively damaging the structure.

On the other hand, products carbonized at lower temperatures were expected to be more reactive. Hence, they were observed to be more easily oxidized by the action of steam. As appeared in Figure 13, charcoals produced at 650 °C by fast and slow heating were easily oxidized upon activation to 25 % and 45 % burn offs respectively. Carbons produced at these points had 99 and 95 hardness and 555 m2/g and 800 m2/g surface area for fast and slow carbonized active carbons, respectively. As a result, it was noticed that hazelnut shells yielded relatively weak carbons with lower surface area values as compared to that of coconut shell carbons.

#### 5.2.2.2. Apricot Stones

Figure 15 depicted the surface area formation (hence development of pore system) in the active carbons under exposure to the action of steam at 900 °C. This

temperature appeared as the optimum activation temperature for apricot stones charcoals that were carbonized at a faster heating. Therefore, effects of rate of heating and elevated temperature carbonization on the surface area formation were examined at this activation temperature. It appeared in the figure that charcoals from fast and slow carbonization behaved similarly and typically in activation conditions at 900 °C. The highest surface areas were obtained at 54 % and 55 % with 906 $m^2/g$ and 850 $m^2/g$, respectively, for slow and fast carbonization. This was due to the micropore formation upto nearly 50 % burn off. Further deep oxidation widened the micropores by removing the walls between neighboring pores and transformation of pores to larger sizes started henceforth. This caused no more increase in $N_2$ BET numbers and particles were composed of mixed pores; micropores, mesopores and macropores. The particular importance of occurrence of mixed pores in the structure comes from the fact that these pores function to serve transport arteries that make the internal parts of the carbon granules readily accessible to the molecules being adsorbed. Figure 15 also indicated that the surface area of active carbons previously carbonized at elevated temperature increased upto 1,150 m2/g even at very deep oxidation levels (68.8 % burn off). This could be explained by strongly compacted structure of charcoals. The action of oxidizing agent occurred preliminary on the lateral surfaces of microcrystallites because of the rate of chemical reaction of steam with disorganized carbon and tars rised faster than diffusion into this hardly compacted structure. As activation further proceeded, oxidizing agent diffused through the compacted material and additional micropores were developed between the layers and on the surfaces of inferior microcrystallites. But, this led to the weakening of the structure as indicated in Figure 16.

Figure 16 also indicated that the hardness of active carbons from fast and slow carbonization sharply increased to maximum values being 105 and 107, respectively, and then, decreased gradually near 50 % burn off. In contrast to these results, hardness of active carbons from high temperature carbonization started from 135.4 and decreased down to 98 at very high level of oxidation. The decrease in the hardness values of slow and fast carbonized carbons was a result of pore transformation. But, the effect of steam upon strongly compacted structure

to open porosity resulted a decrease in hardness values of carbons from high temperature carbonization.

Beside of this theoretical interpretation of experimental results, considering % 50 weight loss as optimum activation condition to yield carbon with largest surface area, apricot stones previously carbonized at different heating yielded active carbons with hardness values all above 100 that competed very well with the hardness of coconut shell carbons. Thus, apricot stones had appreciable importance in active carbon production and considered as a valuable source of raw material that yield suitable carbon to resist highly abrasive CIP and CIL operating conditions.

### 5.2.2.3. Peach Stones

It was deduced from the carbonization results that peach stones when carbonized by fast heating could be very well activated at 800 °C to 44.3 % burn off. This resulted in an excellent carbon with 911 $m^2/g$ $N_2$ BET and 103.4 hardness values. Therefore, effects of slower heating in carbonization on the properties of final products were studied by activating the charcoals at 800 °C and the results obtained are plotted in Figures 17 and 18.

As indicated in Figure 17, the surface area of active carbons of slow carbonization increased gradually upto 962 $m^2/g$ at 52.6 % burn off while a lower value of 911 $m^2/g$ $N_2$ BET surface area at relatively lower burn off of 44.3 % was seen for carbons of fast carbonization. Similarly nearly half of the original weight had to be burnt out for slow carbonization to reach this maximum surface area. Thus, the finding that carbons had largest surface area (hence enrichment in micropores) when they were activated at between 40-60 % burn off was supported by these results. It was also noticed from the same figure that heating manner did not affect the surface area formation significantly. However, carbons of slow carbonization appeared slightly harder than that of fast carbonization when oxidation continued near to 50 % burn off as seen in Figure 18. Figure 18 also dedicated that the peach

stones of both kind could yield active carbon with hardness number around 100 that could be very well comparable to that of coconut shells.

Generally considering both surface area and hardness of products in activation, peach stones behaved similarly to apricot stones and to some extent hazelnut shells. As a result, peach stones were also considered as valuable source of raw material for activated carbon production for gold metallurgy.

### 5.3. Chemical Activation

Some basic information about active carbon production by chemical activation from hazelnut shells will be presented in this section. It was recognized from the results in Table 7 that $ZnCl_2$ influenced the pyrolytic process so that the formation of tar and other aqueous phase products were restricted. The yield of carbon after chemical activation was increased accordingly contradicting that from KOH treatment. It was because of the fact that the aspect of $ZnCl_2$ action was reactions which change the chemical nature of the cellulosic substance in the raw material; the most important of these was dehydration that assists in the decomposition of organic substances by the action of heat and prevented the formation of non-carbonized degradation product (tar).

However, surface area of products in all cases except that obtained in 80 w/w $ZnCl_2$ impregnation were very low being in the range of 12-215 $m^2/g$ and thus, further oxidation by steam was applied to these previously chemically activated products. This was suspected to enhance the porosity formation by acting mainly in the internal parts of the particles.

Table 8 shows the results obtained by steam oxidation of the chemically activated carbons. Active oxygen in steam and chemical agent acted together so that the surface area sharply increased to 980 $m^2/g$ for 5/100 (w/w) KOH impregnation and 604 $m^2/g$ and 1,237 $m^2/g$ for 5/100 (w/w) and 80/100 (w/w) $ZnCl_2$ impregnations. The observed burn offs were very high for KOH treatment, but very low in the case of $ZnCl_2$ treatment. It was recognized that although the surface area values were

acceptable for gold hydrometallurgy, hardness values appeared extremely low that restricted any industrial uses.

## 5.4. Carbon Adsorption Characterization

### 5.4.1. Gold Loading Capacity of Coconut Shell Carbons

The primary requisites for a granular activated carbon to be used in gold-recovery applications are such that the carbon must have a high gold activity (including gold adsorption rate and gold loading capacity) and the carbon must have high mechanical strength. These properties enable gold processor to obtain the highest possible yield from ores. Thus, low level of capital investment and energy requirements will also be realized.

In previous sections, the optimum conditions for manufacturing granular activated carbons from hazelnut shells, peach and apricot stones, with well developed pore structure associated with a high surface area, with minimum loss of carbon content through carbonization and oxidation and a product with sufficient structural strength to withstand abrasion without excessive attrition to particles were outlined. Characterization of active carbons produced at these optimum conditions comprised the second part of thesis and will be discussed in sections henceforth for each raw material.

In this sense, it was firstly aimed to evaluate the appropriateness of chosen experimental methodology for carbon characterization by testing a commercially used coconut shell carbon for gold loading capacity and kinetic aspects for gold adsorption. Then, the data obtained hereby were compared with product specifications presented in data sheet. This section constitutes the discussion of gold loading capacity results obtained from coconut shell carbon.

As indicated in Figure 19, the gold adsorption isotherm approximated a straight line with logarithmic plotting in accordance with Freundlich equation (2.5). This expressed the fact that for data on adsorption obtained at a uniform temperature,

there is a mathematical correlation between the quantity of gold absorbed on carbon and the quantity that is left unabsorbed. The magnitude of this relation in terms of concentration was specific and hence, expected to vary numerically for each carbon.

This figure was further used to obtain K-value in mg.Au/gr as the gold loading capacity of coconut shell carbons at 1 ppm residual gold concentration. Slope of isotherm and maximum attainable capacity by carbon were also measured in the same figure for a comparison. The results are given in Table 9 which showed that the gold loading capacity of coconut shell carbon was measured very high as 31.6 mg.Au/g with a very steep slope of 0.266 indicating the adsorption is large at strong concentrations, but is much less at dilute concentrations. The isotherm with steep slope further disclosed the potential utility of this type carbons in counter current uses such as CIP and CIL operations. It was so expected since carbons with steep slope had reverse adsorptive capacity such that in counter current applications, the once used carbon after being screened from the completely purified slurry is re-used to bring another untreated slurry in subsequent adsorption tanks to an respectively intermediate gold concentrations; thus, the amount of gold adsorbed by each gram of carbon simultaneously increases upto maximum levels and the carbon is moved sequentially from the last tank of adsorption unit to the former ones.

Gold loading capacity of coconut shell carbons measured as 31.6 mg Au/g of carbon indicated very high adsorption capacity even at very low gold concentrations. However, only a small fraction of this capacity utilized in plant practice. It has been shown that loading of gold an carbon in CIP plants seldom exceeds 10 mg Au/g. There are sound practical and economic reasons for this; firstly, the aurocyanide ion adsorbs relatively rapidly onto carbon in the initial stages of the extraction reaction during which adsorption occurs in the relatively large macro and mesopores. Contact times of weeks or even months are required, however, to fully utilize the total surface area available for aurocyanide adsorption. Secondly, carbon breaks down slowly in the adsorption contactors as a result of the abrasive action of the ore in the leach slurry. This carbon is lost from the circuit screens, and this would result in significant gold losses if the carbon were loaded to

excessively high gold values. This problem is exacerbated by the fact that the rate of the reversible desorption reaction is slow and therefore, a highly loaded carbon granule would only desorb gold slowly if it fractured and flowed con-currently with the slurry out of the plant. A third reason for keeping gold loading on the carbon at a relatively low level relates to lock-up of gold in the CIP plant. Carbon inventories on large CIP plants range from 50 to 100 tons or more and the gold loaded on this carbon is removed from an income earning capacity for the life time of the plant. This can have a critical effect on cash-flow during start-up and ultimately, on the economic viability of a new operation.

Consequently, the results obtained from coconut shell carbons implied that the method of evolution of carbons for gold loading capacity is eligible such that K-value presented in data sheet of coconut shell carbons by manufacturers, 31 mg.Au/g is satisfactorily measured as 31.6 mg.Au/gr in this study.

### 5.4.2. Gold Loading Capacity of Hazelnut Shell Carbons

As seen in Figure 20, the lines obtained by plotting the amount of adsorbed per unit mass of carbon against residual gold concentration resulted in isotherm equilibrium curves (the mass of carbon was assumed to be proportional to its surface area) by Freundlich adsorption relationship in accordance with equation (2.5).

Table 11 included the results obtained from this figure as mentioned in previous section. The results in the table showed that hazelnut shell carbons from fast and slow carbonization had 24 mg.Au/gr K-value with 0.23 slope and 19.5 mg.Au/gr K-value with 0.34 slope, respectively, while carbon from elevated temperature carbonization had higher K-value of 30.7 mg.Au/g , with relatively gentle slope of 0.14. In this sense, carbons from fast and slow carbonization had the same reverse adsorption capacity as coconut shells. Furthermore, carbon from slow carbonization and to some extent, from fast carbonization had very close maximum capacity to that of coconut shell carbons. The K-values of these carbons appeared to be lower than that obtained from carbon of elevated temperature carbonization

and coconut shell carbons. However, they fell in the range of practical importance for plant operations in which a loading value of 1-10 mg.Au.gr$^{-1}$ was generally utilized (Shipman, 1982). On the other hand, carbon from elevated temperature carbonization with as much K-value as coconut shell carbons had negligible reverse capacity with a gentle slope of 0.14 that expressed the adsorption is uniform throughout the wide range of gold concentration.

The differences in the results were attributed to the different charcoal preparation (heating pattern) that led to the difference in pore system and pore structure developed in the particles. Therefore, eventhough the surface area of these carbons were similar, their behavior was dissimilar in the adsorption of gold aurocyanide complexes.

### 5.4.3. Gold Loading Capacity of Apricot Stone Carbons

It was seen in Figure 21 that apricot stone carbons of any kind also yielded isotherms in accordance with equation (2.5). This expressed that a mathematical correlation between the quantity of gold adsorbed and the quantity that is left unadsorbed is valid for apricot stone carbons as in the case of coconut shell and hazelnut shell carbons. The isotherm data including K-value measured at 1 ppm residual gold concentration are tabulated in Table 13. Table 13 showed that apricot stone carbons produced differently had very close K-value in the range of 25.8-27.5 mg.Au.gr$^{-1}$ with steeper slope of 0.26 for slow carbonized product and relatively gentle slopes of 0.17 and 0.22 for carbons from fast and elevated temperature carbonization, respectively. It appeared in the same table that carbons of slow carbonization had the same reverse capacity with a slope of 0.26 as coconut shell carbons. Others were considered to have less reverse adsorption capacity as deduced from relatively gentle slopes.

The similar results in the table indicated that the kinds of heating the source material in oxygen free atmosphere (hence charcoal preparation) did not have significant effect on the gold loading capacities of apricot stone carbons. This can

be attributed to structural resistance of apricot stones to high temperature deformation in carbonization.

The K-values eventhough smaller than that of coconut shell carbons to a small extent fell in the range of K-values of a carbons used in industry and thus, apricot stone carbons are believed to be able to strip most of the gold in solution when the mixing in tanks is sufficient.

### 5.4.4. Gold Loading Capacity of Peach Stone Carbons

It is indicated in Figure 22 that the gold adsorption isotherms of peach stone carbons carbonized at a slower and faster heating approximated straight lines and yielded K-values of 27 and 24 mg.Au/g, respectively as seen in Table 15. A gentle slope of 0.21 was observed for both carbons in the same table.

Therefore, it was concluded that rate of heating the source material upto 650 °C in oxygen free atmosphere had no effect in gold adsorption capacity of peach stone carbons.

K-values were similar to those obtained with apricot stones and hazelnut shells, but, smaller than that of coconut shell carbons. However, they fell in the range of K-values of carbons used in industry and thus, they were considered as a valuable source of raw material for active carbon production.

### 5.4.5. Gold Adsorption Kinetics of Coconut Shell Carbons

The objective of the kinetic experiments was to determine the rate at which the target adsorbate; i.e. gold in the form of aurocyanide complex, is adsorbed from the solution containing 5 ppm $KAu(CN)_2$ onto a specific size fraction of active carbons in a laboratory-scale agitated batch reactor. The adsorption data were fitted to a empirical equation (2.6). The reciprocal of the line obtained from the plotting of data in accordance with equation yielded the R-value which was widely

accepted as being a well measure of the rate of gold adsorption. Coconut shell carbons have been reported to have R-value of 0.075 as a usual characteristics as included in data sheet of manufacturers.

On this basis, experimental results were obtained from coconut shell carbons for the evolution of experimental methodology and results of R-values from tested raw materials as alternative source material for active carbon production to coconut shells.

Figure 23 showing the change in the gold adsorption with respect to time by coconut shell carbons indicated that the initial rate of aurocyanide adsorption onto carbon is rapid and that is expected to be controlled by the hydrodynamics in the adsorption reactor. This initial film diffusion controlled reaction, which is known to result in the establishment at between 50 - 70 % of the equilibrium gold capacity. This appeared in the figure to occur in between first three hour. Subsequently, gold cyanide continued to be adsorbed slowly onto the carbon almost indefinitely through the micropores under pore diffusion controlled adsorption to establish overall true equilibrium. But, in practice, the establishment of true equilibrium is difficult and gold cyanide diffuses through the micropores until the cross-sectional area of micropores approaches to that of aurocyanide ions; i.e., adsorption of gold onto the carbon as seen after 8 hour exposure in the figure.

Adsorption data were then plotted in Figure 24 for R-value determination in accordance with equation (2.6). It was seen from the figure that the variation of experimental points was linear with respect to the reaction time. This indicated that the adsorption data could very well be expressed by the equation. This figure was consequently used to obtain the reciprocal of the R-value as the intercept at zero time, which was latter converted to R-value and tabulated in Table 16. $t_{50}$ and $C_s$ at 1 hr values were also included in the table for comparison purposes.

It was seen in Table 16 that coconut shell carbons had 0.059 R value and 3.25 ppm and 120 min, $C_s$ at 1 hr and $t_{50}$ values, respectively. This showed that R-value obtained experimentally was lower than the R-value presented in data sheet,

indicating the relatively gentle agitation used in the experiments since it was known that the rate is greatly influenced by the rate of agitation in batch reactors.

$t_{50}$ values could be approximated as the establishment of initial film diffusion and end of adsorption of gold by mesopores and macropores. It was so expected since as seen in Figure 23, a decrease was observed in the rate of gold adsorption, indicating the transition of film diffusion adsorption towards pore diffusion adsorption. On this basis, 120 minutes was required for completion of initial adsorption and this short time further resulted a quick establishment of adsorption in micropores (establishment of overall adsorption).

### 5.4.6. Gold Adsorption Kinetics of Hazelnut Shell Carbons

In the same sense mentioned in previous section for coconut shell carbons, adsorption data were obtained with hazelnut shell carbons and plotted in Figure 25 and 26 to determine R-value.

As indicated in Figure 25, the rate of gold adsorption was rapid in the initial period of exposure for all the carbons and the adsorption was similar quantitatively upto nearly 50 % adsorption to that observed for coconut shell carbons. However, the rate slowed down thereafter. This was so expected since in the initial period of adsorption, gold was mainly adsorbed onto the external surfaces of carbons; mainly in meso and macropores, and the rapid rate was replaced by slow rate of adsorption in later stages of adsorption due to the slow pore diffusions of gold through the ways on arteries between these pores and micropores. Therefore, the size and shapes of these arteries and less amount of micropores in these carbons (as deduced from lower $N_2$ BET values) affected the rate of adsorption in this region so that the adsorption curves of these carbons leveled off prior than that of coconut shell carbons.

As appeared in Table 17, hazelnut shell carbons had R-values in a very close range of 0.050 - 0.057. These values although relatively smaller than that of the coconut shell carbons, could be considered very high for the carbons with $N_2$ BET

numbers around 785 - 825 $m^2/g$. It is known that the rate of adsorption is proportional to the available surface area of the carbons. Therefore, this finding that contradicts the last statement is attributed to the high ash content of hazelnut shell carbons since it was stated that $Ca^{++}$ present in ash in the from of oxides and hydroxides would favor the gold adsorption. (Bailey, 1986)

It was also, recognized in the same table that $t_{50}$ and $C_s$ at 1 hr values in the range of 130-150 min and 3.70 - 3.35 ppm, respectively, were higher, indicating relatively poor adsorption characteristics, than that of coconut shell carbons.

### 5.4.7. Gold Adsorption Kinetics of Apricot Stone Carbons

The adsorption data obtained from apricot stone carbons were plotted in Figure 27 to investigate the change in adsorption of gold onto the carbons with respect to time. It was recognized in the figure that carbon of slow carbonization (with previously determined K-value of 25.8 $mg.Au.gr^{-1}$) had the same adsorption curve as coconut shell carbon had in all the range of adsorption period covered in the tests. This represented a product with very high activity and appreciable loading capacity in gold adsorption.

It was also recognized in the figure that while active carbons from fast and slow carbonization had the same rate upto 50 % adsorption (film diffusion region), active carbons from elevated temperature carbonization appeared with significantly slower adsorption rates even in the initial period of adsorption. The same phenomena has also been observed for hazelnut shell carbons discussed in previous section. In second portion of adsorption; normally pore diffusion controlled adsorption dominates, different size and shapes of access ways to micropores and low degree of micropore formation affected the gold adsorption. Thus, adsorption curves leveled off at different sequence near to the end of overall adsorption.

Table 17 including the R-values of each carbon from apricot stones indicated that while carbons from fast and slow carbonization had nearly the same R-value as coconut shell carbons, carbons of elevated temperature had lowest R-value of

0.043. It was also recognized in the table that high R-values of carbons decreased the time required to lower the gold concentration by 50 %, accordingly, as deduced from smaller $t_{50}$ values in the table.Thus, these carbons had the same $t_{50}$ value of 120 minutes as coconut shell carbons had.

As a result, it was concluded that the gold adsorption data could also very well be expressed by the rate equation for apricot stone carbons and that apricot stones could yield active carbons with the same adsorption characteristics as coconut shell carbons yielded. For this, apricot stones would be carbonized at 650 °C and then, activated by steam to nearly 50 % of original weight loss at 900 °C.

### 5.4.8. Gold Adsorption Kinetics of Peach Stone Carbons

Last series of kinetic experiments for R-value determination were conducted with peach stone carbons. The adsorption data were plotted in Figure 29 so that the change in the gold adsorption with respect to time was observed easily. It was recognized in the figure that the initial rate of adsorption is rapid as in the case of other tested raw materials, but this continued upto a relatively lower level of adsorption of 30 %. The rate slowed down thereafter and no change was observed after 80 % adsorption for fast carbonized products and 90 % adsorption for slow carbonized products. Thus, it was deduced that the establishment of true equilibrium would take place at a very longer times. This indicated relatively poor activity of products in gold adsorption. Table 19 shows the R-values of peach stone carbons. R-values of these carbons appeared significantly lower than that of coconut shell carbons, and other tested raw materials. However, these carbons were considered to be easily improved with deeper oxidation since structure of these carbons would allow some more weakening that will be created by deeper oxidation. The $t_{50}$ and $C_s$ values in the table indicated low adsorption in meso and macropore region.

As a result, it was concluded that peach stones yielded relatively poor products in adsorption at this level of activation and that longer activation would probably increase the activity by opening up new pores and enlarging the already existing pores.

# CONCLUSIONS

In the light of experimental results, it was recognized that carbonaceous raw materials tested for active carbon production liberated thermally unstable residues in an inert atmosphere in the form of gases including water and high molecular weight tarry substances. This was accompanied by shrinkage in the pores as the carbonization temperature was progressively increased.

Since hazelnut shells, peach and apricot stones have similarities in their chemical structure (same origin), they behaved similarly in carbonization. Hence, the physical and chemical properties of charcoals from these raw materials were allied to each other. The results showed that heating rate upto 650 °C had no significant effect on hardness and surface area of charcoals. However, heating the raw materials at elevated temperatures in carbonization resulted in a strongly compacted granules. This indicated that raw materials with weak structure such as hazelnut shells would be carbonized at elevated temperatures. Charcoals from all raw materials expelled poor activity in this form.

Carbons obtained from chemical activation with $ZnCl_2$ and KOH had poor activity and hence, had to be re-activated afterthen by steam. In this case, eventhough very active products were obtained, steam activation of chemically activated carbons yielded very soft products in any case. So, it obscured the granular use for gold production and only some general aspects about chemical activation were obtained.

It was recognized from the steam activation tests that the activity ( measured by $N_2$ BET value) and hardness expressing the mechanical strength of the material were related to the total weight loss (% burn off) sustained during activation, although the general utility of this relationship in case of activity has been qualified by the

observation that some part of loss occurred by internal burning and some part by reduction in the size of granules. This was attributed to the fixed bed activation of the charcoals from raw materials, in which the action of oxidizing agent was not uniform on the surface of particles. Hence, a fludized bed environment in activation reactors would favor the internal burning of charcoals. During activation, the active oxygen in steam was firstly used in the reactions with disorganized carbon and residual tarry products.Then, It burnt away the more reactive portion of carbon skeleton and the reactions yielded city gas; $CO+H_2$ ( having ability to burn), in accordance with equation (2.1). Finally, a structure enriched in mainly micropores was obtained when nearly half of the original weight was burnt. However, a mixed pore structure with micropores, mesopores and macropores was obtained after 50 % weight loss. This indicated that the activation of raw materials of cellulosic origin would proceed upto this levels. This would also enhance the adsorption by allowing the ions towards the micropore region.

The gold loading capacities in the range of 19.5-30.7 mg.Au/g, 25.8-27.5 mg.Au/g and 24-27 mg.Au/g were obtained for hazelnut shell carbons, apricot and peach stone carbons, respectively. The close values indicated that the loading capacity depended on largely the origin of raw materials. These values although lower than that of the coconut shell carbons fell in the range of K-values of activated carbon used in the industry.

The kinetic results indicated that apricot stones with an R value of 0.060 and $t_{50}$ of 120 minutes had the same adsorption rate as coconut shells with 0.059 and 120 minutes, R and $t_{50}$ values, respectively; hazelnut shells and peach stones seemed to give slower adsorption rate.

Comparing the hardness, surface area, K and R values, it might be stated that hazelnut shells would be carbonized at elevated temperature and then activated by steam to 52.7 % weight loss. However, hazelnut shells yielded weakest carbon with poor adsorption characteristics. Peach and apricot stones, on the other hand, would be carbonized at lower temperatures and then activated at 800 °C and 900 °C, respectively, to yield the best carbon. In this case, nearly half of the original weight was burnt away under the oxidative action of steam. It might also be stated

that activated carbons from peach and apricot stones with higher hardness numbers than coconut shells can be improved with longer activation. This will lead to the weakening of the carbon structure hence somewhat lowers the hardness, however increases the BET surface area by opening up the micropores. Longer activation will also have a beneficial effect on the adsorption capacity by allowing more gold cyanide complexes into enlarged pores and on the adsorption rate by faster diffusion in macropores than in micropores.

In the light of results obtained in this study, it can be concluded that active carbons produced from apricot and peach stones can possibly be employed in gold processing plants. However, it is imperative that further studies to improve the properties of the carbons under investigation be carried out. Moreover, behaviors of these carbons in real life applications; e.g. CIP, CIL etc. shall also be studied.

# REFERENCES


**.....,1994(Annon.).** Gold Mining in Türkiye . A Public Report in Turkish

**Adams, M.D.** The Mechanism of Adsorption of Aurocyanide onto Activated Carbon-Relation between the Effects of Oxygen and Ionic Strength. Hydrometallugy, 25, 1990,pp.171-184

**Adams, M.D., and Fleming, C.A.** The Mechanism of Adsorption of Aurocyanide onto Activated Carbon .Metall. Trans., Vol.20B, 1989, pp.315-325

**Adams, M.D., Friedl, J., and Wagner, F.E.** The Mechanisms of Aurocyanide Adsorption onto Activated Carbon. Hydrometallurgy, 31, 1992, pp.265-275

**Adams, M.D., McDougall, G.J., and Hancock, R.D.** Models for the Adsorption of Aurocyanide onto Activated Carbon- Comparison between the Extraction of Aurocyanide by Activated Carbon. Hydrometallurgy, Vol.19, 1987, pp.95

**Adamson, R.J., (ed).** The Leaching of Gold. Gold Metallurgy in South Africa. Johannesburg, Chamber of Mines of South Africa, 1972, pp.304-327

**Agrawal, R.K.** Kinetics of Reactions Involved in Pyroliysis of Cellulose . Can. J. of Chem. Eng., Vol.66, 1988, pp.403-412

**Agrawal, R.K.** Kinetics of Reactions Involved in Pyrolysis of Cellulose Using Modified Kilser-Broida Model. Can. J. of Chem. Eng., Vol.66, 1988, pp.413-418

**Agrawal, R.K.,and McCluskey, R.J.** The Low Pressure Pyrolysis . J. of App. Poly. Sci., Vol.27, 1983, pp.367-382

**Anderson, T.N., and Porr, J.C.** Gold and Silver Assay Methods in the Mining and Metallurgical Industry- Gold and Silver Leaching, Recovery and Economy. Schlitt, W.J., Larson, W.L., and Hiskey, J.B,(eds). Soc. of Min. Engng of AIME

**ASTM 1762-64.** Chemical Analysis of Wood Charcoal

**ASTM 1991.** Standard Test Method for Iodine Adsorption by Carbon

**ASTM 2367-70.** Standard Test Method for Moisture in Activated Carbon

**ASTM 2854-70.** Standard Test Method for Apparent Density of Activated Carbon

**ASTM 3037-78.** Standard Test Method for Surface Area by Nitrogen Adsorption

**Bailey, R.R.** The Extractive Metallurgy of Gold in South Africa. Stanley, G.G. (ed). The Chamber of Mines of South Africa, 1986

**Bevia, F.R., Rico, D.P., and Gomis, A.F.** Activated Carbon from Almond Shells-Chemical Activation 1. Activating Agent Selection and Variables Influence. Ind. Eng. Prod. Res. Dev., 23, 1984, pp.266-269

**Bocris, J.C.** In Chemistry and Physics of Carbon. Walker, P.C., ( ed ) , Vol.5, New York, Marcel Dekker, 1969

**Browning, R.S.** The Chemistry of Wood . Interscience Pub., New York, London, 1963

**Calgon Carbon Brochure.** Gold Adsorption with Calgon Granular Carbon

**Calgon Test Method 1983.** Gold Adsorption Rate Tests

**Calgon Test Method 53.** Determination of the Gold Adsorptive Capacity of Carbons

**Cheremisinoff, P.N., and Ellesbusch, F., (eds).** Carbon Adsorption Handbook. Ann Arbor, Science Publishers Inc., 1978

**Davidson, R.J.** The Mechanism of Gold Adsorption on Activated Charcoal . J. S. Afr. Inst. Min. Metall., November, 1974, pp.67-76

**Davidson, R.J., Veronese, V., and Nkosi, M.V.** The Use of Activated Carbon for the Recovery of Gold and Silver from Gold Plant Solutions. J. S. Afr. Inst. Min. Metall., 79 (10) , 1979, pp.287-297

**Ermakov, E.A., Shenfeld, B.E., and Lozhkın, A.F.** Activation of Carbonized Granules by Steam. Khimiya Tverdoga Topliva, Vol.12, No.2, 1978, pp.86-89

**Faulkner, W.D.** Carbon Selection Vital. Mining Mothly, March, 1984

**Faust, S.D., and Aly, O.M.** Chemistry of Water Treatment . Butterworth Publishers, Woburn, MA, 1983

**Flowsorb 2300.** Manual Book

**Fornwalt, H.J., Helbig, W.A., and Scheffer, G.H.** Activated Carbon for Liquid Phase Adsorption. Br. Chem. Eng., Vol.8, !963

**Garten, V.A., and Weiss, D.E.** A New Interpretation of the Acidic and Basic Structures in Carbons- The Chromene-Carbonium Ion Complexes in Carbon . Aust. J. Chem., 10, 309, 1957

**Gonzales, J.D.L., Vilchez, F.M., and Reinoso, F.R.** Carbon, Vol.18, 1980, pp.413-418

**Greaves, M.C.** Determination of Gold and Silver in Solution by AAS. Nature , Vol.199, 1963, pp.552-553

**Gupta, J.G.S.** A Review of the Methods for Determination of the Platinium -Group Metals, Silver and Gold by AAS. Miner. Sci. Engng., Vol.5, No.3, 1977, pp.207-218

**Hall, S.H.** A Rapid Method for Gold Extraction Using MIBK. Atomic Abs. News., Vol.18, No.6, 1979, pp.126-127

**Hassler, J.W, (ed).** Activated Carbon. New York , Chemical Pub. Company, 1963

**Hassler, J.W, (ed).** Purification with Activated Carbon. New York, Chemical Pub. Company , 1974

**Ibrado, A.S., and Fuerstanu, D.W.** Effect of the Structure of Carbon Adsorbents on the Adsorption of Gold Cyanide . Hydrometallugy, 30, 1992, pp.243-256

**John, M.V.** Model Application. Lecture Notes, Johannesburg, 1985

**Kipling, J.J.** Quart.Revs , London, 1956

**Kostorova, M.A., Perederil, M.A., and Surinova, S.I.** Production of Adsorbents from Coals. Khimiya Tverdoga Topliva,Vol.10, No.2, 1976, pp.5-15

**Kuz'miykh, V.M., and Tyurin, N.G.** Effect of the Acidity of Cyanide Solutions on the Adsorption of Gold on Charcoal. Izv. Vyssh. Vcheb. Zaved, Tsvet Metall.,Vol.11, 1968

**Laine, J., Calafat, A., and Labady, M.** Preperation of Activated Carbon from Coconut Shell Impregnated with Phosphoric Acid. Carbon, Vol.27, 1989,pp.191-195

**Laxen, P.A.** Carbon-in-Pulp Processes in South Africa. Hydrometallurgy, 13, 1984, pp.169-192

**Laxen, P.A., Becker, G.S.M., and Rubin, R.** Developments in the Application of Carbon-in-Pulp to the Recovery of Gold from South African Ores. J. S. Afr. Inst. Min. Metall., 79, 1979, pp.315-326

**Lundquist, R.V.** Assaying Cyanide Solutions for Gold. Engng. and Min. Journal, November, 1940

**Mallett, R.C., Taylor, J.D., and Steels, T.W.** The Determination of Gold in Barren Cyanide Solution by AAS. Research Report No.24, National Inst. for Metallurgy (South Africa)

**Mantell, C.L., ( ed ).** Carbon abd Graphite Handbook. Interscience Publishers, John Wiley and Sons. Inc., 1968

**Mattson, J.S., and Mark, H.B., (eds).** Activated carbon.New York, Marcel Dekker,1970

**McDougall, G.J.** Lecture Notes on the Manufacture of Activated Carbon

**McDougall, G.J.** The Physical Nature and Manufacture of Activated Carbon . J. S. Afr. Inst. Min. Metall., Vol.80, 1980, pp.344-356

**McDougall, G.J.** The Physical Nature and Manufacture of Activated Carbon . J. S. Afr. Inst. Min. Metall., Vol.91, No.4, 1991, pp.109-120

**McDoudall, G.J., and Fleming, C.A.** Ion Exchange and Sorption Processes in Hydrometallurgy- Extraction of Precious Metals on Activated carbon. Streat, M.A., and Naden, D.,(eds). Society of Chemistry and Industry , Wiley, Chichester, UK, 1987, pp.56-126

**McDougall, G.J., and Hancock, R.D.** Activated Carbons and Gold- A Literature Survey. Minerals Sci. Eng., Vol.12, No.2, 1980

**McDougall, G.J., and Hancock, R.D.** Gold Coplexes and Activated Carbon. Gold Bull. 14 ( 4 ) , 1981, pp.138-153

**McDougall, G.J., Hancock, R.D., Nicol, M.J., Wellington, O.L., and Copperthwaite, R.G.** The Mechanism of Adsorption of Gold Cyanide on Activated Carbon. J. S. Afr. Inst. Min. Metall., Vol.80, 1980, pp.344-356

**Neast, R.C, (ed).** Handbook of Chemistry and Physics. CRC Press, Cleveland, Ohio, 1974

**Nicol, D.I.** The Adsorption of Dissolved Gold on Activated Charcoal in a NIMCIX Contavtor. J. S. Afr. Inst. Min. Metall., 79 (10 ) , 1979, pp.497-502

**Norit Carbon Brochure.** Gold Recovery with Norit Activated Carbon

**Olson, A.M.** Gold Assay by AAS- A Preliminary Report. Atomic Abs. News., Vol.4, 1965, pp.278-280

**Puri, B.R.** Surface Oxidation of Charcoal at Ordinary Temperatures. Proceedings of the 5th . Conf. on Carbon, New York , Pergamon, 1962, Vol.1, pp.165-170

**Puri, B.R.** Chemisorbed Oxygen Evolved as CO2 and its Influence on Surface Reactivity of Carbons . Carbon, Vol.4, 1966, pp.391-400

**Shipman, A.J., (ed).** Laboratory Methods for Testing Activating Carbons for Use in Carbon-in-Pulp Plants for the Recovery of Gold . Originally Issued Copy from Confidental Communication No.C1753M, June, 1991 (Mintek)

**Simmons, E.L.** Gold Assay by AAS. Atomic Abs. News., Vol.4, 1965, pp.281-287

**Simmons, G.L., Blakeman, D.L., Trimble, J.W., and Banning, S.W.** Noranda's Carbon-in-Pulp Gold-Silver Operation at Happy Camp Mine, CA. Min. and Metall. Process., May, 1985, pp.73-78

**Smisek, M., and Cerny, S., (eds).** Active Carbon- Manufacture, Properties and Applications. Amsterdam, Elsevier, 1970

**Snoeyink, V.L., and Weber, W.J.** The Surface Chemistry of Active Carbons- Discussion of Structure and Surface Functional Groups. Envirom. Sci. Technol., 1 (3), 228, 1967

**Streat, M.A., and Naden, D, (eds).** Ion Exchance and Sorption Processes in Hydrometallurgy. Society of Chemistry and Industry, Wiley, Chichester, UK, 1987.

**Strelow, F.W.E., Feast, E.C., Mathews, P.W., and Vanzyl, C.R.** Determination of Gold in Cyanide Waste Solutions by Solvent Extraction and AAS. Anal. Chem., Vol.38, 1966, pp.115-117

**Tindall, F.M.** Silver and Gold Assay by AAS. Atomic Abs. News., Vol.4, 1965, pp.339-340

**Tsuchida, N., Ruane, M., and Muir, D.M.** Studies of the Mechanims of Gold Adsorption on Carbon. Mintek 50 Congress, 1984, Johannesburg

**Urbanic, J.E., Jula, R.J., and Faulkner, W.D.** Regeneration of Activated Carbon Used for Recovery of Gold. Min. and Metall. Process., November, 1985, pp.193-198

**Van Dam, H.E.** Chemistry of CIP nad Related Processes. Eng. and Min. Journal, June, 1983, pp.26-27

**Weber, W.J.** Physicochemical Processes for Water Quality Control. Wiley Interscience , New York, 1972

**William, F.D., and Richards, G.N.** The Effects of Ion-exchanged Cobalt Catalysts on the Gasification of Wood Chars in CO2. Fuel, Vol.67, 1988, pp.345-350

# APPENDIX A

## DETERMINATION OF HARDNESS NUMBER

Abrasion resistance is the property of activated carbons to resist attrition, or wearing away by friction, resulting from particle-particle or particle-container interactions. Dry impact methods measure the percentage retention of carbons, by weight, which is retained on a sieve whose openings are closest to one-half the openings of the sieve that defines the minimum particle size of original weight after the particles were exposed to the action of steel balls in a test pan (ASTM D 3802-79)

The method used in the study provide a quick procedure to determine hardness numbers of activated carbons by using hardgrove machine. The experimental manner of the test was the same as in the case of ASTM standard. Conceding the fact that the test does not actually measure in-service hardness numbers of carbons, it was correlated by a constant that was obtained from equalization of data from coconut shell carbons to standard numbers . The ball-pan hardness number of coconut shell carbon is presented in data sheet as 97.0. Thus, correction factor is obtained.

A screened (-7+14 mesh ) and weighed sample ( 10 gr ) of the carbon was placed in hardgrove machine with a number of stainless steel balls, then subjected to rotating action for 1 minutes. At the end of this period, the amount of particle size degradation was determined by measuring the quantity of carbon by weight which was retained on a 25 # sieve. The hardness numbers were then obtained from equation ;

$$H = 100 (B/A) F \quad (A.1)$$

Where,

H is hardness number,

B is weight of sample retained on 25 # sieve ,gr

A is weight of sample loaded to Hardgrove machine, gr

F is correction factor obtained from the measurements of the hardness number of coconut shell carbons

# APPENDIX B

## DETERMINATION OF BET SURFACE AREA BY NITROGEN ADSORPTION

Surface area of carbons were determined with Flowsorb 2300 machine which measures the specific surface area of samples from the volume of 30 % $N_2$/70 % He mixtures that is adsorbed or (desorbed) by the carbons at liquid nitrogen temperatures. The weight of the sample should be adjusted to give between 0.5 and 25 $m^2$ for the most accurate results. Degassing of the carbon prior to testing, to drive off whatever gases and vapor, most especially water vapor picked up from the atmosphere, was performed at 300 ° C for half an hour. Therefore, the results obtained gave a specific surface area in terms of square meters per gram of carbon when sample weight was established.

The adsorption of gases upon a solid surface is described by one of the well-known BET equation (B1) (Flowsorb 2300 manual ) as follows.

$$(P/P_\infty)/V\,(1-(P/P_\infty)) = 1/(Vm.C) + ((C-1)/(Vm.C))P/P_\infty \qquad (B.1)$$

Where V is the volume (at STP) of gas adsorbed at pressure P, $P_\infty$ the saturation pressure which is the vapor pressure of liquefied gas at the adsorbing temperature, Vm the volume of gas (STP) required to form an adsorbed monomolecular layer, and C a constant related to the energy of adsorption.

The surface area S of the sample giving the monolayer adsorbed gas volume Vm (STP) is then calculated from;

$$S = Vm\ A\ N/M \qquad (B.2)$$

Where A is Avagadro's number which expresses the number of gas molecules in a mole of gas at standard conditions ; M the molar volume of the gas ,and N the area of each adsorbed gas molecule.

The constant C of equation (B.1) is typically a relativelly large number; i.e.; C>> 1, from which equation (B.1) reduces very nearly to

$$(P/P_{\infty}) / V (1-(P/P_{\infty})) = (1/Vm) . ((1/C) + (P/P_{\infty})) \qquad (B.3)$$

Now, if $P/P_{\infty} >> 1/C$, equation (B.3) can be further represented by;

$$(P/P_{\infty})/ V (1-(P/P_{\infty})) = (1/Vm) . (P/P_{\infty}) \qquad (B.4)$$

Which arranges to

$$Vm = V (1-(1/P_{\infty})) \qquad (B.5)$$

Substituting equation (B.5) into equation (B.2) yields,

$$S = V\ A\ N\ (\ 1-(P/P_{\infty})/M \qquad (B.6)$$

from which the sample surface area is readily determined once the volume of gas adsorbed (or desorbed) is measured and appropriate values for the other terms are incorporated.

For nitrogen gas adsorbed from a mixture of 30 % nitrogen and 70 % helium using a liquid bath, the values are arrived at as follows;

The volume V of gas with which the Flowsorb 2300 is calibrated is injected at room temperatures and the prevailing atmospheric pressure. This volume must thus be

multiplied by the ratios 273.2/(Rm.Temp.,° K). (Atm.Press.,mmHg)/760 to convert it to standard conditions (0° C and 760 mmHg)

Avagadro's number A is $6.023.10^{23}$ molecules/g.mole. The molar volume M of a gas at standard conditions is 22414 $cm^3$/g.mole.

The presently accepted value for the area N of a solid surface occupied by an adsorbed nitrogen molecule is $16.2.10^{-20}$ $m^2$ ( = 16.2 Angstroms $^2$ ).

P is 0.3. the atmospheric pressure in millimeters of mercury since the gas mixture is 30 % nitrogen and adsorption takes place at atmospheric pressure. $P_{\infty}$, the saturation pressure of liquid nitrogen is typically a small amount greater than atmospheric due to thermally induced circulation, dissolved oxygen, and other factors. With fresh, relatively pyre liquid nitrogen, the saturation pressure is typically about 15 mmHg greater than atmospheric pressure.

The result for a 30 % N2 / 70 % He mixture adsorbed at liquid nitrogen temperature when room temperature is 22 ° C and atmospheric pressure is 760 mmHg, is the expression;

**$S = v. ( 273.2/Rm.Temp.). ( Atm.Pres./760 ). ( 6.02.10^{-20}.16.2.10^{-20}/ 22.4.10^3) . (1-(\%N2/100).Atm.Pres.)/Sat.Pres.)$** **(B.7)**

**$S = 2.84.v$**

Where S is the surface area in square meters. For calibration purposes, this means that a strenge injection of v= 1.00 cm3 of nitrogen at 22 ° C and 760 mmHg should produce an indicated surface area of 2.84 $m^2$. Thus, once the calibration completed, testing of sample carbon will result the specific surface area provided that the weight after degassing should be established.

# APPENDIX C

## DETERMINATION OF K-VALUE OF CARBONS

To determine K-value expressing the gold loading capacity of carbons, firstly adsorption isotherm of carbons was obtained. To do this, a sample of washed and ovendired carbon was ground to a size less than 95% passing 325 mesh. Then, four to six samples of carbon in the range of 0.020-0.50 gr in weight were separated and each sample was exposed to a 100 ppm gold containing 100 ml borate buffered solution at pH 10. The reaction took place approximately 20 hr for the utilization of a full adsorption of gold by carbon. Then, the residual gold concentration in each sample solution was measured by AAS. From the residual gold concentration, gold adsorbed on carbon (X/M) in mg.Au/g was calculated in the manner presented in the table below this text for coconut shell carbon and plotted in logarithmic form with respect to residual gold concentration in the solution. Thus, an isotherm was obtained. K-value of carbons was obtained as gold loading capacity at 1 ppm residual gold concentration from the graph.

| PH | Grams of carbon (M) | Conc. of Au in equilib. (C) mg/l | mg | mg Adsorbed (X) | Carbon Loading (X/M) |
|---|---|---|---|---|---|
| 10 | ---- | 100 | 10 | ---- | ---- |
| | .330 | 0.8 | 0.08 | 9.92 | 30 |
| | .250 | 2 | 0.2 | 9.80 | 39.2 |
| | .150 | 10.7 | 1.07 | 8.93 | 59.9 |
| | .050 | 54 | 5.4 | 4.6 | 92.2 |
| | .025 | 74 | 7.4 | 2.6 | 104.36 |

# APPENDIX D

## DETERMINATION OF R-VALUE OF CARBONS

Rate of gold adsorption (hence, gold adsorption kinetics) was studied by obtaining R-values of the best carbons from gold adsorption data since this value is generally accepted as a measure of rate of gold adsorption (Urbanic et al., 1985). It was determined by Calgon Test Method 1983 as exposing the 1 gr. of a specific particle size fraction of the activated carbon sample to 1.7 L of a borate buffered 5-ppm $KAu(CN)_2$ solution at pH 10. The exposure took place in a glass reaction vessel. The reaction vessel was magnetically stirred at a rate that the particles were continually suspended in the solution. The gold concentration of the solution was measured periodically over an eight hour exposure by Atomic Absorption Spectrophotometer (AAS) at a wavelength at 242,8 nm. Data obtained were tabulated as in the following table (presented for coconut shell carbon) to fit to the equation (2.6) that yields a straight line in normal cases. R-value was the reciprocal of the intercept at zero time when the time divided by loading on carbon was plotted against time.

| Time (hr) | Residual Au ppm | Adsorbance % | Au Adsorbed mg (X) | T/X/M |
|---|---|---|---|---|
| 1 | 3.25 | 35 | 2.975 | 20.20 |
| 2 | 2.50 | 50 | 4.250 | 28.28 |
| 3 | 1.83 | 63.4 | 5.389 | 33.45 |
| 4 | 1.38 | 72.4 | 6.154 | 39.06 |
| 5 | 0.95 | 81 | 6.895 | 43.64 |
| 6 | 0.70 | 86 | 7.310 | 49.32 |
| 7 | 0.40 | 92.0 | 7.820 | 53.79 |
| 8 | 0.18 | 96.4 | 8.190 | 58.70 |

# VITA

Mustafa Yalçın was born in Ilgaz, Çankırı on July 7, 1964. He received his B.S. degree in Mining Engineering Department from the Middle East Technical University in July 1987. He worked in Demir Export AŞ. as a research engineer from 1987 to 1989. Then, he worked as a graduate assistant in the Department of Mining Engineering until 1993. He has been an Expert in the Undersecretariat of Treasury since 1993. His main areas of interest are gold adsorption unit processes and foreign investments in Türkiye for gold production.